RBL-2H3 MAST CELLS AS A MODEL SYSTEM FOR STUDYING RECEPTOR-STIMULATED Ca^{2+} OSCILLATIONS, PHOSPHOINOSITIDE SYNTHESIS, AND ACTIVITIES DISRUPTED BY ALPHA-SYNUCLEIN

A Dissertation

Presented to the Faculty of the Graduate School

of Cornell University

in Partial Fulfillment of the Requirements for the Degree of

Doctor of Philosophy

By

Marcus M. Wilkes

August 2016

RBL-2H3 MAST CELLS AS A MODEL SYSTEM FOR STUDYING RECEPTOR-STIMULATED Ca^{2+} OSCILLATIONS, PHOSPHOINOSITIDE SYNTHESIS, AND ACTIVITIES DISRUPTED BY ALPHA-SYNUCLEIN

Marcus M. Wilkes

Cornell University, 2016

Due to the complexity of cellular life, model systems are often utilized to simplify multifaceted biological processes, and questions, into their most simple components. Much of what we understand about life, and its associated diseases, has come from studying cellular processes in model systems such as bacteria, yeast, flies, worms, mice, and cell lines. RBL-2H3 cells are a model system used for studying the characteristics and functions of mast cells *in vitro*. Mast cells are a type of white blood cell traditionally known for controlling the allergic immune response, and more recently appreciated for their role in both innate and adaptive immunity, autoimmune diseases, and cancer.

RBL-2H3 cells are a particularly powerful model system for studying receptor-stimulated Ca^{2+} responses, a critical component of mast cell signaling. Cells invest much of their energy to maintain an ~20,000 fold gradient between the concentration of extracellular and intracellular Ca^{2+}. This enables minor changes in intracellular Ca^{2+} levels to regulate a wide range of physiological processes, including the Ca^{2+} response that triggers life at fertilization, the Ca^{2+} response that often triggers cell death, and the majority of cellular processes in between. In this thesis we investigate the puzzling, yet fascinating, phenotype of Ca^{2+} oscillations, a process by which cells rapidly increase, and then subsequently decrease, intracellular Ca^{2+} levels enough to signal, without triggering apoptosis. We report that Ca^{2+} oscillations are controlled, in part, by

the Rho GTPase Cdc42 which plays a critical role in regulating levels of PIP_2, the necessary phosphoinositide cleaved to initiate Ca^{2+} oscillations.

In addition we report that RBL-2H3 cells are also a useful tool for studying processes regulated by alpha-synuclein, a protein long implicated in the pathology of Parkinson's disease. The physiological function of alpha-synuclein is poorly understood and here we describe that this protein is a regulator of stimulated recycling endosomal exocytosis and endocytosis, and that the capacity to control these processes changes depending on alpha-synuclein expression levels in cells. In summary, using RBL-2H3 cells as a model system has enabled us to improve our understanding of the processes that regulate receptor-stimulated Ca^{2+} oscillations, phosphoinositide synthesis, and alpha-synuclein function.

BIOGRAPHICAL SKETCH

Marcus was born May 23, 1987 to Wynn and Teresa Wilkes in Idaho Falls, Idaho. He enjoyed the attention of being the youngest member of his family, for 14 months, before his younger sister joined the family. Despite being born 7th , he would go on to become the exact middle of Wynn and Teresa's 13 children, with four older brothers, four younger brothers, two older sisters, and two younger sisters. At age five his family moved to Cedar Hills, Utah where he lived until he was 18, spending the majority of his time going to school, and playing sports with his friends and siblings. In high school he became acquainted with a new neighbor, Dr. David Bearss, a cancer biologist, previously a professor at the University of Arizona. Dr. Bearss had recently relocated to Utah to start his own pharmaceutical company, developing small molecule kinase inhibitors for cancer therapeutics. Dr. Bearss allowed Marcus to tour his company's research facilities, triggering an interest in biomedical and translational research.

At age 18 Marcus enrolled at Brigham Young University. Following his freshman year Marcus left to serve a mission for The Church of Jesus Christ of Latter-day Saints (LDS) in Hiroshima, Japan, where he lived for two years and became fluent in the Japanese language. Upon completion of his LDS mission, Marcus returned to Brigham Young University where he majored in molecular biology and minored in Japanese. After his sophomore year Marcus reconnected with Dr. Bearss, and subsequently worked as a cancer biology intern at Dr. Bearss' company for three summers, where he grew to love conducting his own experiments and thinking about the applications of biological research.

In May of 2010 Marcus married his best friend Kendra Duncan, and together they had their first child, Sophie, in July of 2011. In August of 2011 Marcus and Kendra, with one month old Sophie in tow, moved 2,000 miles to Ithaca, New York, for Marcus to begin a PhD program,

having been accepted into the Field of Pharmacology at Cornell University. At Cornell, Marcus joined the lab of Professor Barbara Baird and Dr. David Holowka where his thesis researched focused on understanding the connection between Rho GTPases, Ca^{2+} oscillations, and phosphoinositide synthesis. Three years into his PhD, at the encouragement of Professor Baird and Dr. Holowka, Marcus began a collaboration with Dr. David Eliezer at Weill Cornell Medicine, investigating the physiological function of the protein alpha-synuclein, and why disruption of this function leads to Parkinson's disease. This research also developed into a significant part of his thesis research.

While at Cornell Marcus and Kendra had two more children, Duncan in March of 2013, and Ruby in July of 2015. Marcus has enjoyed learning to balance the rigors of graduate work, with the parenting of three young children, and is grateful for the time management skills that he is learning to develop. In the summer of 2016 Marcus, Kendra, and their three children, will relocate to New Jersey for Marcus to work in the pharmaceutical consulting industry. The Wilkes will forever miss, and cherish, the many memories they have created in Ithaca and at Cornell

.

For Kendra:

愛しているよ

ACKNOWLEDGEMENTS

Words cannot adequately express the appreciation and respect I have for Professor Baird and Dr. Holowka. Before joining graduate school, and during my rotations, I was torn about what type of research group I should join. Did I want to join a large group and be mentored by postdoctoral fellows? Did I want to join a small lab with daily interactions with my advisor? Upon beginning my rotation I quickly realized that the Baird-Holowka research group was a perfect fit for my research interests and for my personality. Most importantly I recognized that Barbara and Dave had created an amazing environment where graduate students were given not only the freedom, but the responsibility, to learn and make mistakes, all while constantly being pushed and encouraged to be become better scientists.

I will always be grateful to Barbara for asking tough questions. Especially for her constant emphasis on connecting the fine details of each experiment with the bigger picture of why we are trying to answer, and understand, these complex biological questions and processes in the first place. These conversations came up again and again, whenever we discussed the mutant C1 cells, and more recently as we tried to interpret our alpha-synuclein studies in RBL-2H3 cells. Thank you Barbara for your patience, encouragement, and for constantly setting a high standard that you expected me to reach.

My gratitude for, and relationship with Dave, can be summed up by a short conversation I had with a senior graduate student, from another lab, when I was a first year PhD student. This student had been struggling for months to optimize his experiments, with no success. He said that one day, while extremely frustrated, he looked out his lab window and saw me, walking with Dave, ice buckets in hand, to Weill Hall to do microscopy together. This student then said to me,

"What I wouldn't give to have an advisor who would help me like that!" Thank you Dave, for your constant mentorship, encouragement, and friendship.

I also need to acknowledge the mentorship of Drs Sondermann, Lin, and Casey who were instrumental in helping me write, submit, and fortunately be awarded, my NSF-GRFP fellowship. Dr. Sondermann specifically proofread and edited the science proposal part of the NSF-GRFP application. Without his edits, which helped my science proposal sound like actual science, I never would have been awarded the fellowship. Thank you Holger.

Before I even applied to Cornell I reached out to several professors inquiring about their research. Understandably, very few responded. However, on November 2, 2010, I received a friendly and informative response, from Dr. Richard Cerione telling me a little about his research, encouraging me to apply, and wishing me luck with my applications. I am grateful for the many Cdc42 constructs, in addition to the expertise and advice, Dr. Cerione has offered to help move the Cdc42 project forward. I also appreciate his willingness to allow me to be added to his research group's radiation permit, because without his help we never would have been able to quantitatively show that the B6A4C1 cells are deficient in antigen-stimulated PIP_2 synthesis.

Baird-Holowka group members, past and present, have had a significant impact on my research career. Dr. Kirsten Bryant, a former lab member and pharmacology PhD student, recruited me to the Baird-Holowka group, and then took the time to meticulously mentor me, for which I am grateful. Alice Wagenknecht-Wiesner has been a great friend and offered much advice, and most importantly, has constantly kept the treat jar full of high quality chocolate! Norah, Marek, Lily, Devin, Amit, Kate, Kari, Jordan, Eshan, and Arianna have created a fun environment that make people want to be in the lab doing experiments. Meraj Ramezani has been incredibly helpful with cloning, and in carrying out experiments for the alpha-synuclein

project. I also need to specifically thank Dr. Josh Wilson for creating many of the constructs, particularly VAMP8-pHluorin, that I used in almost all of my experiments. I also would like to thank Dr. Ruth Collins and Dr. Toshimitsu Kawate for allowing me to rotate in their labs, Dr. David Eliezer for assistance with the alpha-synuclein project, Dr. John Erickson for frequent advice, and Dr. Maurine Linder for accepting me as a student in the Field of Pharmacology.

Finally I would like to thank my wife Kendra, for moving 2000 miles away from your family to be with me in graduate school. Thank you for always being patient when I worked nights and weekends, and for always expecting me to better than I thought I could be. Thank you to my children Sophie, Duncan, and Ruby. I promise I will now play more games with you, and make you watch fewer movies.

TABLE OF CONTENTS

LIST OF FIGURES

LIST OF ABBREVIATIONS

a-syn	Alpha-synuclein
BIM	Bisindolylmaleimide I
BMMCs	Bone marrow-derived mast cells
BSS	Buffered saline solution
Ca^{2+}	Calcium ion
CBD	Crib-binding domain
Cdc42	Cell division control protein 42
Cdc42 T17N	Dominant negative form of Cdc42
Cdc42-G12V	Constitutively active form of Cdc42
Cdc42-G12V/QQ	Constitutively active Cdc42-G12V with the C-terminal di-arginine motif mutated to glutamines
CRAC	Ca^{2+} release-activated Ca^{2+} channel
DAG	Diacylglycerol
DHR	Dock Homology Region
DNP-BSA	2,4-Dinitrophenyl hapten conjugated to bovine serum albumin
DOCK	Dedicator of cytokinesesis
DU40	Geranylgeranyl transferase inhibitor
ER	Endoplasmic reticulum
FcεRI	High-affinity receptor for the Fc region of immunoglobulin E
FITC	Fluorescein isothiocyanate
GAP	GTPase-activating protein
GCaMP3	Genetically encoded Ca^{2+} indicator
GDP	Guanosine diphosphate
GEF	Guanine nucleotide exchange factor

GFP	Green Fluorescent Protein
GTP	Guanosine triphosphate
GTPase	Guanosine triphosphate hydrolase enzyme
GWAS	Genome Wide Association Study
IgE	Immunoglobulin E
IP_3	Inositol-trisphosphate
ITAMS	Immunoreceptor tyrosine-based activation motifs
MARCKS	Myristoylated alanine-rich protein kinase C substrate
Mg^{2+}	Magnesium ion
mRFP	Monomeric Red Fluorescent Protein
NAC	Non-amyloid B component
PD	Parkinson's Disease
PH	Plekstrin homology domain
PI3-kinase	Phosphatidylinositol 4,5-bisphosphate 3-kinase
PI4P	Phosphatidylinositol 4-phosphate
PIP_2	Phosphatidylinositol 4,5-bisphosphate
PIP_3	Phosphatidylinositol 3,4,5-triphosphate
PIP5K	Phosphatidylinositol-4-phosphate 5-kinase
PKC	Protein kinase C
PLC	Phospholipase C
RBL	Rat basophilic Leukemia
R.S.	Ca^{2+} release from stores
SN	Catalytically inactive DU40 geranylgeranyl transferase analog
SNARE	Soluble N-ethylmaleimide-sensitive factor attachment protein receptor

SNCA	Synuclein, Alpha (Non A4 Component of Amyloid Precursor)
SOCE	Store operated Ca^{2+} entry
STIM1	Stromal interaction molecule-1
VAMP	Vesicle-associated membrane protein
Wt	Wild type

Chapter 1: Introduction

Part 1: The Role of Antigen-Stimulated Ca^{2+} Signaling, Rho GTPase Activation, and PIP_2 Synthesis in Mast Cell Degranulation

1.1 Why Ca^{2+} is a Dynamic Regulator of Cellular Signaling

To adapt to frequently changing environments cells must internally send messages based on information received from external stimuli. This process of cellular communication is referred to as signaling, and to effectively signal, cells need messengers whose concentration can be variable over time. Over millions of years calcium ions (Ca^{2+}) evolved into one such messenger, in large part because of the evolution of cellular membranes, which maintain an approximate 20,000 fold gradient between the concentration of extracellular and intracellular Ca^{2+}. In contrast, the concentration of magnesium (Mg^{2+}), an ion closely related to Ca^{2+}, varies only slightly across the plasma membrane (Clapham 2007). Cells invest much of their energy to maintain this Ca^{2+} concentration gradient and even small changes in intracellular Ca^{2+} levels lead to a wide range of physiological processes, from the sub-second release of synaptic neurotransmitters, to the regulation of gene expression over months or years (Thul et al. 2008). As a result, it is well established that Ca^{2+} plays a crucial role in essential cellular events that include, but are not limited to, motility, fertilization, proliferation, and exocytosis.

Cells have evolved a variety of methods to regulate both Ca^{2+} influx and efflux. At physiological levels agonists stimulate increases in cytoplasmic Ca^{2+}, which is then followed by rapid or gradual expulsion of Ca^{2+} from cells because, despite being an essential component of cell signaling, a sustained increase in cytoplasmic Ca^{2+} also has the capacity to trigger apoptosis and necrosis (Thul et al. 2008). To avoid initiating cell death, non-excitable cells often undergo Ca^{2+} oscillations, a well-studied, yet poorly understood phenomenon where external stimulants

lead to rapid Ca^{2+} influx into the cytoplasm, followed by rapid Ca^{2+} efflux from the cytoplasm out of the cell, or into the endoplasmic reticulum (ER) or into mitochondria. Despite being stimulated by an agonist only once, the cell then repeats this Ca^{2+} mobilizing process in an oscillatory manner, sometimes for seconds, sometimes for minutes, and sometimes for hours.

Figure 1.1 depicts many of the receptors, pumps, and second messengers that cells have evolved to regulate the flow of Ca^{2+} between the extracellular space, cytoplasm, mitochondria, and the ER, which is known to be a large storage site for intracellular Ca^{2+}, capable of storing up to mM concentrations (Bygrave and Benedetti 1996). Figure 1.1 also depicts one of the most common ways that Ca^{2+} signaling is initiated. Receptor simulation leads to a phosphorylation cascade that activates the protein phospholipase C (PLC), which then cleaves the phosphoinositide phosphatidylinositol 4,5-bisphosphate (PIP_2) at the plasma membrane, producing the second messenger inositol-trisphosphate (IP_3). IP_3 then activates its receptor located on the ER, which results in release of Ca^{2+} into the cytoplasm. This initial release of Ca^{2+} from the ER is known to generate the initial Ca^{2+} oscillation in the cytoplasm (Prince WT 1973; Woods, Cuthbertson, and Cobbold 1986), although there is still much controversy over the exact processes that enable Ca^{2+} oscillations to continue. Ca^{2+} oscillations play a critical role in many non-excitable cell types and this thesis will explore the mechanisms that govern Ca^{2+} oscillations as they pertain to the activation and subsequent signaling of mast cells. Specifically, it will address how the regenerative discharge of stored intracellular Ca^{2+} (Dupont et al. 2011) from the ER drives stimulated mast cell exocytosis and leads to an allergic response.

1.2 Ca^{2+} in Mast Cell Signaling and Degranulation.

Mast cells are a type of white blood cell originally described in the late 1800's in a doctoral

Figure 1.1. **Receptors, pumps, and channels important for maintaining Ca^{2+} gradients**.

From: Clapham, 2007.

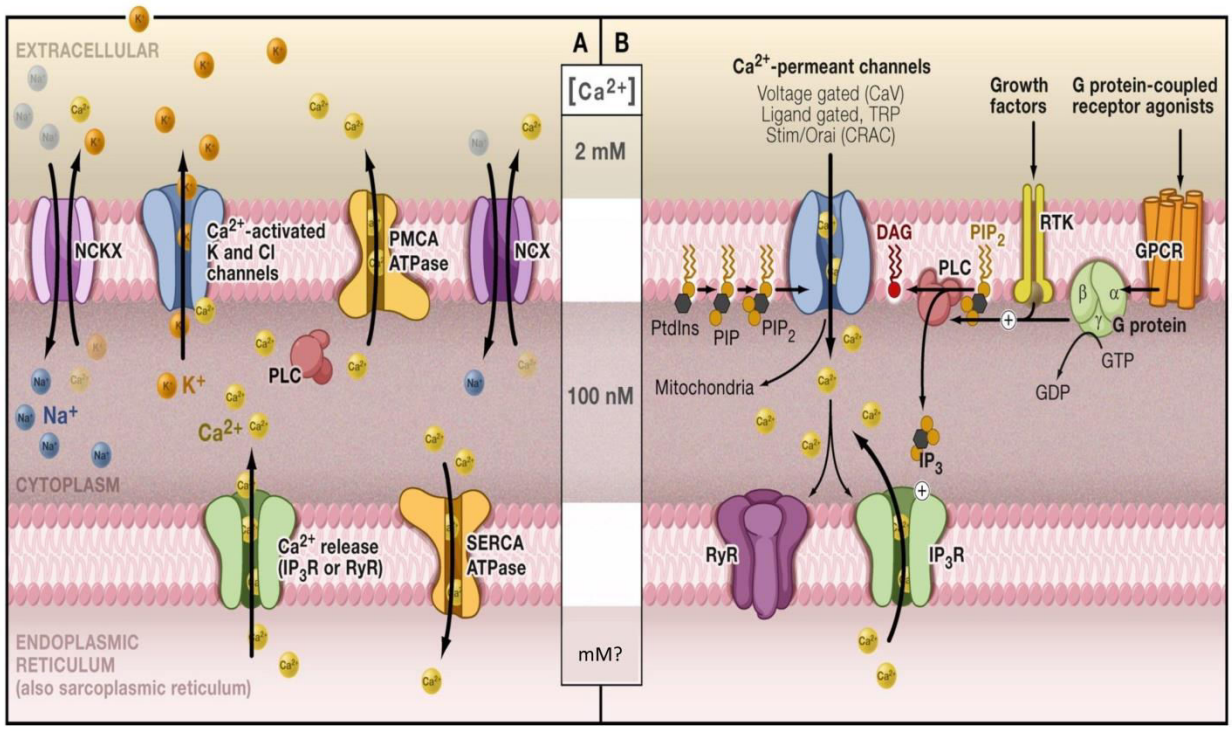

thesis written by future Nobel Laureate Paul Ehrlich. Identified for their unique staining characteristics and large granules, Dr. Ehrlich named these cells *Mastzellen*, incorporating the German word *Mast,* meaning fattening, because he incorrectly believed these cells function was to nourish surrounding tissues. This observation, although misinterpreted, was correct in part because, unlike some white blood cell types that circulate in the blood, such as basophils, mast cells typically remain closely affiliated with mucosal and connective tissues (Beaven 2009). Over 70 years later, in the mid-1900's, a correct biological function was discovered for mast cells when it was recognized that their granules were repositories for the chemical mediator histamine, the secretion of which leads to allergic inflammatory responses. Shortly thereafter, mast cells became one of the first experimental cellular models for studying Ca^{2+} signaling, as influx of extracellular Ca^{2+} was revealed to be essential for histamine secretion and the allergic response that followed (Beaven 2009).

In addition to allergic responses, mast cells also play critical roles in innate and adaptive immune responses to infections, inflammatory autoimmune diseases, and incipient tumors (Abraham and St John 2010; Galli, Maurer, and Lantz 1999; Metz, Siebenhaar, and Maurer 2008). Mast cells assist in these responses in part by undergoing a signaling process known as degranulation, which is the release of histamine and other preformed chemical mediators such as serine proteases and proteoglycans. These mediators are released in response to antigen binding and crosslinking of immunoglobulin E (IgE) bound to the unique FcεRI receptor highly expressed on the mast cell surface. Crosslinking of IgE-FcεRI complexes leads to their association with detergent resistant plasma membrane domains, more commonly referred to as lipid rafts (Field et al., 1995). Crosslinking leads to the phosphorylation of immunoreceptor

tyrosine-based activation motifs (ITAMs) on FcεRI receptors by the Src family kinase Lyn and ultimately leads to the activation of phospholipase Cγ (PLCγ) (Gilfillan and Rivera 2009). Phosphorylation of these ITAMs only occurs after IgE-FcεRI complexes have become associated with lipid rafts and their components (Kenneth A. Field, Holowka, and Baird 1997; K A Field, Holowka, and Baird 1999).

When PLC is activated, it cleaves PIP_2 localized at the inner leaflet of the plasma membrane and produces diacylglycerol (DAG), which remains membrane-associated, and IP_3 which binds to its receptors on the ER and induces depletion of Ca^{2+} from ER stores. This depletion of Ca^{2+} from the ER activates influx of extracellular Ca^{2+}, a process now commonly referred to as store operated Ca^{2+} entry (SOCE). The increase and sustained elevation of Ca^{2+} levels within the cytoplasm that result from SOCE are essential for mast cell activation and degranulation.

Within the last 10 years it has been demonstrated that the underlying mechanism for SOCE is the interaction between the ER Ca^{2+} sensor, stromal interaction molecule-1 (STIM1) and a pore-forming subunit of the Ca^{2+} release-activated Ca^{2+} (CRAC) channel, Orai1, which is located at the plasma membrane (Soboloff et al. 2006). Depletion of Ca^{2+} from the ER leads to the oligomerization of STIM1, which then interacts with Orai1, allowing influx of extracellular Ca^{2+}. This influx of Ca^{2+} then leads to granules fusing with the plamsa membrane, and exocytosis, resulting in histamine secretion. This Ca^{2+} influx via stimulated STIM1-Orai1 coupling is also necessary to refill intraceullular Ca^{2+} stores such as the ER. This refilling is critical for sustained Ca^{2+} oscillations to occur. If SOCE is blocked, or if extracellular Ca^{2+} is

Figure 1.2. **Antigen-mediated Ca^{2+} signaling and degranulation pathways in mast cells**.

From: Holowka et al., 2015.

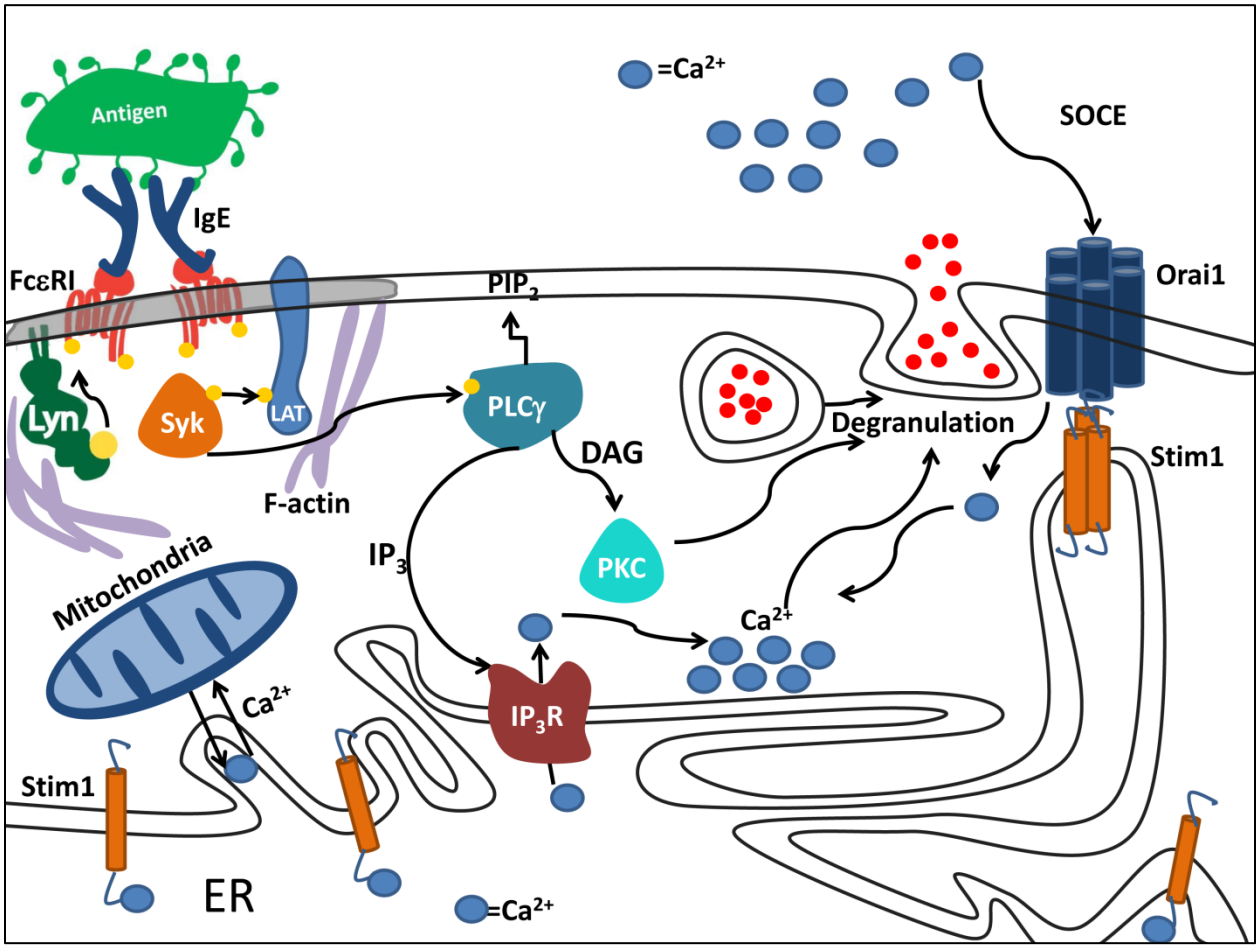

removed from the cellular environment, preventing refilling of stores, initial Ca^{2+} oscillations will still be triggered, although they will prematurely stop, and exocytosis of histamine containing granules will not occur. The mast cell degranulation process, as currently understood, is depicted in Figure 1.2. Although well-studied, there are still many unanswered questions as to how certain steps in this signaling cascade are controlled, and many questions specifically revolve around the fundamental regulation of Ca^{2+} mobilization, signaling, and oscillations. Chapter 2 of this thesis addresses some of these important questions.

To further investigate stimulated Ca^{2+} signaling and degranulation responses in mast cells, scientists have taken advantage of a model mammalian cell line known as Rat Basophilic Leukemia-2H3 (RBL-2H3) cells. Basophils are white blood cells that are similar in both appearance and function to mast cells, despite developing from different hematopoietic lineages. The original designation of RBL cells as basophils is a mis-identification of these mucosal-type mast cells (Seldin et al. 1985). RBL-2H3 cells express the FcεRI receptor which is activated by crosslinking, making this mammalian cell line a valuable tool for investigating the biochemical pathways necessary for mast cell activation. Even scientific studies that claim RBL-2H3 cells are an imprecise model for many mast cell responses (Passante et al. 2009) conclude that RBL-2H3 cells are an accurate and reliable model for mast cell degranulation, which is the primary biological function evaluated in this thesis.

1.3 Rho GTPases and Mast Cell Degranulation

Using RBL-2H3 cells as a model system, the Baird-Holowka Research Group has made several contributions to our understanding of mast cell signaling. One particular discovery recognized proteins known as Rho GTPases as playing an important role in stimulated Ca^{2+}

signaling and degranulation. Rho GTPases are a family of small signaling G proteins that are homologous to the α-subunit of large heterotrimeric G proteins. The most highly conserved members of this family, RhoA, Rac, and Cdc42, are frequently referred to as molecular switches due to their capacity to shift between active GTP-bound and inactive GDP-bound forms. Rho GTPases are activated by guanine nucleotide exchange factors (GEFs), and inactivated by GTPase-activating proteins (GAPs). When bound to GTP, Rho GTPases interact with many downstream effector proteins, stimulating a variety of processes such as microtubule dynamics, changes in gene transcription, chemotaxis, axonal guidance, cell cycle progression, cell adhesion, and oncogenic transformation ((Jaffe and Hall 2005; Heasman and Ridley 2008). Historically, it is through their regulation of actin cytoskeletal dynamics that Rho GTPases are thought to play a central role in many of these diverse biological processes.

Rho GTPases have conserved functions across many eukaryotic species and were first implicated in mast cell signaling over 20 years ago (Norman et al. 1994; Price et al. 1995). However, despite many studies and contributions from several different research groups, the mechanism by which Rho GTPases regulate mast cell signaling has yet to be elucidated. Previous research demonstrated that antigen stimulation results in activation of Cdc42 and Rac1 (El-Sibai and Backer 2007), and that expression of constitutively active Cdc42 and Rac1 in RBL-2H3 cells enhances antigen-stimulated Ca^{2+} responses and degranulation (Elizabeth Hong-Geller and Cerione 2000). Subsequent research demonstrated that expression of these same constitutively active Cdc42 and Rac1 mutants in a mutant RBL-2H3 cell line, referred to as B6A4C1, deficient in antigen stimulated Ca^{2+} responses and degranulation, reconstituted both Ca^{2+} mobilization and degranulation (E Hong-Geller et al. 2001). However, despite *in vitro*

results demonstrating that Rho GTPases could interact with and enhance activation of PLCγ, potentially explaining the mechanism by which Rho GTPases enhance Ca^{2+} and therefore degranulation responses, this finding was never observed in stimulated RBL-2H3 cells. More recent studies, described in Chapter 2 of this thesis, also demonstrate that constitutively active Cdc42 enhances antigen-mediated Ca^{2+} mobilization in B6A4C1 cells. However, new insights from this study indicate that Cdc42 may regulate Ca^{2+} signaling indirectly, by stimulating synthesis of PIP_2, whose hydrolysis is essential for Ca^{2+} mobilization.

1.4 Phosphoinositides and Ca^{2+} Signaling

Beginning with their discovery in the 1970's, phosphoinositides have come to be recognized as powerful pleiotropic regulators of cell signaling, despite making up only a small portion of cellular phospholipids. Over the last 15 years it has been recognized that in eukaryotes, not only do phosphoinositides play a fundamental role in transducing signals received from cell receptors, but they also play critical roles in shaping cellular membranes, controlling vesicular trafficking, and regulating events such as exocytosis and endocytosis (Balla 2013).

Phosphoinositides are phosphorylated forms of phosphatidylinositol, and Figure 1.3 shows the important shape of these molecules that enables their phosphorylation at positions 3, 4, and 5 of the inositol ring. Figure 1.3 also depicts many of the kinases and phosphatases known to regulate the different phosphoinositide species, all of which have unique, yet important cellular functions.

The phosphoinositide PIP_2 plays a fundamental role in Ca^{2+} signaling. PIP_2 hydrolysis following PLC activation is an essential Ca^{2+} signaling step in non-excitable cells (Figure 1.1)

Figure 1.3. **Phosphoinositide basics**. *A*: Agranoff's turtle demonstrating the orientation of the hydroxyl groups in *myo*-inositol. *B*: interconversions between various phosphoinositides and the enzymes catalyzing these reactions. The yeast enzymes are listed in parentheses. Where there is some ambiguity it is indicated by "??". *It is worth pointing out that contrary to their designation, PIP5K2s are 4-kinases that act on PtdIns5P. From: Balla, 2013.

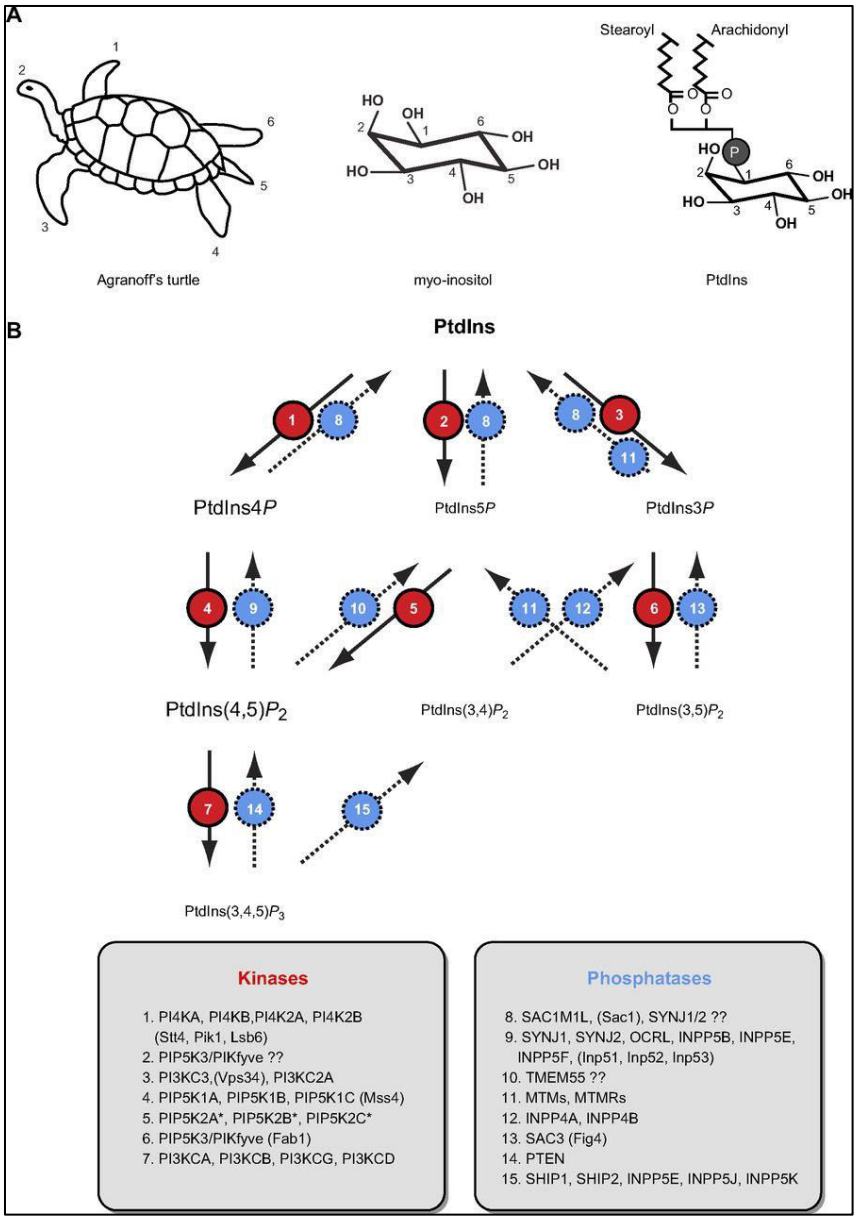

such as mast cells (Figure 1.2), and it can also play an important role in Ca^{2+} signaling in excitable neuronal cells. PIP_2 makes up only a small fraction of the total phosphoinositide found in cells and so its necessary, and frequent, hydrolysis suggests that a mechanism must exist to constantly replenish a pool of PIP_2 at the plasma membrane. In addition, the hydrolysis and cleavage of PIP_2 directly results in the production of IP_3, whose binding to its receptor at the ER initiates Ca^{2+} mobilization and Ca^{2+} oscillations. Thus, not only must PIP_2 be replenished, but it must be replenished rapidly in order for Ca^{2+} oscillations to occur over the time course of several minutes, often with durations of several hours.

A previous study suggests that the entire pool of PIP_2 at the plasma membrane is depleted and replenished several times over a ten minute stimulation (Creba et al. 1983). A mechanism must exist to control the constant replenishment of a pool of PIP_2 at the plasma membrane for as long as PLC remains activated and functional. Based on previous literature and our recent results, we now hypothesize that the Rho GTPase Cdc42, and potentially Rac1 and RhoA, regulates mast cell Ca^{2+} mobilization and degranulation, at least in part, through facilitation of antigen-stimulated PIP_2 synthesis. We begin to evaluate this hypothesis at the end of Chapter 2 and revisit it more fully in Chapter 3 as we aim to uncover the specific mechanism by which Rho GTPases regulate receptor-stimulated PIP_2 synthesis.

1.5 Rho GTPases and PIP_2 Synthesis

The first evidence implicating Rho GTPases in PIP_2 synthesis was published in 1994 when it was shown that the inhibitor lovastatin, which inhibits modification of small-GTPase binding proteins like Rho GTPases, decreased PIP_2 levels in Swiss 3T3 and the C3H 10 ½ cell lines (Chong et al. 1994). This manuscript also described how reduced PIP_2 levels leads to

decreased stimulated Ca^{2+} mobilization in these cell lines. A later study demonstrated that overexpression of RhoA, Rac1, and Cdc42 in human embryonic kidney 293 cells also increases PIP_2 levels (Weernink et al. 2004). This study also shows that overexpression of RhoA, Rac1, and Cdc42 increases expression of three type 1 phosphatidylinositol 4-phosphate 5-kinases (PIP5-kinase), which stimulate the production of PIP_2 from its precursor phosphatidylinositol 4-phosphate (PI4P). However this study shows that although RhoA and Rac1 increase type 1 PIP5-kinase levels, and therefore PIP_2 levels, through a direct interaction, Cdc42 does not appear to directly bind to these PIP5-kinases, despite its overexpression also leading to increased PIP5-kinase and PIP_2 levels.

Although these findings strongly implicate a role for Rho GTPases in regulation of PIP_2 synthesis, both studies only quantify PIP_2 levels following overexpression of Rho GTPases in cells, and not by looking at PIP_2 levels following receptor stimulation. As we are particularly interested in how PIP_2 is rapidly re-synthesized following receptor stimulation, PIP_2 hydrolysis, and onset of Ca^{2+} oscillations, we searched the literature to determine a potential mechanism by which Cdc42 regulates PIP_2 synthesis, and also searched for potential methods that we might employ to evaluate receptor-stimulated PIP_2 synthesis in RBL-2H3 cells.

1.6 Potential Mechanisms for Rho GTPase Regulation of PIP_2 Synthesis

A 1995 manuscript from a previous Baird-Holowka lab collaborator quantified receptor-stimulated PIP_2 synthesis using RBL-2H3 cells as a model system. The author of this study, Dr. John Apgar, discovered that antigen-stimulation of crosslinked IgE-receptor complexes resulted in increased PIP_2 synthesis that could be quantified for several minutes following biosynthetic labeling with PIP_2 precursors and mast cell stimulation. This study also demonstrated that direct

activation of protein kinase C (PKC) by a phorbol ester resulted in PIP_2 synthesis in mast cells (Apgar 1995).

PKC has long been known to be involved in mast cell signaling, although its function was not clearly understood. A recent study from our lab demonstrated that, in RBL-2H3 cells, the protein known as myristoylated alanine-rich protein kinase C substrate (MARCKS) binds to negatively charged phospholipids at the inner leaflet of the plasma membrane, particularly PI4P and PIP_2 (Gadi et al. 2011). Following antigen stimulation and PIP_2 hydrolysis, the second messenger DAG is produced and assists in the activation of PKC, which phosphorylates three essential serine residues on MARCKS, causing the protein to disassociate from the phosphoinositides it sequesters. This then allows for the previously sequestered PIP_2 to be available to participate in exocytosis, which is known to be a PIP_2 dependent process (Kabachinski et al. 2014). This process also makes available PI4P, the precursor for PIP_2, making this a potential point for the recruitment of PIP5-kinases and replenishment of PIP_2 at the plasma membrane. It is summarized in Figure 1.4, which depicts mast cell signaling immediately following PLC activation. Previous studies have identified some PKC isoforms as Cdc42 effector proteins (Cook et al. 2006; Coghlan, Chou, and Carpenter 2000), suggesting a possible mechanism by which Cdc42 could activate these isoforms. Another study in RBL-2H3 cells demonstrated that the PKC inhibitor bisindolylmaleimide I (BIM) does not inhibit Cdc42 activation (El-Sibai and Backer 2007), suggesting that Cdc42 is activated and acts upstream of PKC activation. Based on these findings and the research of Gadi et al. (Gadi et al. 2011) and Apgar (Apgar 1995), we hypothesized that Cdc42 regulates PKC activation, and it is through

Figure 1.4. **Role of PKC in regulating PIP_2 availability and, possibly, PIP_2 synthesis.**

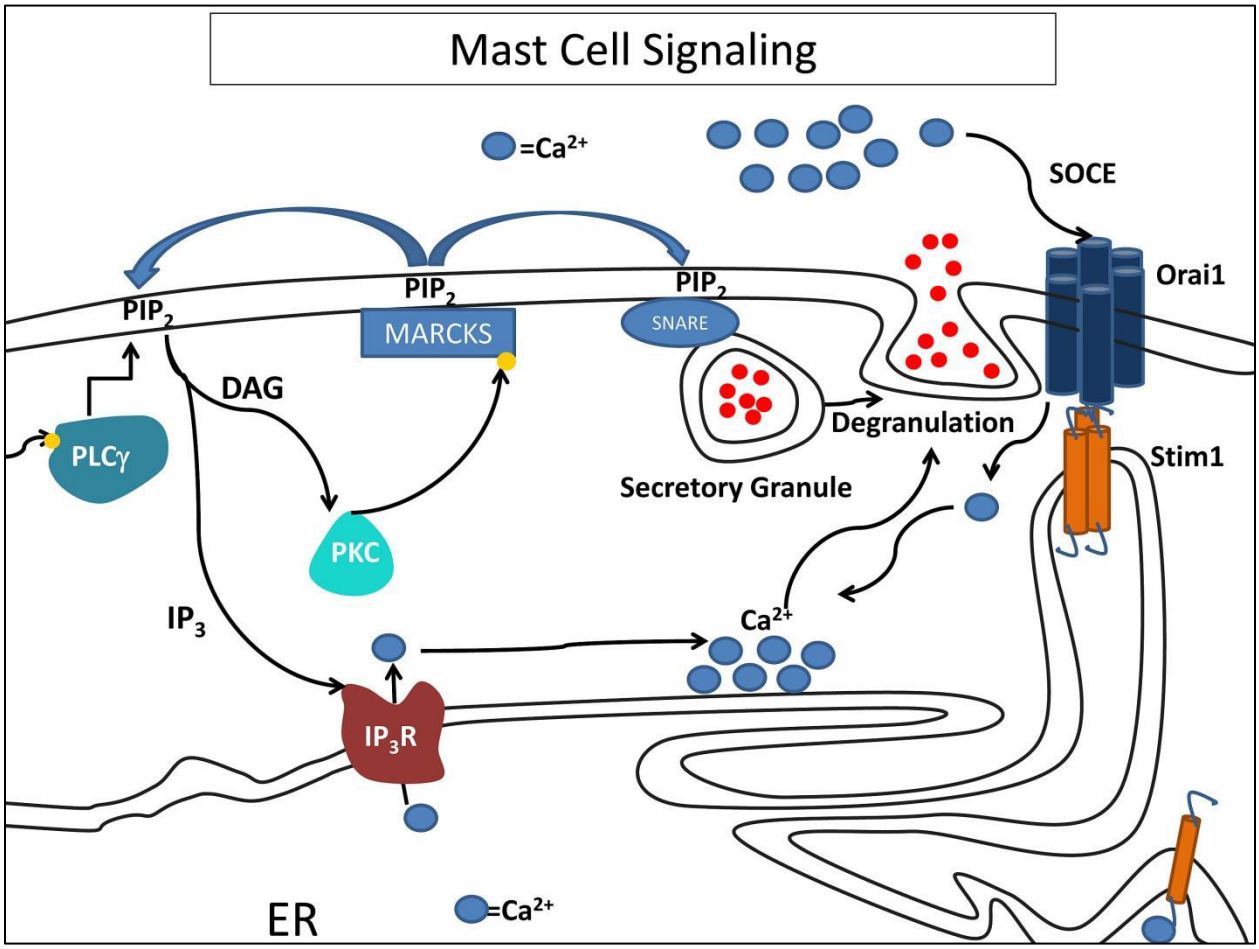

this indirect mechanism that Cdc42 regulates receptor-stimulated PIP_2 synthesis. Our findings exploring this hypothesis are described in Chapter 3.

Two other studies recently observed that, following antigen stimulation in RBL-2H3 cells, not only did Ca^{2+} levels oscillate, but many proteins known to be important for mast cell signaling events oscillate as well (Wollman and Meyer 2012; Wu, Wu, and De Camilli 2013). These studies discovered that by expressing the fluorescent construct PH-PLCδ-EGFP in RBL-2H3 cells, PIP_2 levels at the plasma membrane could be monitored in real time to oscillate synchronously but out of phase with Ca^{2+} oscillations in the cytoplasm. Using a method similar to those described in these manuscripts, we show in Chapter 2 that B6A4C1 cells, which are deficient in antigen stimulated Cdc42 and Rac1 activation, are also deficient in antigen-stimulated PIP_2 oscillations. However, PIP_2 oscillations are reconstituted when constitutively active Cdc42 is expressed in B6A4C1 cells. We continue to use this method in Chapter 3 as we further investigate the mechanism by which Cdc42 regulates PIP_2 synthesis in a receptor stimulation-dependent manner. Although through PKC, or a direct interaction with PIP5-kinases are two possible mechanisms by which Cdc42 regulates PIP_2 synthesis following receptor stimulation, a third intriguing group of Cdc42 effectors that could be relevant to these processes are PI3-kinases.

1.7 Rho GTPases and PI3-Kinases

Over 20 years ago it was first demonstrated that Cdc42 could directly bind to PI3-kinases (Tolias, Cantley, and Carpenter 1995). It was later shown that PI3-kinases plays an important, yet not well-understood, role in antigen-stimulated Ca^{2+} responses in mast cells (Ching et al. 2001). In 2013 it was again confirmed that Cdc42 can bind directly to PI3-kinase isoforms, and

that this interaction is mediated by a GEF protein that belongs to the atypical DOCK GEF family. However, Dbl GEF family members, the canonical Rho GTPase activating GEF family, did not mediate a Cdc42-PI3-kinase interaction (Fritsch et al. 2013). This finding is particularly interesting because in Chapter 2 of this thesis we show that an atypical DOCK GEF family member, DOCK7, capable of activating both Cdc42 and Rac, reconstitutes Ca^{2+} oscillations in B6A4C1 cells to normal RBL-2H3 levels. However, a member of the more canonical Dbl GEF family, the protein Cool2, showed no reconstitution effects (Wilkes et al. 2014). Based on these results we compared the effect of the known PI3-kinase inhibitor wortmannin for mast cell signaling (Yano et al. 1993), to a geranylgeranyl transferase inhibitor, DU40, that inhibits Rho-GTPase anchoring to the plasma membrane, a step needed for Rho GTPase activation and function (Peterson et al. 2006). Our findings and interpretations of this data are described in Chapter 3. Although PIP_2 is the substrate for PI3-kinase, there are known phosphatases which convert phosphatidylinositol 3,4,5-triphosphate (PIP3) back to PIP_2, shown in Figure 1.3, and it is potentially through regulating this type of process that Cdc42 could affect total PIP_2 levels (Balla 2013).

In chapter 3 we also begin to further investigate whether DOCK7, or another DOCK family member, is mutated or deficient in B6A4C1 cells, and whether this defect leads to inhibition of degranulation. As both constitutively active Cdc42 and Rac1 reconstitute Ca^{2+} mobilization and degranulation in B6A4C1 cells, we suspect that a GEF defective in activating both of these Rho GTPases is responsible for loss of signaling. Other members of the DOCK GEF family are also capable of activating both Cdc42 and Rac1, and we begin to compare one of these GEFs, DOCK8, with DOCK7 in Chapter 3 as we attempt to further elucidate a mechanism

by which Cdc42 regulates PIP_2 synthesis. An alternative hypothesis to a defective GEF in B6A4C1 cells is that an overactive GAP immediately switches off activated Cdc42 and Rac1 following antigen stimulation before they can interact with necessary effectors. However, data in Chapter 3 shows that, following antigen stimulation, Cdc42 does not appear to be become activated in the mutant B6A4C1 cells, leading us to further believe that the defect in B6A4C1 cells is with a specific GEF.

1.8 Part 1 Conclusion

Antigen-stimulated activation of Rho GTPases is a critical step for mast cell signaling and degranulation. Although Rho GTPases are implicated in many cellular events, their capacity to regulate PIP_2 synthesis is often overlooked, despite this being an evolutionarily conserved function (Cotteret and Chernoff 2002). This key function of Rho GTPases is overlooked partially because receptor-stimulated PIP_2 synthesis is technically difficult to study, and partially because a clear mechanism by which Rho GTPases activate PIP_2 synthesis has yet to be established. Even regulation of the actin cytoskeleton, one of the most well-known functions attributed to Rho GTPases, may be regulated in part because Rho GTPases have the capacity to regulate phosphoinositide levels (Tolias, Cantley, and Carpenter 1995). This thesis describes our key findings exploring the connection between antigen-stimulated Rho GTPase activation, Ca^{2+} oscillations, and PIP_2 synthesis, and it begins to make clear the important connection between receptor-stimulated Rho GTPase activation and PIP_2 synthesis, an event that most likely plays an essential signaling role in many different cell types.

Part 2: RBL-2H3 Cells as a Model Mammalian System for Investigating a Physiological Function for Alpha-Synuclein

1.9 Model Systems in Biological Research

As described in Part I of this introduction, RBL-2H3 cells are most commonly used as a model system for studying mast cell activation and signaling. RBL-2H3 cells are mucosal-type mast cells (Seldin et al. 1985), and their characteristics offer many advantages as a model system over other mast cell subtypes, such as bone marrow-derived mast cells (BMMCs), that are closer in subtype to serosal mast cells. These advantages include RBL-2H3 cells being an adherent cell line, and more stable in biological tissue culture, making them easier for *in vitro* experimentation. BMMCs, on the other hand, lack adherence, which causes additional technical difficulties for biological research, and have more variable expression of the FceRI receptor. RBL-2H3 cells also have a measurable IgE-mediated degranulation response, making them an ideal model system for studying mast cell degranulation.

The principle of using models to simplify and understand complex problems is common throughout many academic disciplines. In biology, model cell lines, and more broadly model organisms, are an essential part of research because they allow scientists to simplify complex organisms, and their complex cellular processes, into more basic and fundamental components. Many of these biological processes are essential for life and therefore are highly conserved from the simplest to the most complex eukaryotic organism (Tugendreich et al. 1994). Fundamental principles learned from simple models are often directly applicable to more complex systems. In biology the majority of what we know and understand about cellular processes was discovered because of basic research using model organisms such as yeast, flies, worms, fish, and mice. Three benefits of using model organisms for research are, first, these organisms are typically less

expensive than complex organisms. Second, model systems are more ethically justifiable, and thirdly, model organisms often grow and develop faster than complex organisms, especially when compared to humans. This is a huge advantage when it comes to studying diseases which often take many years to develop in humans, but may only take weeks or months to develop in a model organism.

1.10 Model Organisms and Cell Lines in Disease-Oriented Research

Studying complex diseases is both difficult, and sometimes unethical, in human patients. Model systems are frequently used to try to simplify the disease process, to hasten the onset of disease, and to identify key proteins or genes that are essential for disease progression. However, because of technological advancements that now enable the sequencing of entire genomes, the manner by which scientists and doctors identify and recognize disease-related genes is changing (Gonzaga-Jauregui, Lupski, and Gibbs 2012). In response to new technological advancements, and because of the known short comings of model cell lines and model organisms, some have speculated that simplified model systems may become irrelevant in the near future (Hunter 2008). However, most in the scientific community recognize that new technological advances, coupled with intelligent use of model organisms, will strengthen and improve disease-focused biological research (Aitman et al. 2008; Aitman et al. 2011).

Model organisms have become even more relevant in disease-related research with the advancement of genetic techniques that allow scientists to knockdown, or completely knockout, specific genes within animal models. Specific phenotypes are now more easily attributed to one specific gene of interest, offering new insight into the physiological roles of many previously poorly understood proteins. However, despite the many advances that have come from the

development of Cre-Lox knockout mice (Sauer 1998), and more recently CRISPR-Cas9-mediated genome editing (O'Connell et al. 2014), model systems, no matter the disease of interest, have limitations (Hunter 2008; Kamb and Kamb 2005; Crawley 2007).

Model systems have proven particularly difficult to develop for neurodegenerative diseases, in part because an animal such as a mouse, with a lifespan of approximately only two years, is not an ideal candidate for recreating disease phenotypes that typically take five to six decades to manifest in humans. An alternative to using model organisms that is commonly used with all disease-related research is the use of cellular models which allow studies to be conducted more quickly and with less complex variables (Dawson, Ko, and Dawson 2010). Use of a cellular model can be particularly insightful when knockout or knockdown animal models are inconclusive in their findings. This was the case initially for many knockout mice created for the purpose of studying Alzheimer's and Parkinson's disease (PD) because genetically modified mice failed to develop clear phenotypes that mimicked disease states and behaviors observed in humans (Harvey, Wang, and Hoffer 2008; Taymans and Cookson 2010; Ke et al. 2012). However, researchers have learned from earlier mistakes and many animal models for neurodegenerative diseases now exist (Lim and Ng 2009; Bilkei-Gorzo 2014). Unfortunately, much of the data gleaned from neurodegenerative animal models has been difficult to interpret. Hence, scientists are frequently returning to cellular based systems in an attempt to improve understanding of the basic mechanisms that lead to onset of neurodegenerative diseases. One such cellular based strategy has recently proven insightful in Alzheimer's research (Choi et al. 2014) and these authors suggest that researchers consider using novel cellular based approaches for other neurodegenerative diseases. Chapter 4 of this thesis details a unique cell-based

approach taken by the Baird-Holowka lab using RBL-2H3 cells as a non-traditional model system to investigate the physiological role of a protein known as alpha-synuclein (a-syn), which has long been implicated in onset and progression of PD.

1.11 Alpha-synuclein in Parkinson's Disease

A-syn is a small, 140 amino acid protein (Figure 1.5) with an unknown function found predominantly in neurons, although its expression has also been detected in red blood cells and other tissues (Barbour et al. 2008). It is expressed in the nucleus and in the cytosol, making up approximately 1% of all cytosolic proteins in neurons (Iwai et al. 1995). A-syn was named after it was found to localize to synaptic vesicles and on nuclear envelopes isolated from the Torpedo electric organ (Maroteaux, Campanelli, and Scheller 1988). Shortly thereafter, this protein was characterized in studies investigating Alzheimer's patients, and a-syn was identified as the non-amyloid component of β-amyloid plaques (Uéda et al. 1993). Since its discovery over 20 years ago, synuclein has been linked to a group of overlapping neurodegenerative disorders, known as alpha-synucleinopathies, which include PD, PD dementia, dementia with Lewy bodies, multiple system atrophy, as well as many other less extensively studied conditions (Kim, Kågedal, and Halliday 2014; Burré 2015). Pathological identification of β-amyloid plaques, or tau aggregates, is typically used to identify Alzheimer's disease. However, a-syn aggregates have also been found in the brains of ~50% of all Alzheimer's disease patients (Lippa et al. 1998; Arai et al. 2001; Marsh and Blurton-Jones 2012). Despite this, a-syn is most commonly associated with PD, as a-syn is the primary component of Lewy bodies, the pathological hallmark of PD, and synucleinopathies in general (Spillantini 1999; Irwin, Lee, and Trojanowski 2013; Norris, Giasson, and Lee 2004).

Figure 1.5. **Structural characteristics of a-syn.** From: Xu & Chan 2015. *Biomolecules*, 5(2), pp. 1122-1142

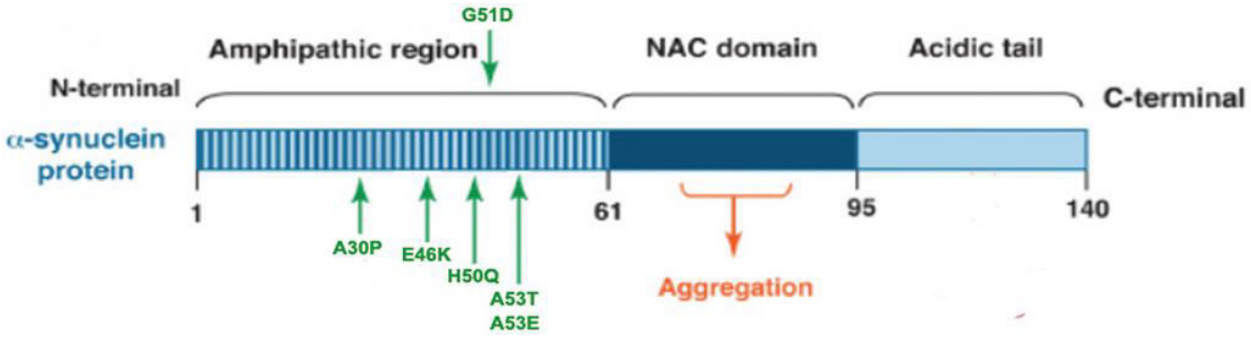

A-syn has also been intensely studied because, in some cases, onset of PD appears to be hereditary. A genetic link between a-syn and PD was first established in 1997, and several rare mutations, as well as duplications and triplications to the SNCA gene, which encodes for a-syn, have since been discovered. Families with these mutations are said to have autosomal dominant familial PD, which frequently leads to early disease onset (Polymeropoulos et al. 1997; Hope et al. 2004). Despite this genetic link, mutations to the SNCA gene are quite rare, accounting for less than 10% of all PD cases (Schulte and Gasser 2011). However, elevated levels of a-syn are observed in many patients who develop sporadic, not genetic, forms of PD, suggesting a critical role for this protein in either form of the disease (Chiba-Falek, Lopez, and Nussbaum 2006; Murphy et al. 2014).

1.12 The Physiological Role of A-syn

For over two decades, a-syn and its associated synucleinopathies have been intensively studied, yet the normal cellular function of this protein remains elusive. Alpha-synucleinopathies are typically toxic to cells, although it is not clear whether this toxicity results from a loss of normal a-syn function, or a toxic gain of function due to a-syn oligomerization and aggregation (Snead and Eliezer 2014). What is clear is that overexpression of a-syn is toxic in both humans and animal models, having a more severe effect than knockout or knockdown of a-syn (Masliah et al. 2000; Abeliovich et al. 2000; Cabin et al. 2002). Recent studies have recognized that two alternative isoforms of synuclein, beta and gamma, may compensate for a loss of a-syn function, and mice lacking all three synuclein isoforms show age-dependent neuronal dysfunction to a stronger extent than a-syn knockout alone (Greten-Harrison et al. 2010; Burré et al. 2010). These and other recent results suggest that, although synucleinopathies often exhibit toxic gain of

function effects, a-syn displacement from synapses due to aggregation and misfolding, may also result in a loss of function effect that is equally responsible for neuronal toxicity (Collier et al. 2016)

Part of the difficulty in studying a-syn function comes from its unique structure and intrinsically disordered state when free in solution (Weinreb et al. 1996; Eliezer et al. 2001; Mantsyzov et al. 2014). The a-syn protein can be divided into three distinct parts, as shown in Figure 1.5. Region 1 consists of N-terminal residues 1-60 that encode for a lipid binding domain that contains 7 imperfect 11-residue repeats each centered on a variation of a KTKEGV core consensus sequence (Snead and Eliezer 2014; Bussell, Ramlall, and Eliezer 2005). All known a-syn familial genetic mutations, A30P, E46K, H50Q, G51D, and A53T, are located within this N-terminal region. Despite being disordered in solution, this N-terminal domain adopts an amphipathic helical structure in the presence of membranes. The second distinct region of a-syn contains the N-terminal residues 61-95 which forms a hydrophobic domain referred to as the non-amyloid B component (NAC), and this region is essential for a-syn aggregation and oligomerization (Pfefferkorn, Jiang, and Lee 2012). The third distinct region of the protein is the final ~40 residues that constitute the acidic C-terminus that remains disordered even in the presence of membranes. In Chapter 4, we evaluate the essential roles that the N-and C-terminal regions play in regulating stimulated cellular responses, specifically investigating exocytosis and endocytosis.

1.13 A-syn and Synaptic Vesicle Trafficking

Although the physiological function of a-syn in neurons has yet to be established, several studies suggest it could play an important role in many cellular processes, as depicted in Figure

1.6. While many processes have been implicated, strong evidence suggests that a-syn plays a critical role in the regulation of synaptic vesicle trafficking and homeostasis, although it is not clear at which step in this process a-syn acts (docking, priming, fusion, exocytosis, endocytosis, etc.). One previous study demonstrated that overexpression of wild type a-syn (Wt a-syn), or A30P a-syn, inhibited stimulated dopamine release in PC-12 cells, a chromaffin cell line used to model neuronal dopamine release. This study also showed evidence that this inhibitory mechanism occurs downstream of Ca^{2+} mobilization, but before Ca^{2+}-dependent membrane fusion of vesicles, most likely interfering with a late exocytic step such as docking or priming (Larsen et al. 2006). Stimulated dopamine release is essential for movement in humans, and PD is classified primarily as a movement disorder. The neurons that are responsible for stimulated dopamine release and movement are located in the substantia nigra region of the brain, and in PD patients the majority of these neurons die, and the neurons that remain are unhealthy and filled with Lewy bodies.

When healthy and functioning, neurons release neurotransmitters at presynaptic terminals, often thousands of times per minute, and evidence points to this location as a prime target for initiation of neurodegeneration (Kramer and Schulz-Schaeffer 2007). Tightly coordinated membrane fusion machinery is necessary for frequent neurotransmitter exocytosis, and recent studies indicate that a-syn as a key regulator of this machinery. Soluble N-ethylmaleimide-sensitive factor attachment protein receptor (SNARE) proteins are essential for synaptic vesicle fusion, which is mediated by formation of a SNARE complex consisting of three proteins: syntaxin-1, SNAP-25, and synaptobrevin-2. Recent evidence suggests a-syn binds directly to synaptobrevin-2, acting as a chaperone for SNARE complex assembly (Burré et al. 2010),

Figure 1.6: **Potential physiological roles for a-syn.** From: Snead & Eliezer 2014.

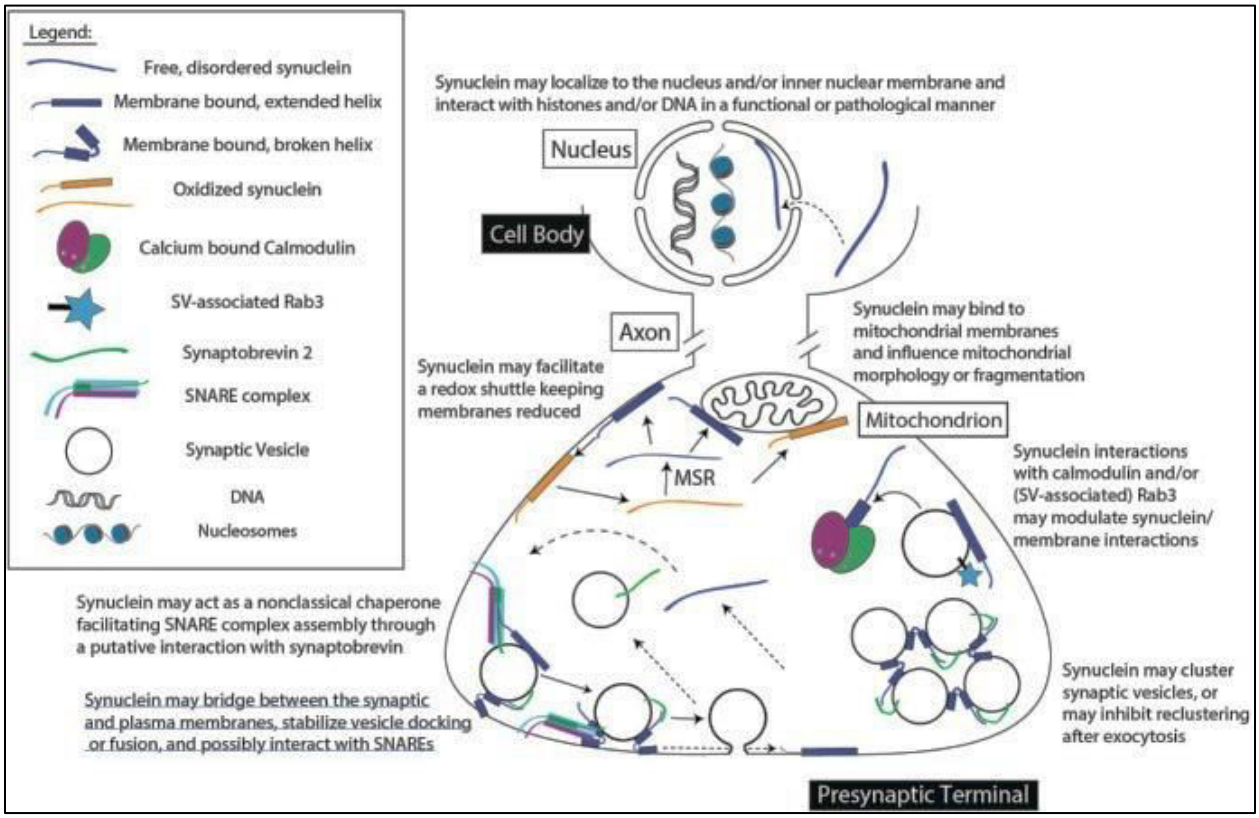

although other studies suggest a-syn does not directly bind synaptobrevin-2, but regulates SNARE complex assembly indirectly (Darios et al. 2010). Despite conflicting data, both of these studies point to a-syn regulating key synaptic vesicle exocytic events. Understanding mechanistically how, and if, a-syn regulates synaptic vesicle exocytosis physiologically, pathologically, or both, is necessary for understanding onset of PD, and potentially for developing more effective treatments and therapeutics against disease onset and progression.

1.14 Part 2 Conclusion

Despite progress made over the past ten years, understanding how a-syn regulates synaptic vesicle trafficking in neurons remains difficult. The rapid kinetics by which neurons undergo stimulated exocytosis and subsequent endocytosis makes studying, and distinguishing, between these two major cellular events difficult. Many studies recognize that overexpression of a-syn inhibits synaptic vesicle trafficking, but the majority focus on a-syn's effect on endocytosis (Busch et al. 2014; Vargas et al. 2014). In Chapter 4 we demonstrate that, by using RBL-2H3 cells as a non-conventional model system to study a complex, neurological process, we can monitor the effect of a-syn on stimulated exocytosis independently from endocytosis. This allows us to offer unique insights into questions that scientists have struggled to answer for decades (Bolker 2012). We demonstrate that a-syn regulates exocytosis and endocytosis inversely, in a concentration dependent manner, strengthening the proposal that PD-causing neuronal toxicity stems from a combination of both gain and loss of function events.

REFERENCES

Abeliovich, A, Y Schmitz, I Fariñas, D Choi-Lundberg, W H Ho, P E Castillo, N Shinsky, et al. 2000. "Mice Lacking Alpha-Synuclein Display Functional Deficits in the Nigrostriatal Dopamine System." *Neuron* 25 (1): 239–52. doi:10.1016/S0896-6273(00)80886-7.

Abraham, Soman N, and Ashley L St John. 2010. "Mast Cell-Orchestrated Immunity to Pathogens." *Nature Reviews. Immunology* 10 (6): 440–52. doi:10.1038/nri2782.

Aitman, Timothy J, Charles Boone, Gary a Churchill, Michael O Hengartner, Trudy F C Mackay, and Derek L Stemple. 2011. "The Future of Model Organisms in Human Disease Research." *Nature Reviews. Genetics* 12 (8): 575–82. doi:10.1038/nrg3047.

Aitman, Timothy J, John K Critser, Edwin Cuppen, Anna Dominiczak, Xose M Fernandez-Suarez, Jonathan Flint, Dominique Gauguier, et al. 2008. "Progress and Prospects in Rat Genetics: A Community View." *Nature Genetics* 40 (5): 516–22. doi:10.1038/ng.147.

Apgar, J R. 1995. "Activation of Protein Kinase C in Rat Basophilic Leukemia Cells Stimulates Increased Production of Phosphatidylinositol 4-Phosphate and Phosphatidylinositol 4,5-Bisphosphate: Correlation with Actin Polymerization." *Mol Biol Cell* 6 (1): 97–108. http://www.ncbi.nlm.nih.gov/pubmed/7749199\nhttp://www.ncbi.nlm.nih.gov/pmc/articles/PMC275817/pdf/mbc00021-0104.pdf.

Arai, Yasushi, Mineo Yamazaki, Osamu Mori, Hiromi Muramatsu, Goro Asano, and Yasuo Katayama. 2001. "Alpha-Synuclein-Positive Structures in Cases with Sporadic Alzheimer's Disease: Morphology and Its Relationship to Tau Aggregation." *Brain Research* 888 (2): 287–96. doi:10.1016/S0006-8993(00)03082-1.

Balla, T. 2013. "Phosphoinositides: Tiny Lipids with Giant Impact on Cell Regulation." *Physiological Reviews* 93 (3): 1019–1137. doi:10.1152/physrev.00028.2012.

Barbour, Robin, Kristin Kling, John P. Anderson, Kelly Banducci, Tracy Cole, Linnea Diep, Michael Fox, et al. 2008. "Red Blood Cells Are the Major Source of Alpha-Synuclein in Blood." *Neurodegenerative Diseases* 5 (2): 55–59. doi:10.1159/000112832.

Beaven, Michael A. 2009. "Our Perception of the Mast Cell from Paul Ehrlich to Now." *European Journal of Immunology*. doi:10.1002/eji.200838899.

Bilkei-Gorzo, Andras. 2014. "Genetic Mouse Models of Brain Ageing and Alzheimer's Disease." *Pharmacology and Therapeutics*. doi:10.1016/j.pharmthera.2013.12.009.

Bolker, Jessica. 2012. "Model Organisms: There's More to Life than Rats and Flies." *Nature*, 3–5. doi:10.1038/491031a.

Burré, Jacqueline. 2015. "The Synaptic Function of α-Synuclein." *Journal of Parkinson's Disease*. doi:10.3233/JPD-150642.

Burré, Jacqueline, Manu Sharma, Theodoros Tsetsenis, Vladimir Buchman, Mark R Etherton,

and Thomas C Südhof. 2010. “Alpha-Synuclein Promotes SNARE-Complex Assembly in Vivo and in Vitro.” *Science (New York, N.Y.)* 329 (5999): 1663–67. doi:10.1126/science.1195227.

Busch, David J, Paul A Oliphint, Rylie B Walsh, Susan M L Banks, Wendy S Woods, Julia M George, and Jennifer R Morgan. 2014. “Acute Increase of α-Synuclein Inhibits Synaptic Vesicle Recycling Evoked during Intense Stimulation.” *Molecular Biology of the Cell* 25 (24): 3926–41. doi:10.1091/mbc.E14-02-0708.

Bussell, Robert, Trudy Fiona Ramlall, and David Eliezer. 2005. “Helix Periodicity, Topology, and Dynamics of Membrane-Associated Alpha-Synuclein.” *Protein Science : A Publication of the Protein Society* 14 (4): 862–72. doi:10.1110/ps.041255905.

Bygrave, Fyfe L., and Angelo Benedetti. 1996. “What Is the Concentration of Calcium Ions in the Endoplasmic Reticulum?” *Cell Calcium* 19 (6): 547–51. doi:10.1016/S0143-4160(96)90064-0.

Cabin, Deborah E, Kazuhiro Shimazu, Diane Murphy, Nelson B Cole, Wolfram Gottschalk, Kellie L McIlwain, Bonnie Orrison, et al. 2002. “Synaptic Vesicle Depletion Correlates with Attenuated Synaptic Responses to Prolonged Repetitive Stimulation in Mice Lacking Alpha-Synuclein.” *The Journal of Neuroscience : The Official Journal of the Society for Neuroscience* 22 (20): 8797–8807. doi:22/20/8797 [pii].

Chiba-Falek, Ornit, Grisel J. Lopez, and Robert L. Nussbaum. 2006. “Levels of Alpha-Synuclein mRNA in Sporadic Parkinson Disease Patients.” *Movement Disorders* 21 (10): 1703–8. doi:10.1002/mds.21007.

Ching, Tsui Ting, Ao Lin Hsu, Amy J. Johnson, and Ching Shih Chen. 2001. “Phosphoinositide 3-Kinase Facilitates Antigen-Stimulated Ca2+ Influx in RBL-2H3 Mast Cells via a Phosphatidylinositol 3,4,5-Trisphosphate-Sensitive Ca2+ Entry Mechanism.” *Journal of Biological Chemistry* 276 (18): 14814–20. doi:10.1074/jbc.M009851200.

Choi, Se Hoon, Young Hye Kim, Matthias Hebisch, Christopher Sliwinski, Seungkyu Lee, Carla D’Avanzo, Hechao Chen, et al. 2014. “A Three-Dimensional Human Neural Cell Culture Model of Alzheimer’s Disease.” *Nature* 515 (7526): 274–78. doi:10.1038/nature13800.

Chong, L D, a Traynor-Kaplan, G M Bokoch, and M a Schwartz. 1994. “The Small GTP-Binding Protein Rho Regulates a Phosphatidylinositol 4-Phosphate 5-Kinase in Mammalian Cells.” *Cell* 79 (3): 507–13. doi:10.1016/0092-8674(94)90259-3.

Clapham, David E. 2007. “Calcium Signaling.” *Cell* 131 (6): 1047–58. doi:10.1016/j.cell.2007.11.028.

Coghlan, M P, M M Chou, and C L Carpenter. 2000. “Atypical Protein Kinases Clambda and -Zeta Associate with the GTP-Binding Protein Cdc42 and Mediate Stress Fiber Loss.” *Molecular and Cellular Biology* 20 (8): 2880–89. http://www.pubmedcentral.nih.gov/articlerender.fcgi?artid=85517&tool=pmcentrez&render

type=abstract.

Collier, Timothy J., D. Eugene Redmond, Kathy Steece-Collier, Jack W. Lipton, and Fredric P. Manfredsson. 2016. “Is Alpha-Synuclein Loss-of-Function a Contributor to Parkinsonian Pathology? Evidence from Non-Human Primates.” *Frontiers in Neuroscience* 10 (January): 1–7. doi:10.3389/fnins.2016.00012.

Cook, Anthony C, Cojen Ho, Jennifer L Kershner, Steve a Malinowski, Heath Moldveen, Brigid a Stagliano, and Simon J Slater. 2006. “Competitive Binding of Protein Kinase Calpha to Membranes and Rho GTPases.” *Biochemistry* 45 (48): 14452–65. doi:10.1021/bi0612420.

Cotteret, Sophie, and Jonathan Chernoff. 2002. “The Evolutionary History of Effectors Downstream of Cdc42 and Rac.” *Genome Biology* 3 (2): REVIEWS0002. doi:Artn 0002.1.

Crawley, J N. 2007. *What’s Wrong with My Mouse? Behavioural Brain Research*. Vol. 179. doi:10.1016/j.bbr.2007.01.023.

Creba, Judith A, C Peter Downes, Phillip T Hawkins, Glenn Brewster, Robert H Michell, and Christopher J Kirk. 1983. “Other Ca2 + -Mobilizing Hormones.” *Reactions* 212: 733–47.

Darios, Frédéric, Violeta Ruipérez, Inmaculada López, Jose Villanueva, Luis M Gutierrez, and Bazbek Davletov. 2010. “Alpha-Synuclein Sequesters Arachidonic Acid to Modulate SNARE-Mediated Exocytosis.” *EMBO Reports* 11 (7): 528–33. doi:10.1038/embor.2010.66.

Dawson, Ted M., Han Seok Ko, and Valina L. Dawson. 2010. “Genetic Animal Models of Parkinson’s Disease.” *Neuron*. doi:10.1016/j.neuron.2010.04.034.

Dupont, Genevie` ve, Laurent Combettes, Gary S. Bird, and and James W. Putney. 2011. “Calcium Oscillations.” *Cold Spring Harbor Perspectives in Biology* 1 (3): a004226.

Eliezer, D, E Kutluay, R Bussell, and G Browne. 2001. “Conformational Properties of Alpha-Synuclein in Its Free and Lipid-Associated States.” *Journal of Molecular Biology* 307 (4): 1061–73. doi:10.1006/jmbi.2001.4538.

El-Sibai, Mirvat, and Jonathan M. Backer. 2007. “Phospholipase C?? Negatively Regulates Rac/Cdc42 Activation in Antigen-Stimulated Mast Cells.” *European Journal of Immunology* 37 (1): 261–70. doi:10.1002/eji.200635875.

Field, K A, D Holowka, and B Baird. 1999. “Structural Aspects of the Association of FcepsilonRI with Detergent- Resistant Membranes.” *J Biol Chem* 274 (3): 1753–58. http://www.ncbi.nlm.nih.gov/htbin-post/Entrez/query?db=m&form=6&dopt=r&uid=9880557\nhttp://www.jbc.org/cgi/content/full/274/3/1753.

Field, Kenneth A., David Holowka, and Barbara Baird. 1997. “Compartmentalized Activation of the High Affinity Immunoglobulin E Receptor within Membrane Domains.” *Journal of Biological Chemistry* 272 (7): 4276–80. doi:10.1074/jbc.272.7.4276.

Fritsch, Ralph, Inge De Krijger, Kornelia Fritsch, Roger George, Beth Reason, Madhu S. Kumar, Markus Diefenbacher, Gordon Stamp, and Julian Downward. 2013. "XRAS and RHO Families of GTPases Directly Regulate Distinct Phosphoinositide 3-Kinase Isoforms." *Cell* 153 (5). doi:10.1016/j.cell.2013.04.031.

Gadi, Deepti, Alice Wagenknecht-Wiesner, David Holowka, and Barbara Baird. 2011. "Sequestration of Phosphoinositides by Mutated MARCKS Effector Domain Inhibits Stimulated Ca(2+) Mobilization and Degranulation in Mast Cells." *Molecular Biology of the Cell* 22 (24): 4908–17. doi:10.1091/mbc.E11-07-0614.

Galli, Stephen J., Marcus Maurer, and Chris S. Lantz. 1999. "Mast Cells as Sentinels of Innate Immunity." *Current Opinion in Immunology* 11 (1): 53–59. doi:10.1016/S0952-7915(99)80010-7.

Gilfillan, Alasdair M., and Juan Rivera. 2009. "The Tyrosine Kinase Network Regulating Mast Cell Activation." *Immunological Reviews* 228 (1): 149–69. doi:10.1111/j.1600-065X.2008.00742.x.

Gonzaga-Jauregui, Claudia, James R. Lupski, and Richard A. Gibbs. 2012. "Human Genome Sequencing in Health and Disease." *Annual Review of Medicine* 63 (1): 35–61. doi:10.1146/annurev-med-051010-162644.

Greten-Harrison, Becket, Manuela Polydoro, Megumi Morimoto-Tomita, Ling Diao, Andrew M Williams, Esther H Nie, Sachin Makani, et al. 2010. "Aβγ-Synuclein Triple Knockout Mice Reveal Age-Dependent Neuronal Dysfunction." *Proceedings of the National Academy of Sciences of the United States of America* 107 (45): 19573–78. doi:10.1073/pnas.1005005107.

Harvey, B K, Y Wang, and B J Hoffer. 2008. "Transgenic Rodent Models of Parkinson's Disease." *Acta Neurochirurgica. Supplement* 101: 89–92. http://www.ncbi.nlm.nih.gov/pubmed/18642640.

Heasman, Sarah J, and Anne J Ridley. 2008. "Mammalian Rho GTPases: New Insights into Their Functions from in Vivo Studies." *Nature Reviews. Molecular Cell Biology* 9 (9): 690–701. doi:10.1038/nrm2476.

Hong-Geller, E, D Holowka, R P Siraganian, B Baird, and R a Cerione. 2001. "Activated Cdc42/Rac Reconstitutes Fcepsilon RI-Mediated Ca2+ Mobilization and Degranulation in Mutant RBL Mast Cells." *Proceedings of the National Academy of Sciences of the United States of America* 98 (3): 1154–59. doi:10.1073/pnas.98.3.1154.

Hong-Geller, Elizabeth, and Richard A. Cerione. 2000. "Cdc42 and Rac Stimulate Exocytosis of Secretory Granules by Activating the IP3/calcium Pathway in RBL-2H3 Mast Cells." *Journal of Cell Biology* 148 (3): 481–93. doi:10.1083/jcb.148.3.481.

Hope, Andrew D., Ronny Myhre, Jennifer Kachergus, Sarah Lincoln, Gina Bisceglio, Mary Hulihan, and Matthew J. Farrer. 2004. "??-Synuclein Missense and Multiplication

Mutations in Autosomal Dominant Parkinson's Disease." *Neuroscience Letters* 367 (1): 97–100. doi:10.1016/j.neulet.2004.05.100.

Hunter, P. 2008. "The Paradox of Model Organisms." *EMBO Reports* 9: 717–20. doi:10.1038/embor.2008.142.

Irwin, David J., Virginia M-Y M.-Y. Lee, and John Q. Trojanowski. 2013. "Parkinson's Disease Dementia: Convergence of α-Synuclein, Tau and Amyloid-β Pathologies." *Nature Reviews. Neuroscience* 14 (9): 626–36. doi:10.1038/nrn3549.

Iwai, Akihiko, Eliezer Masliah, Makoto Yoshimoto, Nianfeng Ge, Lisa Flanagan, H. A. Rohan de Silva, Agnes Kittel, and Tsunao Saitoh. 1995. "The Precursor Protein of Non-ABeta Component of Alzheimer's Disease Amyloid Is a Presynaptic Protein of the Central Nervous System." *Neuron* 14 (2): 467–75. doi:10.1016/0896-6273(95)90302-X.

Jaffe, Aron B., and Alan Hall. 2005. "RHO GTPASES: Biochemistry and Biology." *Annual Review of Cell and Developmental Biology* 21 (1): 247–69. doi:10.1146/annurev.cellbio.21.020604.150721.

Kabachinski, Greg, Masaki Yamaga, D Michelle Kielar-Grevstad, Stephen Bruinsma, and Thomas F J Martin. 2014. "CAPS and Munc13 Utilize Distinct PIP2-Linked Mechanisms to Promote Vesicle Exocytosis." *Molecular Biology of the Cell* 25 (4): 508–21. doi:10.1091/mbc.E12-11-0829.

Kamb, Alexander, and Alexander Kamb. 2005. "What's Wrong with Our Cancer Models?" *Nature Reviews. Drug Discovery* 4 (2): 161–65. doi:10.1038/nrd1635.

Ke, Yazi D., Alexandra K. Suchowerska, Julia Van Der Hoven, Dineeka M. De Silva, Christopher W. Wu, Janet Van Eersel, Arne Ittner, and Lars M. Ittner. 2012. "Lessons from Tau-Deficient Mice." *International Journal of Alzheimer's Disease*. doi:10.1155/2012/873270.

Kim, Woojin Scott, Katarina Kågedal, and Glenda M Halliday. 2014. "Alpha-Synuclein Biology in Lewy Body Diseases." *Alzheimer's Research & Therapy* 6 (5): 73. doi:10.1186/s13195-014-0073-2.

Kramer, Michael L., and Walter J. Schulz-Schaeffer. 2007. "Presynaptic α-Synuclein Aggregates, Not Lewy Bodies, Cause Neurodegeneration in Dementia with Lewy Bodies." *The Journal of Neuroscience* 27 (6): 1405–10. doi:10.1523/JNEUROSCI.4564-06.2007.

Larsen, Kristin E, Yvonne Schmitz, Matthew D Troyer, Eugene Mosharov, Paula Dietrich, Abrar Z Quazi, Magali Savalle, et al. 2006. "Alpha-Synuclein Overexpression in PC12 and Chromaffin Cells Impairs Catecholamine Release by Interfering with a Late Step in Exocytosis." *The Journal of Neuroscience : The Official Journal of the Society for Neuroscience* 26 (46): 11915–22. doi:10.1523/JNEUROSCI.3821-06.2006.

Lim, Kah-Leong, and Chee-Hoe Ng. 2009. "Genetic Models of Parkinson Disease." *Biochimica*

et Biophysica Acta 1792 (7): 604–15. doi:10.1016/j.bbadis.2008.10.005.

Lippa, Carol F., Hideo Fujiwara, David M.A. Mann, Benoit Giasson, Minami Baba, Marie L. Schmidt, Linda E. Nee, et al. 1998. "Lewy Bodies Contain Altered α-Synuclein in Brains of Many Familial Alzheimer's Disease Patients with Mutations in Presenilin and Amyloid Precursor Protein Genes." *The American Journal of Pathology* 153 (5): 1365–70. doi:10.1016/S0002-9440(10)65722-7.

Mantsyzov, Alexey B., Alexander S. Maltsev, Jinfa Ying, Yang Shen, Gerhard Hummer, and Ad Bax. 2014. "A Maximum Entropy Approach to the Study of Residue-Specific Backbone Angle Distributions in α-Synuclein, an Intrinsically Disordered Protein." *Protein Science* 23 (9): 1275–90. doi:10.1002/pro.2511.

Maroteaux, L, J T Campanelli, and R H Scheller. 1988. "Synuclein: A Neuron-Specific Protein Localized to the Nucleus and Presynaptic Nerve Terminal." *The Journal of Neuroscience : The Official Journal of the Society for Neuroscience* 8 (8): 2804–15.

Marsh, Samuel E, and Mathew Blurton-Jones. 2012. "Examining the Mechanisms That Link β-Amyloid and α-Synuclein Pathologies." *Alzheimer's Research & Therapy* 4 (2): 11. doi:10.1186/alzrt109.

Masliah, E, E Rockenstein, I Veinbergs, M Mallory, M Hashimoto, a Takeda, Y Sagara, a Sisk, and L Mucke. 2000. "Dopaminergic Loss and Inclusion Body Formation in Alpha-Synuclein Mice: Implications for Neurodegenerative Disorders." *Science (New York, N.Y.)* 287 (5456): 1265–69. doi:10.1126/science.287.5456.1265.

Metz, Martin, Frank Siebenhaar, and Marcus Maurer. 2008. "Mast Cell Functions in the Innate Skin Immune System." *Immunobiology* 213 (3-4): 251–60. doi:10.1016/j.imbio.2007.10.017.

Murphy, Karen E., Amanda M. Gysbers, Sarah K. Abbott, Nahid Tayebi, Woojin S. Kim, Ellen Sidransky, Antony Cooper, Brett Garner, and Glenda M. Halliday. 2014. "Reduced Glucocerebrosidase Is Associated with Increased Alpha-Synuclein in Sporadic Parkinson's Disease." *Brain* 137 (3): 834–48. doi:10.1093/brain/awt367.

Norman, James C., Leo S. Price, Anne J. Ridley, Alan Hall, and Anna Koffer. 1994. "Actin Filament Organization in Activated Mast Cells Is Regulated by Heterotrimeric and Small GTP-Binding Proteins." *Journal of Cell Biology* 126 (4): 1005–15. doi:10.1083/jcb.126.4.1005.

Norris, Erin H, Benoit I Giasson, and Virginia M-Y Lee. 2004. "Alpha-Synuclein: Normal Function and Role in Neurodegenerative Diseases." *Current Topics in Developmental Biology* 60: 17–54. doi:10.1016/S0070-2153(04)60002-0.

O'Connell, M R, B L Oakes, S H Sternberg, A East-Seletsky, M Kaplan, and J A Doudna. 2014. "Programmable RNA Recognition and Cleavage by CRISPR/Cas9." *Nature* 516 (7530): 263–66. doi:10.1038/nature13769.

Passante, Egle, Carsten Ehrhardt, Helen Sheridan, and Neil Frankish. 2009. "RBL-2H3 Cells Are an Imprecise Model for Mast Cell Mediator Release." *Inflammation Research* 58 (9): 611–18. doi:10.1007/s00011-009-0028-4.

Peterson, Yuri K., Patrick Kelly, Carolyn A. Weinbaum, and Patrick J. Casey. 2006. "A Novel Protein Geranylgeranyltransferase-I Inhibitor with High Potency, Selectivity, and Cellular Activity." *Journal of Biological Chemistry* 281 (18): 12445–50. doi:10.1074/jbc.M600168200.

Pfefferkorn, Candace M., Zhiping Jiang, and Jennifer C. Lee. 2012. "Biophysics of ??-Synuclein Membrane Interactions." *Biochimica et Biophysica Acta - Biomembranes* 1818 (2): 162–71. doi:10.1016/j.bbamem.2011.07.032.

Polymeropoulos, Mihael H, Christian Lavedan, Elisabeth Leroy, Susan E Ide, Anindya Dehejia, Amalia Dutra, Brian Pike, et al. 1997. "Mutation in the Alpha-Synuclein Gene Identified in Families with Parkinson's Disease." *Science (New York, N.Y.)* 276 (5321): 2045–47. doi:doi: 10.1126/science.276.5321.2045.

Price, Leo S., James C. Norman, Anne J. Ridley, and Anna Koffer. 1995. "The Small GTPases Rac and Rho as Regulators of Secretion in Mast Cells." *Current Biology* 5 (1): 68–73. doi:10.1016/S0960-9822(95)00018-2.

Prince WT, Berridge MJ. 1973. "The Role of Calcium in the Action of 5-Hydroxytryptamine and Cyclic AMP on Salivary Glands." *J Exp Biol*, no. 58: 367–84.

Sauer, Brian. 1998. "Inducible Gene Targeting in Mice Using the Cre / Lox System." *Methods* 392 (14): 381–92. doi:10.1006/meth.1998.0593.

Schulte, Claudia, and Thomas Gasser. 2011. "Genetic Basis of Parkinson's Disease: Inheritance, Penetrance, and Expression." *Application of Clinical Genetics*. doi:10.2147/TACG.S11639.

Seldin, D C, S Adelman, K F Austen, R L Stevens, a Hein, J P Caulfield, and R G Woodbury. 1985. "Homology of the Rat Basophilic Leukemia Cell and the Rat Mucosal Mast Cell." *Proceedings of the National Academy of Sciences of the United States of America* 82 (11): 3871–75. doi:10.1073/pnas.82.11.3871.

Snead, David, and David Eliezer. 2014. "Alpha-Synuclein Function and Dysfunction on Cellular Membranes." *Experimental Neurobiology* 23 (4): 292–313. doi:10.5607/en.2014.23.4.292.

Soboloff, Jonathan, Maria A. Spassova, Xiang D. Tang, Thamara Hewavitharana, Wen Xu, and Donald L. Gill. 2006. "Orai1 and STIM Reconstitute Store-Operated Calcium Channel Function." *Journal of Biological Chemistry* 281 (30): 20661–65. doi:10.1074/jbc.C600126200.

Spillantini, M.G. 1999. "Parkinson's Disease, Dementia with Lewy Bodies and Multiple System Atrophy Are α-Synucleinopathies." *Parkinsonism & Related Disorders* 5 (4): 157–62. doi:10.1016/S1353-8020(99)00031-0.

Taymans, Jean Marc, and Mark R. Cookson. 2010. “Mechanisms in Dominant Parkinsonism: The Toxic Triangle of LRRK2, Alpha -Synuclein, and Tau.” *BioEssays* 32 (3): 227–35. doi:10.1002/bies.200900163.

Thul, R, T C Bellamy, H L Roderick, M D Bootman, and S Coombes. 2008. “Calcium Oscillations.” *Adv Exp Med Biol* 641: 1–27. doi:10.1101/cshperspect.a004226.

Tolias, K. F., L. C. Cantley, and C. L. Carpenter. 1995. “Rho Family GTPases Bind to Phosphoinositide Kinases.” *Journal of Biological Chemistry* 270 (30): 17656–59. doi:10.1074/jbc.270.30.17656.

Tugendreich, S, D E Bassett Jr., V A McKusick, M S Boguski, and P Hieter. 1994. “Genes Conserved in Yeast and Humans.” *Human Molecular Genetics* 3 (Spec No): 1509–17.

Uéda, K, H Fukushima, E Masliah, Y Xia, a Iwai, M Yoshimoto, D a Otero, J Kondo, Y Ihara, and T Saitoh. 1993. “Molecular Cloning of cDNA Encoding an Unrecognized Component of Amyloid in Alzheimer Disease.” *Proceedings of the National Academy of Sciences of the United States of America* 90 (23): 11282–86. doi:10.1073/pnas.90.23.11282.

Vargas, Karina J., Sachin Makani, Taylor Davis, Christopher H. Westphal, Pablo E. Castillo, and Sreeganga S. Chandra. 2014. “Synucleins Regulate the Kinetics of Synaptic Vesicle Endocytosis.” *The Journal of Neuroscience : The Official Journal of the Society for Neuroscience* 34 (28): 9364–76. doi:10.1523/JNEUROSCI.4787-13.2014.

Weernink, Paschal A Oude, Konstantinos Meletiadis, Silvia Hommeltenberg, Matthias Hinz, Hisamitsu Ishihara, Martina Schmidt, and Karl H. Jakobs. 2004. “Activation of Type I Phosphatidylinositol 4-Phosphate 5-Kinase Isoforms by the Rho GTPases, RhoA, Rac1, and Cdc42.” *Journal of Biological Chemistry* 279 (9): 7840–49. doi:10.1074/jbc.M312737200.

Weinreb, Paul H., Weiguo Zhen, Anna W. Poon, Kelly A. Conway, and Peter T. Lansbury. 1996. “NACP, a Protein Implicated in Alzheimer’s Disease and Learning, Is Natively Unfolded.” *Biochemistry* 35 (43): 13709–15. doi:10.1021/bi961799n.

Wilkes, Marcus M, Joshua D Wilson, Barbara Baird, and David Holowka. 2014. “Activation of Cdc42 Is Necessary for Sustained Oscillations of Ca2+ and PIP2 Stimulated by Antigen in RBL Mast Cells.” *Biology Open* 3 (8): 700–710. doi:10.1242/bio.20148862.

Wollman, R, and T Meyer. 2012. “Coordinated Oscillations in Cortical Actin and Ca2+ Correlate with Cycles of Vesicle Secretion.” *Nature Cell Biology* 14 (12): 1261–69. doi:10.1038/ncb2614.

Woods, Niall M, K. S. Roy Cuthbertson, and Peter H Cobbold. 1986. “Repetitive Transient Rises in Cytoplasmic Free Calcium in Hormone-Stimulated Hepatocytes.” *Nature* 319 (6054): 600–602. doi:10.1038/319600a0.

Wu, M, X Wu, and P De Camilli. 2013. “Calcium Oscillations-Coupled Conversion of Actin Travelling Waves to Standing Oscillations.” *Proc Natl Acad Sci U S A* 110 (4): 1339–44.

doi:10.1073/pnas.1221538110.

Yano, Hiroshi, Satoehi Nakanishi, Koutarou Kimura, Nobuo Hanai, Yutaka Saitoh, Yasuhisa Fukui, Yoshiaki Nonomura, and Yuzuru Matsuda. 1993. “Inhibition of Histamine Secretion by Wortmannin through the Blockade of Phosphatidylinositol 3-Kinase in RBL-2H3 Cells.” *Journal of Biological Chemistry* 268 (34): 25846–56.

Chapter 2

Activation of Cdc42 is Necessary for Sustained Ca^{2+} and PIP_2 Oscillations Stimulated by Antigen in RBL Mast Cells[1]

2.1 ABSTRACT

Antigen stimulation of mast cells via FcεRI, the high-affinity receptor for IgE, triggers a signaling cascade that requires Ca^{2+} mobilization for exocytosis of secretory granules during the allergic response. To characterize the role of Rho GTPases in FcεRI signaling, we utilized a mutant RBL cell line, B6A4C1, that is deficient in antigen-stimulated Cdc42 activation important for these processes. In response to antigen, we find that B6A4C1 cells exhibit severely attenuated Ca^{2+} oscillations that are restored to wild type RBL-2H3 levels by expression of constitutively active Cdc42 G12V or by a GEF for Cdc42, DOCK7, but not when the C-terminal di-arginine motif of active Cdc42 is mutated to di-glutamine. Antigen-stimulated FcεRI endocytosis is also defective in B6A4C1 cells, and Cdc42 G12V reconstitutes this response as well, indicating that activation of Cdc42 is critical for both Ca^{2+} responses to antigen and receptor endocytosis. To account for these multiple functional consequences, we show that Cdc42 G12V reconstitutes antigen-stimulated oscillations of phosphatidylinositol 4,5-bisphosphate (PIP_2) at the plasma membrane in mutant B6A4C1 cells, implying a role for Cdc42 in the regulation of stimulated PIP_2 synthesis.

2.2 INTRODUCTION

Antigen-mediated crosslinking of the high affinity receptor for IgE, FcεRI, stimulates Ca^{2+} mobilization that is essential for most aspects of mast cell function, including stimulated exocytosis of both secretory granules/lysosomes (degranulation) and recycling endosomes

1. This chapter was previously published. **Wilkes M**, Wilson J, Baird B, Holowka D. Activation of Cdc42 by Antigen Stimulation is Critical for Sustained Ca^{2+} and PIP_2 oscillations in RBL Mast Cells. *Biol Open.* 2014 July. 3: 700-10.

(Holowka et al., 2012). These secretory responses depend on Ca^{2+} influx in a process known as store-operated Ca^{2+} entry (SOCE). In this process, antigen-stimulated hydrolysis of PIP_2 by phospholipase Cγ (PLCγ) results in production of inositol 1,4,5-trisphosphate (IP_3) to cause release of Ca^{2+} from the endoplasmic reticulum (ER), which initiates direct coupling of the ER membrane protein STIM1 with the plasma membrane channel protein Orai1 to activate Ca^{2+} entry (Vig and Kinet, 2009). Defects in this Ca^{2+} mobilization process result in mast cells that fail to undergo exocytosis of secretory granules that contain mediators important for the allergic response (Vig and Kinet, 2009; Vig et al., 2006).

Previous studies provided evidence that antigen stimulation of FcεRI in RBL-2H3 mast cells results in activation of the Rho-GTPases Cdc42 and Rac1 (El-Sibai and Backer, 2007) that participate in Ca^{2+} mobilization leading to exocytosis of secretory granules (Hong-Geller and Cerione, 2000). Subsequently, we showed that Cdc42 G12V, an activated form of Cdc42, reconstitutes full Ca^{2+} mobilization and degranulation in response to antigen in a mutant RBL cell line, designated as B6A4C1, that is defective in these responses (Field et al., 2000; Hong-Geller et al., 2001). These studies suggested that Cdc42 acts upstream of IP_3 production in the Ca^{2+} mobilization process. However, questions remain as to the molecular mechanism by which Cdc42 regulates these mast cell Ca^{2+} responses. A recent study provided evidence that oscillations in antigen-stimulated Cdc42 activation are coupled to oscillations in PIP_2 and Ca^{2+} concentrations important for stimulated exocytosis (Wu et al., 2013). Furthermore, Johnson et al. (2012) demonstrated that a conserved di-arginine motif located near its carboxyl terminus is important for Cdc42 binding to PIP_2-containing membranes and for Cdc42-dependent cell transformation, but not for the role of Cdc42 in actin cytoskeleton-dependent filopodia formation.

To better understand the roles of Rho proteins in FcεRI signaling, we investigated whether the C-terminal di-arginine motif is needed for Cdc42 to mediate Ca^{2+} responses and exocytosis in mast cells. In the course of these studies, we determined that activation of Cdc42 is necessary for antigen-stimulated Ca^{2+} oscillations and exocytosis in RBL mast cells, and its C-terminal di-arginine motif is required for its role in these processes. We further provide evidence that activation of Cdc42 is necessary for antigen-stimulated endocytosis of FcεRI, a Ca^{2+}-independent process, as well as for stimulated PIP_2 synthesis manifested as oscillations in plasma membrane PIP_2.

2.3 RESULTS

B6A4C1 cells are deficient in antigen stimulated Cdc42 activation. B6A4C1 is a chemically mutagenized RBL mast cell subline that was originally selected for deficiency in stimulated degranulation and the expression of a mast cell-specific ganglioside, α−galactosyl GD1b (Stracke et al., 1987; Oliver et al., 1992). Previous studies demonstrated that robust antigen-stimulated Ca^{2+} mobilization and degranulation are reconstituted in mutant B6A4C1 cells by expressing constitutively active forms of Cdc42 or Rac1 (Field et al., 2000; Hong-Geller et al., 2001). To determine directly if these cells are defective in the activation of Cdc42 by IgE/FcεRI crosslinking we used a colorimetric assay to evaluate basal and antigen-stimulated Cdc42-GTP levels in both RBL-2H3 and B6A4C1 cells. As summarized in Figure 2.1, antigen stimulates a ~2.0-fold increase in Cdc42-GTP in RBL-2H3 cells after 1 min that declined to ~1.4-fold increase after 3 min, consistent with a previous study (El-Sibai and Backer, 2007). Under these conditions, B6A4C1 cells showed somewhat higher basal Cdc42-GTP levels when compared to RBL-2H3 cells (~ 15 %), and only a very small increase due to antigen stimulation

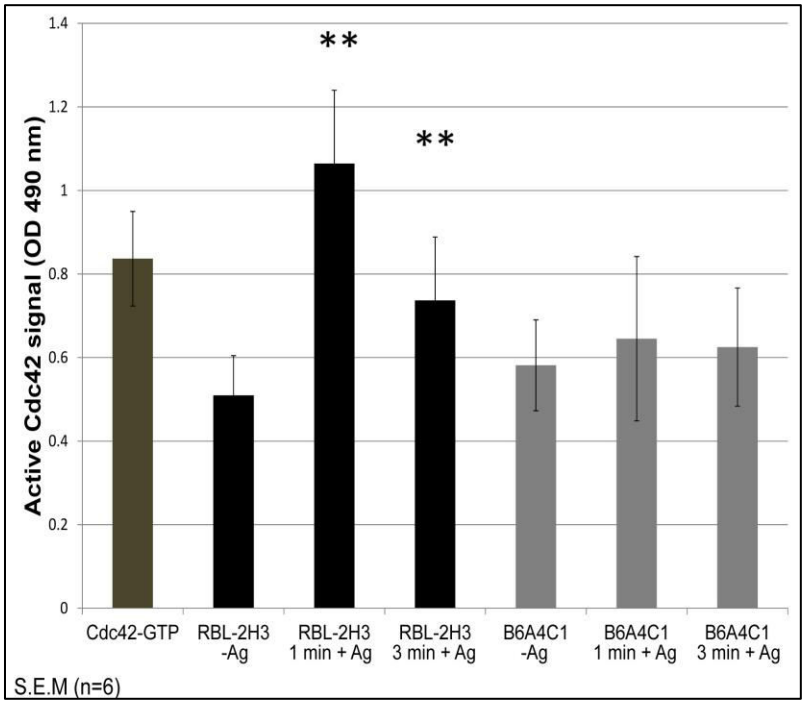

Figure 2.1. **B6A4C1 cells are deficient in antigen stimulated Cdc42 activation**. RBL-2H3 and B6A4C1 cells were sensitized with IgE, stimulated with 0.2 μg/ml multivalent DNP-BSA for one or three minutes, lysed, and analyzed using a colorimetric G-LISA assay. *Error bars* indicate ± standard error of the mean (s.e.m.) of six independent experiments. (** represents P-values <.01).

that is not statistically significant. These results confirm that B6A4C1 cells are defective in FcεRI-mediated activation of Cdc42.

Carboxyl terminal di-arginine motif of Cdc42 is necessary for reconstituting Ca^{2+} mobilization in B6A4C1 cells. In previous studies, Rho family GTPases were expressed in RBL cells using vaccinia infection (Hong-Geller and Cerione, 2000; Field et al., 2000; Hong-Geller et al., 2001). In our current experiments, Cdc42 cDNA constructs were transfected into these cells together with a genetically encoded Ca^{2+} indicator, GCaMP3, using electroporation. As shown in representative experiments in Figure 2.2A and 2.2B, addition of an optimal dose of antigen, in the absence of extracellular Ca^{2+}, stimulates transient increases in cytoplasmic Ca^{2+} due to release from ER stores in both the RBL-2H3 and B6A4C1 cells. This response in B6A4C1 cells is faster and more transient than in 2H3 cells. Subsequent addition of 1.8 mM extracellular Ca^{2+} results in SOCE that is reduced in B6A4C1 cells compared with the response in 2H3 cells (Fig. 2.2A,B). B6A4C1 cells transfected with Cdc42 G12V and GCaMP3 show enhanced Ca^{2+} release from stores and SOCE when compared to B6A4C1 cells expressing GCaMP3 with empty vector pcDNA 3.0 (Fig. 2.2C vs. 2.2A), consistent with previous results using the vaccinia expression system (Hong-Geller et al., 2001).

The previous study by Johnson et al. (2012) provided evidence for a critical role for the C-terminal di-arginine motif of Cdc42 in cell transformation by an activated mutant of this protein, but a short-term assay for the functional role of this motif was lacking. To evaluate the effect of charge neutralization of the di-arginine motif, we compared the capacity of Cdc42 G12V with the di-arginine motif mutated to di-glutamines (Cdc42 G12V/QQ) to substitute for

Figure 2.2 **Carboxyl terminal di-arginine motif of Cdc42 is necessary for reconstituting Ca^{2+} mobilization in B6A4C1 cells**. IgE-sensitized RBL-2H3 mast cells expressing pcDNA and GCaMP3 (**A**), and B6A4C1 mast cells expressing pcDNA and GCaMP3 (**B**), Cdc42 G12V and GCaMP3 (**C**), or Cdc42 G12V/QQ and GCaMP3 cells (**D**) were stimulated in Ca^{2+}-free BSS with 0.2 μg/ml of DNP-BSA (Ag) at 100 sec, then 1.8 mM Ca^{2+} was added at 200 sec. The resulting responses represent Ca^{2+} release from stores and store operated Ca^{2+} entry (SOCE), respectively. **E and F:** Summary of four independent experiments monitoring changes in GCaMP3 fluorescence due to stimulated Ca^{2+} release from stores (**E**) and SOCE (**F**). *Error bars* indicate ± s.e.m. (** represents P-values <0.01).

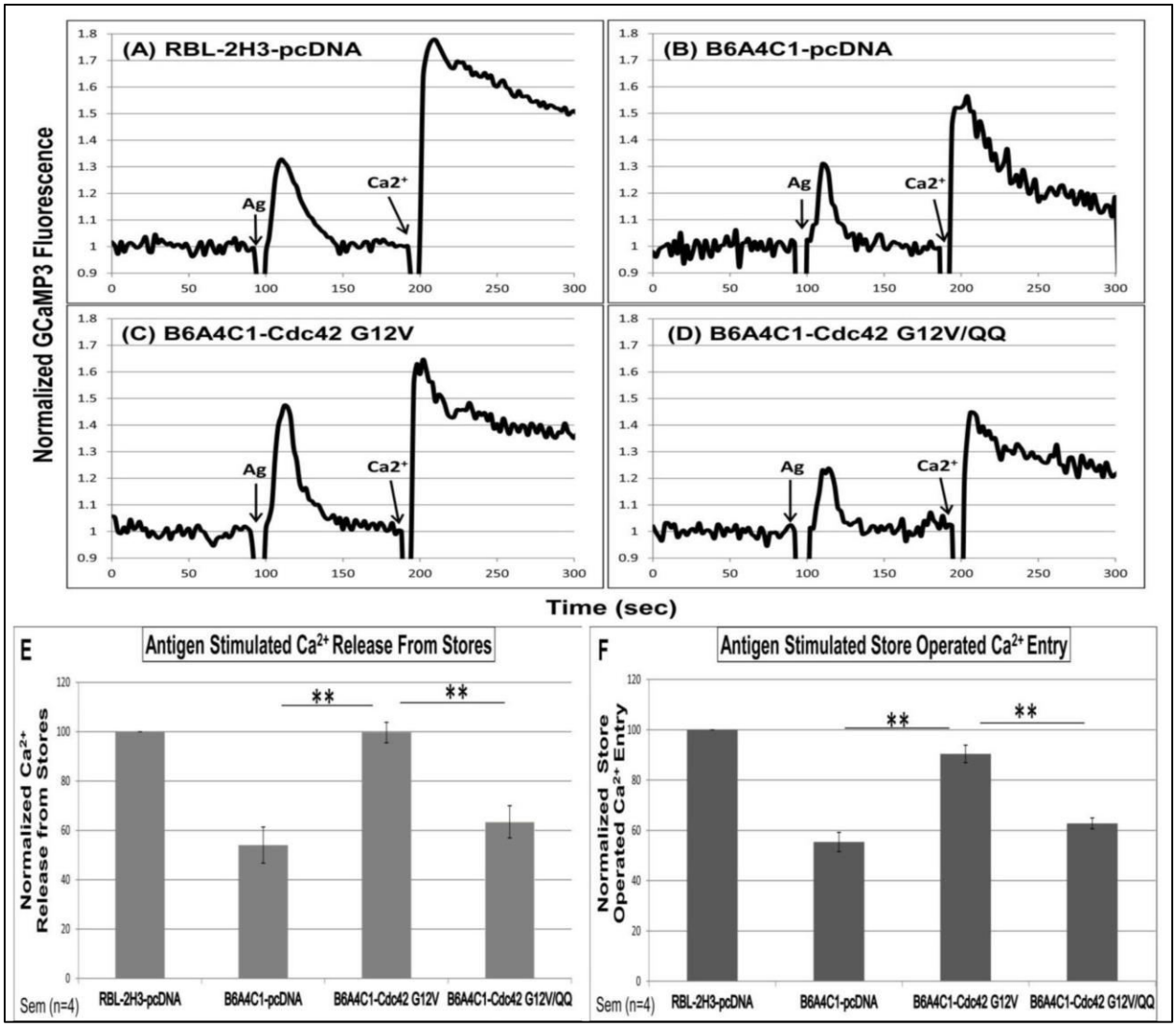
(A) RBL-2H3-pcDNA
(B) B6A4C1-pcDNA
(C) B6A4C1-Cdc42 G12V
(D) B6A4C1-Cdc42 G12V/QQ
Ag
Ca2+
Normalized GCaMP3 Fluorescence
Time (sec)
E
Antigen Stimulated Ca2+ Release From Stores
Normalized Ca2+ Release from Stores
F
Antigen Stimulated Store Operated Ca2+ Entry
Normalized Store Operated Ca2+ Entry
**
Sem (n=4)
RBL-2H3-pcDNA
B6A4C1-pcDNA
B6A4C1-Cdc42 G12V
B6A4C1-Cdc42 G12V/QQ

Cdc42 G12V in our Ca2+ experiments. Expression of Cdc42 G12V/QQ in B6A4C1 cells failed to reconstitute the 2H3-level Ca^{2+} response for antigen-stimulated Ca^{2+} release from stores and to reconstitute the 2H3-level Ca^{2+} response for antigen-stimulated Ca^{2+} release from stores and for SOCE observed with Cdc42 G12V (Fig. 2.2D). These trends are summarized for multiple experiments in Figure 2.2E and 2.2F: they show that the capacity of Cdc42 G12V to reconstitute normal antigen-stimulated Ca^{2+} responses in mutant B6A4C1 cells depends critically on the C-terminal di-arginine motif. These results further establish a straight-forward short term assay in which the molecular basis for the role of this di-arginine motif can be investigated.

The di-arginine motif of Cdc42 is important for FcεRI-stimulated exocytosis in RBL mast cells. Exocytosis of secretory granules requires sustained increases in cytoplasmic Ca^{2+} levels that depend on influx of extracellular Ca^{2+} via SOCE (Ma and Beaven, 2011). A previous study showed that activated Cdc42 enhances FcεRI-mediated granule exocytosis in RBL-2H3 cells (Hong-Geller and Cerione, 2000). Because of limited signal-to noise in B6A4C1 cells, we used a pH-sensitive pHluorin-labeled member of the SNARE protein family, vesicle-associated membrane protein-8 (VAMP8) to monitor stimulated exocytosis in RBL-2H3 cells co-transfected with different Cdc42 constructs (Fig. 2.3). This VAMP8-pHluorin protein localizes to both recycling endosomes and secretory granules, where its fluorescence is very low due to reduced pH environments. Upon exocytosis of these VAMP8-pHluorin labeled vesicles, the fluorescence increases markedly due to exposure to neutral pH at the cell surface. Under the conditions of this experiment, Cdc42 G12V enhanced antigen-stimulated exocytosis by 54% (Fig. 2.3B,D). By comparison, Cdc42 G12V/QQ enhanced exocytosis by only 22% (Fig. 2.3C,D), a level not statistically greater than the vector control (Fig. 2.3A,D). These results, all together, are

Figure 2.3. **The di-arginine motif of Cdc42 is important for FcεRI-stimulated exocytosis in RBL-2H3 mast cells.** IgE-sensitized RBL-2H3 cells co-transfected with VAMP8-pHluorin and pcDNA (**A**), VAMP8-pHluorin and Cdc42 G12V (**B**), or VAMP8-pHluorin and Cdc42 G12V/QQ were stimulated by 0.2 μg/ml Ag in the presence of 2 μM cytochalasin D, and exocytosis was monitored as increased pHlourin fluorescence via steady-state fluorimetry. (D) Summary of percent increase in Vamp8-mediated exocytosis normalized to RBL-2H3 cells expressing pcDNA vector control. *Error bars* indicate ± s.e.m. of four independent experiments. (** represents P-values <.01, * represents P-values <.05, N.S. indicates values are not significantly different).

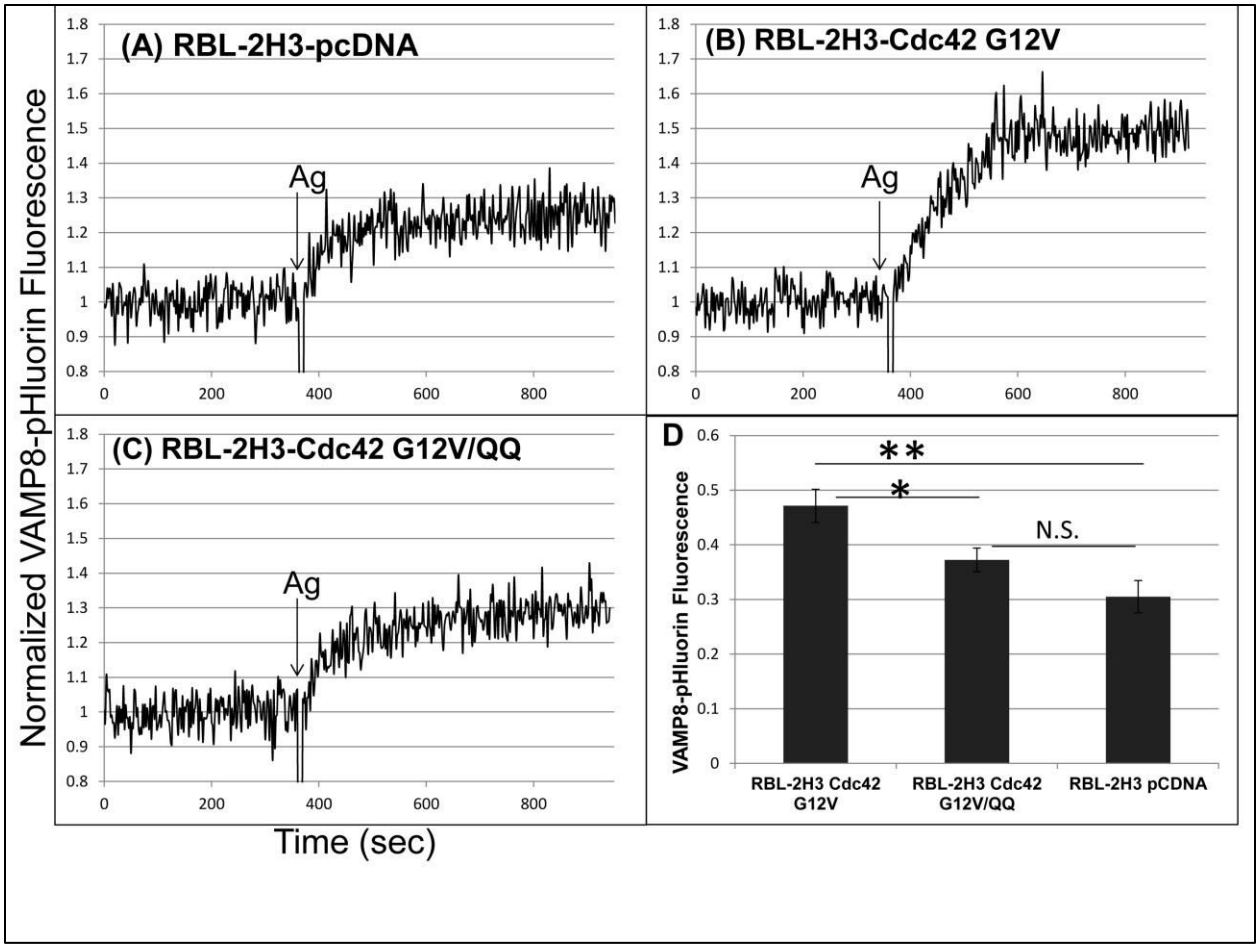
(A) RBL-2H3-pcDNA
(B) RBL-2H3-Cdc42 G12V
(C) RBL-2H3-Cdc42 G12V/QQ
Ag
Normalized VAMP8-pHluorin Fluorescence
Time (sec)
D
VAMP8-pHluorin Fluorescence
**
*
N.S.
RBL-2H3 Cdc42 G12V
RBL-2H3 Cdc42 G12V/QQ
RBL-2H3 pCDNA

consistent with an important role for the di-arginine motif in FcεRI-mediated Ca^{2+} mobilization that is necessary for exocytosis.

Cdc42 is essential for maintaining sustained Ca^{2+} *oscillations in mast cells*. Antigen-stimulated Ca^{2+} oscillations are a hallmark of FcεRI signaling responses (Millard et al., 1989; Parekh and Putney, 2005), and these have been shown to play an important role in granule exocytosis (Kim et al., 1997). Upon addition of antigen, most RBL-2H3 cells exhibit sustained Ca^{2+} oscillations lasting more than 5 min in imaging experiments (representative results in Fig. 2.4A and Supplementary Movie 1). In contrast, B6A4C1 cells typically exhibit only a few oscillations before returning to baseline Ca^{2+} levels, very similar to the response of 2H3 cells in the absence of extracellular Ca^{2+} (Fig. 2.4B,C, and Supplementary Movie 2). Remarkably, expression of Cdc42 G12V in these cells restores sustained Ca^{2+} oscillations with periodicities similar to that of 2H3 cells (Fig. 2.4D). Consistent with its incapacity to restore sustained Ca^{2+} responses in B6A4C1 cells in fluorimetry experiments (Fig. 2.2), Cdc42 G12V/QQ fails to restore sustained Ca^{2+} oscillations in these cells (Fig. 2.4E).

Dock7, a DHR2-containing GEF for Cdc42 and Rac, restores sustained Ca^{2+} *oscillations in B6A4C1 mutant mast cells*. Although Cdc42 G12V and Rac1 G12V restore normal antigen-stimulated Ca^{2+} responses in B6A4C1 cells, wt Cdc42 and wt Rac1 do not reconstitute this response (Hong-Geller et al., 2001), suggesting that these cells are deficient in a guanine nucleotide exchange factor (GEF) capable of activating both Cdc42 and Rac1. We showed previously that expression of o-Dbl, a prototype Rho GEF containing a plekstrin homology domain and a Dbl-homology domain essential for GEF catalytic activity, only partially reconstitutes antigen-stimulated Ca^{2+} responses (Hong-Geller et al., 2001), and we found that a structurally similar GEF, Cool2, also shows only minimal reconstitution (Fig. 2.4G). Because of

Figure 2.4. **Activation of Cdc42 by antigen is necessary for sustained Ca^{2+} oscillations in RBL mast cells.** RBL-2H3 mast cells were co-transfected with GCaMP3 and pcDNA (**A** and **C**) or dominant negative Cdc42 T17N (**H**). B6A4C1 cells were co-tranfected with GCaMP3 and pcDNA (**B**) Cdc42 G12V (**D**), Cdc42 G12V/QQ (**E**), or the Rho family GEFs DOCK7 (**F**) or Cool2 (**G**). Ag (0.2 μg/ml) was added at t = 0, and representative examples of Ca^{2+} responses are shown. (**I**) Summary of quantification of Ca^{2+} oscillations stimulated by 0.2 μg/ml multivalent DNP-BSA. Dark grey histograms are the number of oscillations occurring in the first two minutes following the initial Ca^{2+} spike, and light grey segments are the number of oscillations that occur in the last three minutes of the five minute stimulation time period. 2H3: RBL-2H3 cells; C1: B6A4C1 cells. Error bars refer to the total five minute responses and indicate ± s.e.m. for 110 individual cells for each condition shown (*** represents P-values <.001).

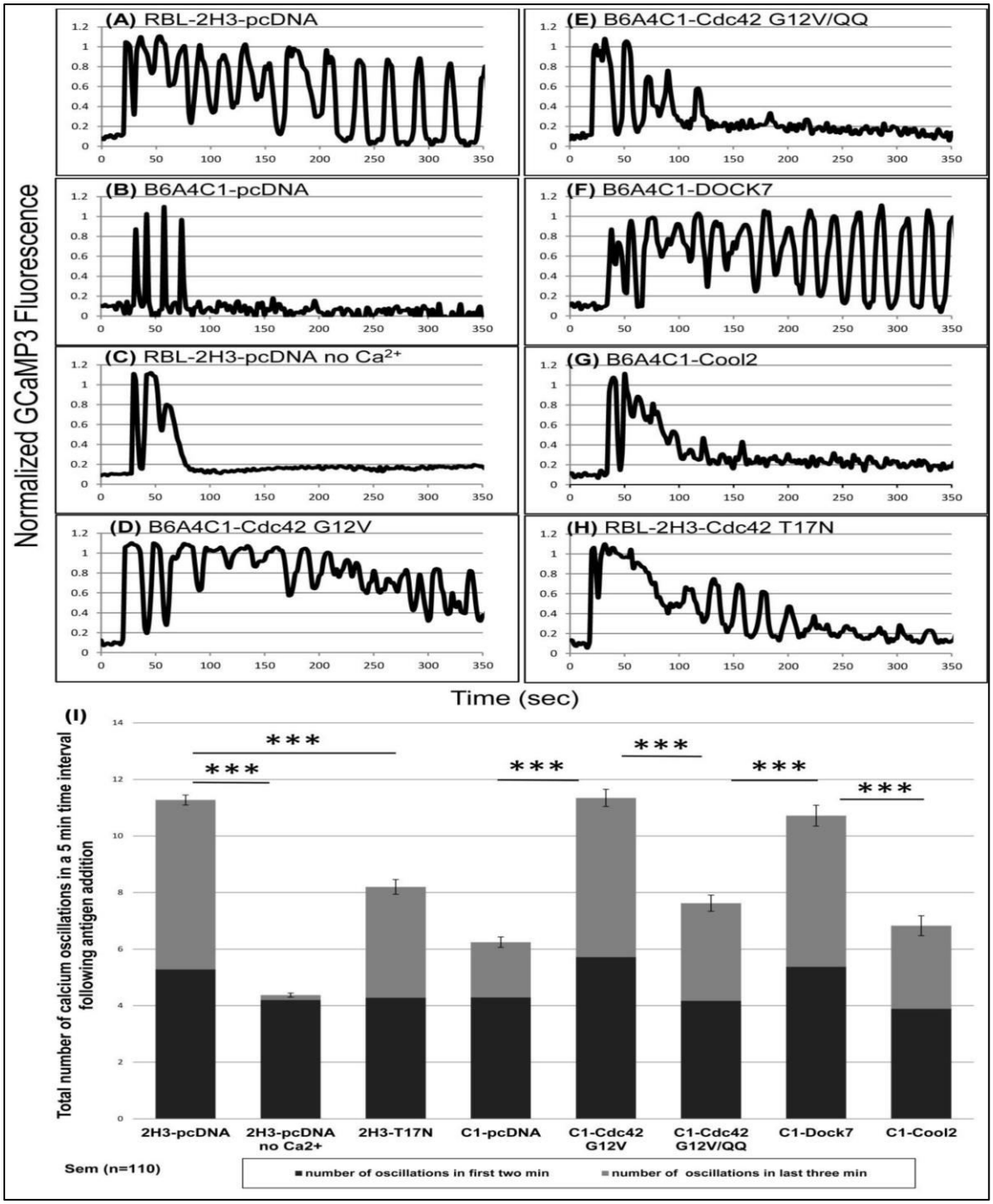
(A) RBL-2H3-pcDNA
(B) B6A4C1-pcDNA
(C) RBL-2H3-pcDNA no Ca2+
(D) B6A4C1-Cdc42 G12V
(E) B6A4C1-Cdc42 G12V/QQ
(F) B6A4C1-DOCK7
(G) B6A4C1-Cool2
(H) RBL-2H3-Cdc42 T17N
Normalized GCaMP3 Fluorescence
Time (sec)
(I)
Total number of calcium oscillations in a 5 min time interval following antigen addition
***
2H3-pcDNA
2H3-pcDNA no Ca2+
2H3-T17N
C1-pcDNA
C1-Cdc42 G12V
C1-Cdc42 G12V/QQ
C1-Dock7
C1-Cool2
Sem (n=110)
number of oscillations in first two min
number of oscillations in last three min

these results, we investigated whether a Dock GEF family protein might more effectively reconstitute the Ca^{2+} response to antigen in B6A4C1 cells, and in these initial studies we chose to evaluate Dock7 due to its capacity to activate both Cdc42 and Rac. In contrast to Cool2, Dock7 consistently enhanced the number of Ca^{2+} oscillations in B6A4C1 cells to levels similar to RBL-2H3 cells (Fig. 2.4F vs 2.4A). Dock 7 shares almost no sequence homology with Dbl GEFs, but contains instead a DHR2 domain for its catalytic activity and a DHR1 domain thought to be important for GEF localization (Meller et al., 2005). We also tested the dominant negative form of Cdc42, Cdc42 T17N in a loss-of-function assay. As represented in Figure 2.4H, this construct attenuates Ca^{2+} oscillations in RBL-2H3 cells under our experimental conditions.

Results from these real-time imaging experiments for >100 cells for each construct are summarized in Figure 2.4I. Whereas similar numbers of Ca^{2+} oscillations are observed in all cases during the first 2 min, both in the presence and absence of extracellular Ca^{2+} (4.1-5.7), numbers of oscillations in the time interval from 2 to 5 min vary widely, from 0.1 to 7.0. Most striking is the full reconstitution of Ca^{2+} oscillations during this time period in B6A4C1 cells with both Cdc42 G12V and Dock 7, and the minimal effect of Cdc42 G12V/QQ in this regard.

Cdc42 G12V enhances a Ca^{2+}*-independent process, FcεRI endocytosis, in B6A4C1 cells.* Results described above demonstrate that Cdc42 G12V reconstitutes normal antigen-stimulated Ca^{2+} mobilization in mutant B6A4C1 cells. To distinguish whether this is a direct effect on Ca^{2+} mobilization or on an upstream event, we examined whether Cdc42 G12V reconstitutes a Ca^{2+}-independent response in B6A4C1 cells. Antigen-mediated FcεRI endocytosis was originally determined to be independent of Ca^{2+} in RBL cells (Furuichi et al., 1984), and a recent study shows that a B6A4C1-related cell line is deficient in this process (Mazucato et al., 2011). We confirmed that antigen-stimulated IgE/FcεRI endocytosis occurs independently of Ca^{2+}

Figure 2.5. **Cdc42 G12V reconstitutes antigen-stimulated FcεRI endocytosis in B6A4C1 cells. (A-D)** Representative confocal images of antigen-stimulated IgE receptor endocytosis. RBL-2H3 and B6A4C1 mast cells expressing mRFP to mark positively transfected cells were labeled with Alexa488-conjugated IgE and stimulated with 0.2 μg/ml DNP-BSA for 15 min, then fixed and labeled with Alexa 647-conjugated anti-Alexa488 Ab to monitor endocytosis. Endocytosed Alexa488-IgE is not accessible to Alexa 647-anti-Alexa488 Ab. **E**, quantified results of the number of cells undergoing antigen-stimulated IgE receptor endocytosis. Error bars indicate ± s.e.m. for 4 individual experiments. 300 cells were counted for each individual experiment for a total of 1200 cells quantified for each condition shown (*** represents P-values <.001). Scale bar equals 20 μm.

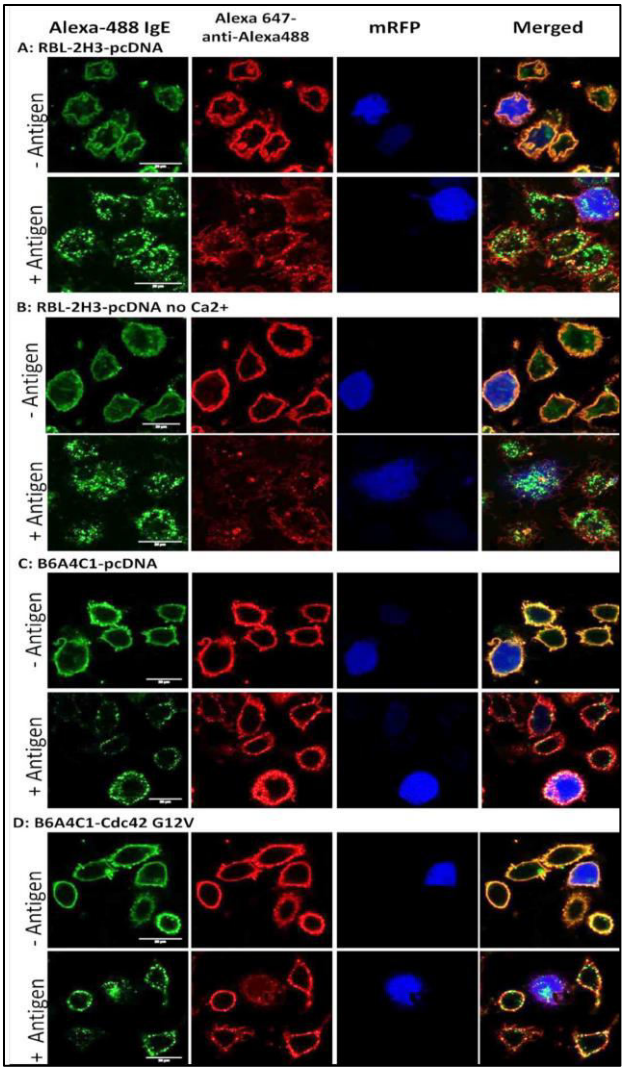
Alexa-488 IgE
Alexa 647-anti-Alexa488
mRFP
Merged
A: RBL-2H3-pcDNA
- Antigen
+ Antigen
B: RBL-2H3-pcDNA no Ca2+
- Antigen
+ Antigen
C: B6A4C1-pcDNA
- Antigen
+ Antigen
D: B6A4C1-Cdc42 G12V
- Antigen
+ Antigen

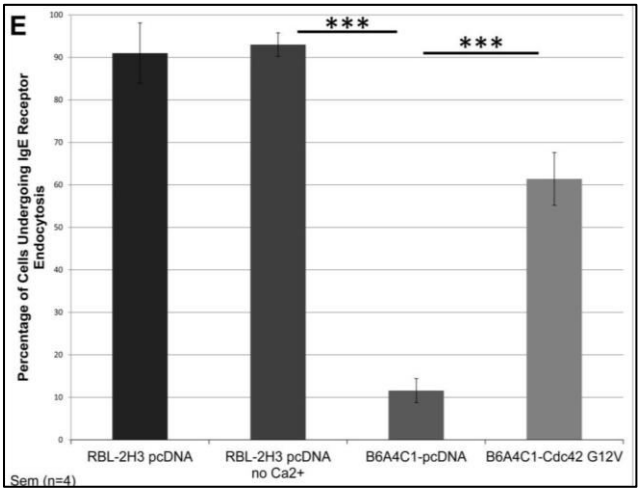
E
Percentage of Cells Undergoing IgE Receptor Endocytosis
***
***
RBL-2H3 pcDNA
RBL-2H3 pcDNA no Ca2+
B6A4C1-pcDNA
B6A4C1-Cdc42 G12V
Sem (n=4)

mobilization in RBL-2H3 cells, such that >90% of these cells undergo this process in the presence and absence of extracellular Ca^{2+} (Fig. 2.5A,B,E). Under the same conditions, we found that most B6A4C1 cells fail to undergo antigen-stimulated IgE/FcεRI endocytosis, and these complexes were retained as puncta at the plasma membrane in all but ~12% of these cells (Fig. 2.5C,E). In contrast, expression of Cdc42-G12V in these cells substantially increased the percentage of cells undergoing this process. In four separate experiments, 61% of B6A4C1 cells co-expressing Cdc42-G12V together with the transfection marker mRFP exhibited antigen-dependent IgE/FcεRI endocytosis (Fig. 2.5D,E). These results show that activated Cdc42 contributes to antigen-mediated FcεRI endocytosis in RBL cells, and they suggest that its fundamental role in FcεRI signaling is the activation of an early cellular event that is upstream of Ca^{2+} mobilization and degranulation.

Cdc42 G12V reconstitutes antigen stimulated PIP_2 oscillations in B6A4C1 cells. Recent studies demonstrated that, in addition to Ca^{2+} oscillations, antigen stimulation of RBL-2H3 cells results in oscillating levels of PIP_2 at the plasma membrane that are synchronous with Ca^{2+} oscillations but out of phase (Wu et al., 2013; Wollman and Meyer, 2012). Using PH-PLCδ-GFP to monitor levels of PIP_2 (Stauffer et al., 1998; Varnai and Balla, 1998), we investigated whether activation of Cdc42 is important for the generation of these PIP_2 oscillations. We verified that antigen-stimulated PIP_2 oscillations are frequently observed in RBL-2H3 cells, such that >80% of RBL-2H3 cells examined exhibited sustained oscillations that are typically evident after 200-300 s (Fig. 2.6A,D). In contrast, addition of antigen to B6A4C1 cells causes a time-dependent increase in cytoplasmic PH-PLCδ-GFP fluorescence, presumably due to PLCγ-mediated PIP_2 hydrolysis, but <15% of these cells exhibit stimulated PIP_2 oscillations (Fig. 2.6B,D). Expression of Cdc42 G12V in these cells markedly increased the percentage of cells that exhibit antigen-

Figure 2.6. **Cdc42 G12V reconstitutes antigen stimulated PIP_2 oscillations in B6A4C1 cells.** IgE-sensitized RBL-2H3 mast cells expressing pcDNA and PH-PLCδ-GFP (**A**), and B6A4C1 mast cells expressing pcDNA and PH-PLCδ-GFP (**B**), or Cdc42 G12V and PH-PLCδ-GFP (**C**), were stimulated with 0.2 μg/ml of DNP-BSA (Ag) at ~20 sec in the presence of 2 μM cytochalasin D. **(D)** Quantified results for the percentage of cells undergoing antigen-mediated PIP_2 oscillations. Error bars indicate ± s.d. for 3 individual experiments. 16-17 cells were analyzed for each individual experiment for a total of 50 cells monitored for each condition shown (*** represents P-values <.001).

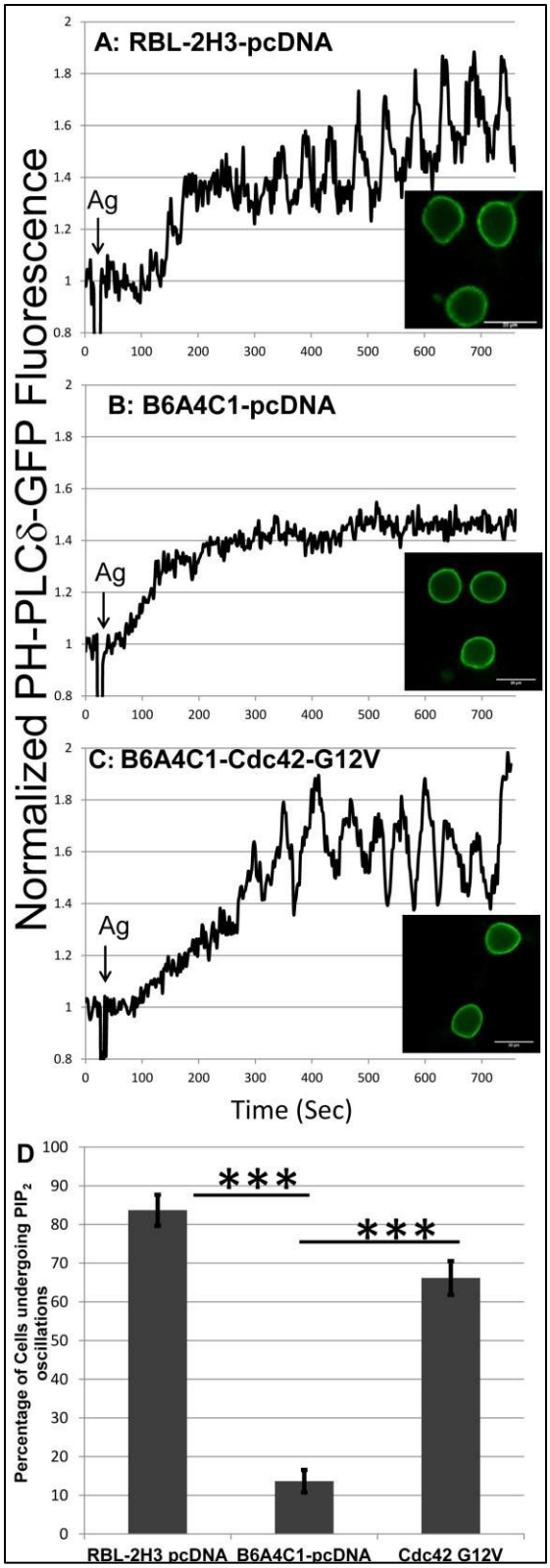
A: RBL-2H3-pcDNA
B: B6A4C1-pcDNA
C: B6A4C1-Cdc42-G12V
Ag
Normalized PH-PLCδ-GFP Fluorescence
Time (Sec)
D
Percentage of Cells undergoing PIP2 oscillations
***
***
RBL-2H3 pcDNA
B6A4C1-pcDNA
Cdc42 G12V

stimulated PIP_2 oscillations, such that ~66% of cells have sustained PIP_2 oscillations in three separate experiments (Fig. 2.6C,D). As for the wild type RBL-2H3 cells, PIP2 oscillations begin 200-300 sec after antigen addition, suggesting that PIP2 hydrolysis is the dominant process activated prior to this time. These findings suggest that antigen-mediated activation of Cdc42 is important for replenishment of PIP_2 at the plasma membrane during hydrolysis by PLCγ, resulting in cycles of PIP_2 hydrolysis and synthesis that results in sustained Ca^{2+} oscillations in antigen-stimulated mast cells.

2.4 DISCUSSION

It has long been recognized that mast cells play an essential role in allergic responses, and there is now evidence that these cells also play critical roles in both innate and adaptive immune responses to infections, inflammatory autoimmune diseases, and incipient tumors (Abraham and St John, 2010; Galli et al., 1999; Metz et al., 2008). Mast cells assist in these responses in part by undergoing the process of degranulation, in which preformed mediators such as histamine, serine proteases, and proteoglycans are released after stimulation by antigen binding and crosslinking of IgE bound to FcεRI receptors at the cell surface. Despite previous studies establishing the importance of Rho GTPases in mast cell signaling (Hong-Geller and Cerione, 2000; Field et al., 2000; Hong-Geller et al., 2001), the mechanism by which they regulate these responses has yet to be elucidated.

We compared normal antigen-stimulated RBL-2H3 cell responses to those of a mutant RBL-2H3 cell line that we have shown to be defective in antigen stimulated Cdc42 activation (Fig. 2.1). Our results demonstrate that in the absence of Cdc42 activation, mast cells undergo attenuated Ca^{2+} mobilization responses to antigen, showing both reduced Ca^{2+} release from stores

and reduced SOCE (Fig. 2.2B). Cdc42 G12V reconstitutes both phases of antigen stimulated Ca^{2+} mobilization, and the polybasic di-arginine motif located at the C-terminus of Cdc42 is important for this capacity (Fig. 2.2C, D). This motif also appears to be important for antigen-stimulated exocytosis, a process that occurs downstream of Ca^{2+} mobilization in these cells (Fig. 2.3). We hypothesize that electrostatic interactions between the positively charged di-arginine motif of Cdc42 and negatively charged phospholipids at the plasma membrane are important for the capacity of Cdc42 to regulate mast cell signaling.

Because Ca^{2+} oscillations are important for antigen-stimulated exocytosis in mast cells, we evaluated the participation of Cdc42 in regulating antigen stimulated Ca^{2+} oscillations. In contrast to the sustained Ca^{2+} oscillations observed in stimulated RBL-2H3 cells, B6A4C1 cells undergo only limited initial oscillations, similar to those in RBL-2H3 in the absence of extracellular Ca^{2+} (Fig. 2.4B,C). We found that Cdc42 G12V reconstitutes sustained Ca^{2+} oscillations in the B6A4C1 cells to wild type RBL-2H3 levels (Fig. 2.4D,I), and we conclude that activation of Cdc42 is necessary for these sustained oscillations and for maximal granule exocytosis. Furthermore, we also find that the GEF DOCK7 reconstitutes this oscillatory Ca^{2+} behavior in B6A4C1 cells (Fig. 2.4F,I), strengthening the conclusion that the activation of Cdc42 is deficient in the mutant RBL cells.

Two distinct families of GEFs have been identified for Rho GTPase activation: the conventional Dbl-family (Hart et al., 1991) and the more recently identified DOCK180 family (Takai et al., 1996; Hasegawa et al. 1996; Erickson and Cerione, 2004), which is divided into four subclasses. DOCK7 belongs to the DOCK-C subfamily, which activates both Cdc42 and Rac (Cote and Vuori, 2007). Although functionally similar to the Dbl-GEF family, DOCK-GEFs do not contain the Dbl-homology domain to mediate GTP-GDP exchange; instead they are

characterized by a DOCK homology region 2 (DHR-2) domain to stimulate nucleotide exchange leading to Rho GTPase activation. We note that recent studies have demonstrated participation of several DOCK GEF family members in immune regulatory functions (Nishikimi et al., 2013), including an important role for DOCK8, which, like DOCK7, activates both Cdc42 and Rac. Mutations or deletions of DOCK8 lead to a form of T and B cell immunodeficiency characterized by recurrent viral infections, greater susceptibility to cancer, and elevated serum levels of IgE (Nishikimi et al., 2013). Another family member, DOCK2, has been shown to be involved in forming the immunological synapse between antigen presenting cells and T lymphocytes following recruitment of this GEF by PIP_3 (Le Floc'h A et al. 2013). Our DOCK7 findings add to this growing body of literature supporting the view that DOCK GEFs play critical roles in regulating various immune responses.

It is unclear why a Dock GEF and not a Dbl-GEF reconstitutes Ca^{2+} responses as demonstrated in our experiments, especially considering *in vitro* data which suggest that Dbl-GEFs have better nucleotide exchange efficiency than DOCK GEF family members (Kulkarni et al., 2011; Miyamoto et al., 2007; Watabe-Uchida et al., 2006; Yamauchi et al., 2008). One possible explanation is that, in addition to mediating GTP-GDP exchange, DOCK7, which is very large (~240 kDa), also acts as an adaptor protein: DOCK7 may recruit and bind specific effector proteins necessary to regulate mast cell responses and thereby mediate essential interactions between Cdc42 and its effectors. This hypothesis is consistent with our findings that the fast cycling mutant Cdc42 F28L, which undergoes spontaneous activation without the assistance of GEF proteins, does not reconstitute Ca^{2+} mobilization in B6A4C1 cells (M.M.W., unpublished observations). Future studies will evaluate previously characterized DOCK7 mutants (Zhou et al., 2013) to determine if structural elements in addition to the nucleotide

exchanging DHR-2 domain of DOCK7 are involved in regulating Ca^{2+} mobilization in mast cells. DOCK6 and DOCK8, the two other DOCK family members capable of activating Cdc42 and Rac, will also be evaluated to determine whether DOCK7 is unique in its capacity as a Rho GEF to reconstitute sustained Ca^{2+} oscillations in the B6A4C1 cells.

Our findings that constitutively active Cdc42, as well as DOCK7, reconstitute antigen-stimulated Ca^{2+} oscillations offer new insights into the mechanism by which Cdc42 regulates Ca^{2+} mobilization in mast cells. Sustained Ca^{2+} oscillations depend on SOCE, as well as on IP_3 generation (Hajnoczky and Thomas, 1997; Meyer and Stryer, 1991). Thapsigargin, which stimulates SOCE and degranulation in both RBL-2H3 and B6A4C1 cells (Field et al., 2000), initiates these responses by inhibiting the SERCA pump necessary for maintaining ER Ca^{2+} levels. Thapsigargin causes cytoplasmic Ca^{2+} to be elevated in a sustained manner (Cohen et al, 2009; Wollman and Meyer, 2012). Normally, however, replenishment of the PIP_2 pool being hydrolyzed by activated PLCγ to generate IP_3 must be maintained for mast cells to sustain Ca^{2+} oscillations accompanying SOCE. We hypothesized that Cdc42 promotes mast cell signaling by acting upstream of IP_3 production by PLCγ and Ca^{2+} release from stores. To test this hypothesis, we evaluated the capacity of Cdc42 to regulate a PIP_2-dependent process that is independent of Ca^{2+} mobilization.

A previous study reported that endocytosis is a Ca^{2+} independent process in RBL-2H3 cells (Furuichi et al, 1984), and because it is also common that endocytosis is a PIP_2-dependent process (Santos et al., 2013), we investigated whether B6A4C1 cells are deficient in stimulated IgE receptor endocytosis, in addition to their Ca^{2+} mobilization defects. We found that B6A4C1 cells are deficient in this endocytic process, and that expression of Cdc42 G12V in mutant RBL cells results in a significant increase in the number of cells capable of undergoing IgE/FcεRI

endocytosis. These results confirm that Cdc42 regulates an event independent and upstream of Ca^{2+} mobilization.

Initial characterization of the B6A4C1 cell line demonstrated defects in Ca^{2+} mobilization mediated by both PLCγ and PLCβ-activating receptors (Field et al., 2000). Although it is possible that activated Cdc42 reconstitutes Ca^{2+} responses in B6A4C1 cells via a direct interaction with PLCγ, PLCβ is activated downstream of an adenosine-specific G-protein coupled receptor in RBL cells, and its structure and mechanism of activation are very different from FcεRI-mediated activation of PLCγ (Rhee, 2001). Thus, it seems unlikely that defective signaling in B6A4C1 cells stems from a specific deficiency in stimulated PLC activity. Although *in vitro* data initially suggested some physical interaction between Cdc42 and PLCγ in RBL-2H3 cells, this was not enhanced by FcεRI activation (Hong-Geller and Cerione, 2000). Furthermore, antigen-stimulated activation of PLCγ, detected as stimulated tyrosine phosphorylation of this protein, occurs equally well in both B6A4C1 and RBL-2H3 cells (Field et al., 2000). As PLCγ and PLCβ share a common substrate (PIP_2), the hydrolysis of which leads to Ca^{2+} mobilization, we hypothesized that a defect in stimulated PIP_2 synthesis is a more likely deficiency in the B6A4C1 cell line. A model summarizing possible mechanisms is presented in Figure 2.7.

A critical step in PIP_2 synthesis is phosphorylation of phosphatidylinositol 4-phosphate (PI4P) at the D-5 position of the inositol ring, by type I phosphatidylinositol 4-phosphate 5-kinases (PIP5K) (Van den Bout and Divecha, 2009). RhoA was the first member of the Rho GTPase family shown to stimulate PIP5K activity (Chong et al., 1994), and subsequent studies revealed that overexpression of either wt Rac1 or wt Cdc42 resulted in positive regulation of specific PIP5-kinase isoforms, leading to increased levels of cellular PIP_2 (Weernink et al., 2004). RhoA and Rac1 both bind directly to PIP5-kinase isoforms in a nucleotide-independent

Figure 2.7**. Model for the mechanism by which Cdc42 regulates Ca^{2+} mobilization in RBL mast cells.** Antigen crosslinks IgE/FcεRI complexes to initiate a tyrosine phosphorylation cascade that results in the activation of both PLCγ and Cdc42. Hydrolysis of PIP_2 by PLCγ produces IP_3 that mediates Ca^{2+} release from ER stores to cause SOCE, which facilitates degranulation. Our results demonstrate that activation of Cdc42 is important for a sustained Ca^{2+} response to antigen, including sustained Ca^{2+} oscillations. Reconstitution of antigen-stimulated PIP_2 oscillations in B6A4C1 cells by Cdc42 G12V suggests that this Rho protein maintains elevated PIP_2 levels during ongoing hydrolysis by PLCγ.

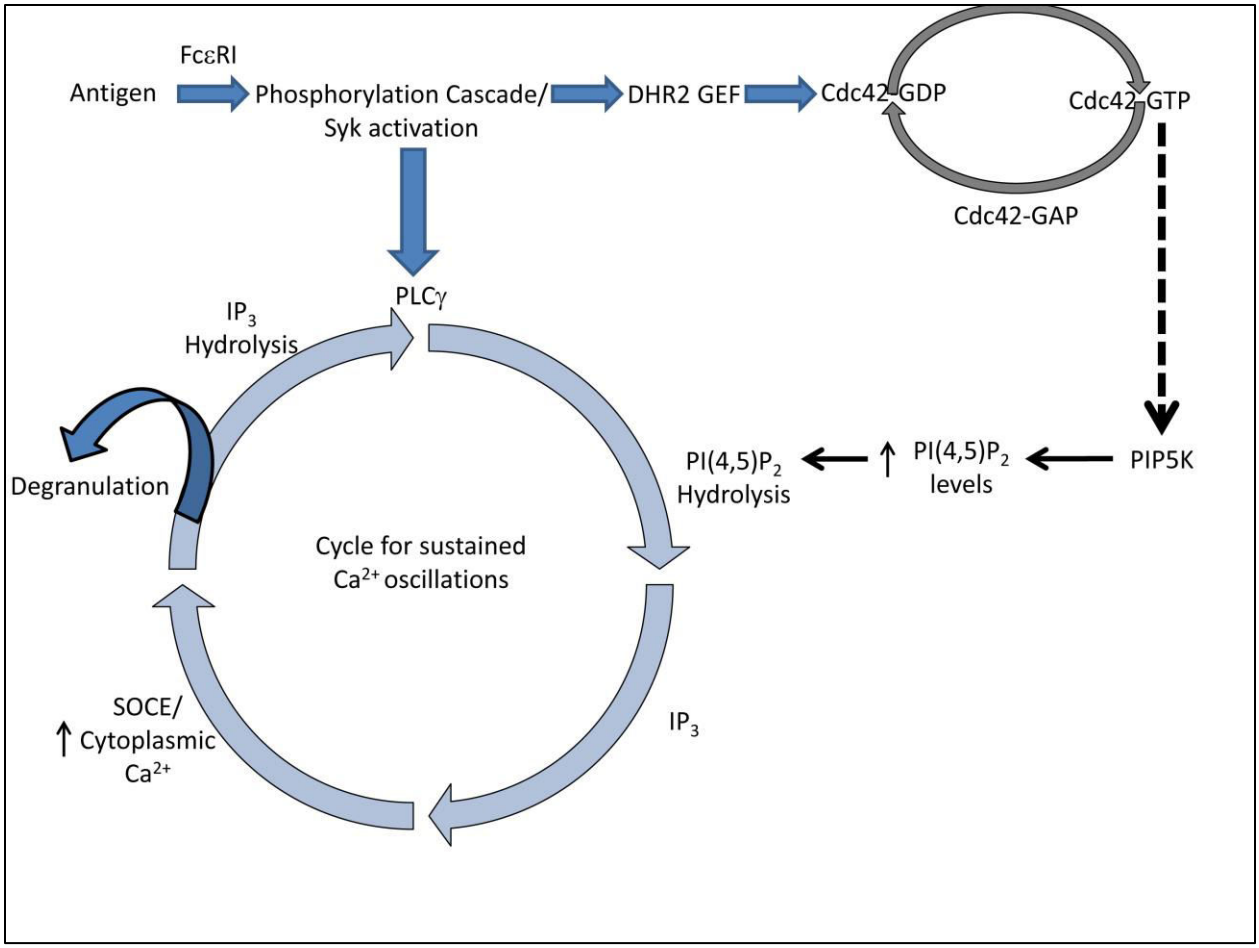
FcεRI
Antigen
Phosphorylation Cascade/
Syk activation
DHR2 GEF
Cdc42-GDP
Cdc42-GTP
Cdc42-GAP
PLCγ
IP3
Hydrolysis
Degranulation
PI(4,5)P2
Hydrolysis
PI(4,5)P2
levels
PIP5K
Cycle for sustained
Ca2+ oscillations
SOCE/
Cytoplasmic
Ca2+
IP3

manner, suggesting an important functional role for these Rho family GTPases in recruiting PIP_2-forming kinases to specific cellular compartments (Chatah and Abrams, 2001). Rac1 has been shown to bind to PIP5-kinase isoforms through an RKR motif located in its C-terminal sequence immediately preceding its CAAX motif (van Hennik et al., 2003), and this motif is positioned similarly to the di-arginine motif of Cdc42 that is critical for Ca^{2+} signaling in RBL mast cells (Figs. 2.2, 2.3, and 2.4), as well as for transformation of NIH 3T3 cells by activated Cdc42 (Johnson et al., 2012). Cdc42 and Rac1 share high sequence homology, and these results emphasize the importance of this polybasic motif for this pathway of Rho-family GTPase-mediated signaling. Our results in Figure 2.6 provide evidence that the regulation of PIP_2 levels at the plasma membrane by antigen activation of Cdc42 is the crucial upstream process that is defective in the B6A4C1 cells and necessary for stimulation of sustained Ca^{2+} oscillations and receptor endocytosis.

In summary, our results support a critical role for the activation of Cdc42 in FcεRI signaling in mast cells. Activated Cdc42 reconstitutes normal antigen-stimulated Ca^{2+} mobilization and consequent exocytosis in mutant B6A4C1 cells, including sustained Ca^{2+} and PIP_2 oscillations, and the conserved polybasic di-arginine motif of Cdc42 is important for this function. Cdc42 G12V, as well as the Rho GEF DOCK7, restores sustained Ca^{2+} oscillations in mutant B6A4C1 cells to normal RBL-2H3 levels. Restoration by activated Cdc42 of crosslinking-dependent FcεRI endocytosis in B6A4C1 cells, a Ca^{2+} independent process, suggests that this Rho family GTPase regulates Ca^{2+} mobilization in mast cells by acting on an event upstream of PLCγ activation, possibly by mediating stimulated synthesis of phosphatidylinositol 4,5-bisphosphate (Fig. 2.7). Future studies will evaluate the molecular mechanism by which activated Cdc42 regulates PIP_2 levels under conditions of FcεRI signaling.

2.5 MATERIALS AND METHODS

Cell Culture: RBL-2H3 and B6A4C1 cells were cultured as monolayers in minimal essential medium (Invitrogen Corp., Carlsbad, CA) with 20% fetal bovine serum (Atlanta Biologicals, Atlanta, GA) and 10 μg/ml gentamicin sulfate (Invitrogen) as previously described (Gosse et al., 2005).

Reagents and Chemicals: Cytochalasin D and other chemicals were purchased from Sigma-Aldrich (St. Louis, MO).

Expression Plasmids: The genetically encoded calcium indicator, GCaMP3, previously described (Tian et al., 2009), was purchased from Addgene (plasmid #22692). DNA plasmids pcDNA3.0, Cdc42 G12V, Cdc42 G12V/QQ, Cdc42 T17N, Dock7, and Cool2 were generously provided by Dr. Richard Cerione (Cornell University, Ithaca, NY). Super-ecliptic pHluorin, as a fusion with transferrin receptor (human) in the vector jPA5 (Merrifield et al., 2005), was obtained from Dr. P. De Camilli (Yale University, New Haven, CT).

To create the VAMP8-pHluorin-fusion construct, the transferrin receptor sequence was removed from the jPA5 construct using EcoRI and AgeI sites and replaced with cDNA encoding VAMP8 (mouse, Open Biosystems). PH-PLCδ-GFP (Varnai and Balla, 1998) was from Dr. Tamas Balla (National Institutes of Health).

Transfection: Both RBL-2H3 and B6A4C1 cell lines were transfected by electroporation under identical conditions for fluorimetry-based Ca^{2+} and exocytosis experiments, and for imaging-based Ca^{2+} and PIP_2 oscillation experiments. Cells were harvested three to five days after passage and ~ 1 x 10^7 cells were electroporated in 0.5 ml of cold electroporation buffer (137 mM NaCl, 2.7 mM KCl, 1 mM $MgCl_2$, 1 mg/ml glucose, 20 mM HEPES (pH 7.4) using 10 μg of reporter plasmid DNA (GCaMP3 for Ca^{2+}measurements, VAMP8-pHluorin for exocytosis

measurements, or PH-PLCδ-GFP for PIP_2 measurements) together with 30 μg of effector plasmid DNA (Cdc42 G12V, Cdc42 G12V/QQ, Cdc42 T17N, Dock7, Cool2, or pcDNA 3.0) at 280 V and 950 μF using Gene Pulser X (Bio-Rad). For fluorimetry-based experiments, cells were then plated in 100 mm dishes. For Ca^{2+} and PIP_2 oscillation experiments, electroporated cells were resuspended in 6 mls of medium and plated in three different MatTek dishes (2 ml/dish) (MatTek Corporation, Ashland, MA). For all experiments, cells were allowed to recover for 24 hours, then sensitized with 0.5 μg/ml anti-2,4-dinitrophenyl (DNP) IgE (Posner et al., 1992) for ~12 hours (total recovery time of 36 hours).

Cdc42 Activation Assay: Relative Cdc42 activities were measured using a colorimetric G-LISA assay (Cytoskeleton, Denver, CO). RBL-2H3 and B6A4C1 cells were plated in 35 mm dishes (Greiner Bio One Cellstar) at a density of 1 X 10^5 cells/ml and sensitized with IgE. Cells were then washed once with buffered saline solution (BSS: 135 mM NaCl, 5 mM KCl, 1 mM $MgCl_2$, 1.8 mM $CaCl_2$ 5.6 mM D(+) glucose, 20 mM HEPES, pH 7.4) and cells were stimulated for either one or three minutes at 37°C with 0.2 μg/ml multivalent DNP-BSA (Posner et al., 1992), then processed according to the manufacturer's instructions, except that a lysis buffer containing 25mM Tris, pH7.4, 100mM NaCl, 1mM EDTA, 1% (v/v) Triton 100, 1 mM sodium orthovanadate, 1 mM β-glycerol phosphate, 1 μg/mL leupeptin, and 1 μg/ml aprotinin was used.

Ca^{2+} Measurements: Cytoplasmic Ca^{2+} levels were measured using an SLM 8100C steady-state fluorimeter (SLM Instruments, Urbana, IL). Cells previously electroporated with GCaMP3 and the effector plasmid DNA of interest were allowed to recover as described above and then harvested using PBS/EDTA and resuspended in 1.8 ml BSS devoid of Ca^{2+}. Cells were then incubated and stirred at 37ºC for 5 minutes, and GCaMP3 levels were monitored (excitation 490 nm, emission 520 nm). Following addition of 5 μM EGTA to chelate trace amounts of

extracellular Ca^{2+} that remain, cells were stimulated with 0.2 µg/ml DNP-BSA to monitor Ca^{2+} release from stores. 1.8 mM $CaCl_2$ was then adder to monitor SOCE. To compare magnitudes of Ca^{2+} responses, cells were then lysed by 0.1% Triton X-100 to obtain the maximum value of GCaMP3 fluorescence, then 5 mM EGTA was added to determine background fluorescence, and this differential was used to normalize Ca^{2+} responses.

Integrated values for antigen-stimulated Ca^{2+} release from stores were determined using GraphPad-Prism software. SOCE was quantified 100 s after addition of 1.8 mM Ca^{2+} to avoid the transient increase in Ca^{2+} that is observed upon Ca^{2+} addition even in the absence of stimulation (Cohen et al., 2009).

For imaging analysis of Ca^{2+}oscillations, cells expressing GCaMP3 were washed into BBS and incubated for 5 minutes at 37ºC within a confined heating chamber prior to live cell imaging. GCaMP3 fluorescence was monitored for twenty seconds prior to addition of 0.2 µg/ml DNP-BSA, and Ca^{2+} oscillations were monitored over a time interval of 10 m using a 40X H_20 heated objective on a Zeiss 710 confocal microscope. GCaMP3 was excited using the 488-nm line of a krypton/argon laser and viewed with a 502-551 nm band-pass filter.

Offline image analysis was conducted using ImageJ (National Institutes of Health). Changes in GCaMP3 fluorescence were normalized by dividing the maximum GCaMP3 fluorescence value by the initial fluorescence basal level monitored before DNP-BSA addition. Transient increases in GCaMP3 fluorescence were scored as oscillations if the transient peak was at least half of the maximum GCaMP3 fluorescence peak response observed for an individual cell.

Statistical analysis of Ca^{2+} oscillations was conducted by counting and averaging the number of oscillatory peaks over a 5 minute time interval, beginning immediately following the initial calcium transient.

Exocytosis Measurements: Antigen-stimulated exocytosis was monitored as time-dependent increases in VAMP8-pHluorin fluorescence using the SLM 8100C steady-state fluorimeter. RBL-2H3 cells were electroporated with VAMP8-pHluorin and an effector plasmid DNA (Cdc42 G12V, Cdc42 G12V/QQ or pcDNA 3.0), then allowed to recover for 24 hours, sensitized as described above, and resuspended in 1.8 ml of BSS as for measurements of Ca^{2+} responses. Cells were preincubated at 37ºC with 0.2 μM of cytochalasin D for 6 minutes, then exocytosis was stimulated by addition of 0.2 μg/ml DNP-BSA, and increases in VAMP8-pHluorin fluorescence levels were monitored over a 10 min time interval. 50 mM NH_4Cl was then added to rapidly neutralize the acidic environment of endosomes, resulting in a dequenching of VAMP8-pHluorin and revealing total values for VAMP8-pHluorin fluorescence. Net exocytosis was typically observed ~5 min following DNP-BSA addition.

Endocytosis Measurements: As described above, ~ 1 x 10^7 RBL-2H3 or B6A4C1 cells were electroporated with 10 μg of mRFP and 30 μg of pcDNA 3.0 or 10 μg of mRFP and 30μg of Cdc42 G12V. Cells were allowed to recover for approximately 24 hours, then sensitized with 2 μg/ml Alexa-488 IgE for 1.5 hours, washed in BSS, and stimulated with 800 ng/ml DNP-BSA at 37ºC for 15 minutes +/- 1.8 mM $CaCl_2$. Cells were then fixed with 4% paraformaldehyde + 0.1% glutaraldehyde, labeled with an anti-Alexa Fluor 488 primary antibody (Invitrogen) followed by Alexa 647-anti-rabbit IgG secondary antibody in PBS with 1 mg/ml BSA, and imaged on a Zeiss 710 confocal microscope using a 63x oil objective. 300 positively transfected cells (detected by mRFP) were scored for IgE receptor endocytosis.

PH-PLCδ-GFP Measurements: ~ 1 x 10^7 RBL-2H3 or B6A4C1 cells were electroporated with PH-PLCδ-GFP and either pcDNA 3.0 or Cdc42 G12V. Cells were allowed to recover for approximately 24 hours, washed into BBS, and preincubated with 2 μM cytochalasin D for 5 minutes at 37ºC prior to live cell imaging to prevent stimulated cell ruffling and spreading. PH-PLCδ-GFP fluorescence was monitored for twenty seconds prior to addition of 0.2 μg/ml DNP-BSA, and PH-PLCδ-GFP oscillations were monitored over a time interval of 15 min using a 40X water objective in a confined heating chamber on a Zeiss 710 confocal microscope. Images were analyzed by selecting a region of interest within the cytoplasm of positively transfected cells using ImageJ and normalized to baseline fluorescence prior to antigen addition. 16-17 cells were analyzed for each individual experiment, and cells were scored as to whether or not they exhibited at least 5 antigen-stimulated PIP_2 oscillations during the time period of 100 to 1000 seconds following addition of antigen.

Statistical Analyses: Statistical analysis was performed with Prism software (Graphpad) and Microsoft Excel. All bar graphs display mean ± SEM unless otherwise noted. For the Cdc42 activation assay statistical significance was determined by a Two-Way ANOVA (Analysis of Variance) with replication followed by Tukey's post test. The statistical significance of all other figures was determined by a One-Way ANOVA (Analysis of Variance) followed by Tukey's post test. Level of significance is denoted as follows: $*P < 0.05$, $**P < 0.01$, $***P < 0.001$.

ACKNOWLEDGEMENTS

We thank Dr. Jon Erickson (Cornell University) for helpful discussions and a critical reading of the manuscript, and Carol Bayles for maintaining the Cornell Imaging Facility. I also thank Dr. Josh Wilson for creating the VAMP8-pHluorin construct used in this chapter. This work was supported by the National Science Foundation Graduate Research Fellowship under Grant No. NSF DGE-1144153 (MMW), and was also supported through grant RO1 AI022499 (DH) from the National Institutes of Health (NIAID) and grant F32GM095183 (JDW) from the National Institutes of Health (NIGMS). This manuscript has been published in the journal Biology Open.

1

REFERENCES

Abraham SN and St John AL. (2010). Mast cell-orchestrated immunity to pathogens. *Nat. Rev. Immunol.* 10, 440-452.

Chatah NE and Abrams CS. (2001). G-protein-coupled receptor activation induces the membrane translocation and activation of phosphatidylinositol-4-phosphate 5-kinase I alpha by a rac- and rho-dependent pathway. *J. Biol. Chem.* 276, 34059-34065.

Chong LD, Traynor-Kaplan A, Bokoch GM, Schwartz MA. (1994). The small GTP-binding protein rho regulates a phosphatidylinositol 4-phosphate 5-kinase in mammalian cells. *Cell* 79, 507-513.

Cohen R, Torres A, Ma HT, Holowka D, Baird B. (2009). Ca2+ waves initiate antigen-stimulated Ca2+ responses in mast cells. *J. Immunol.* 183, 6478-6488.

Cote JF and Vuori K. (2007). GEF what? Dock180 and related proteins help rac to polarize cells in new ways. *Trends Cell Biol.* 17, 383-393.

El-Sibai M, Backer JM. (2007). Phospholipase C gamma negatively regulates Rac/Cdc42 activation in antigen-stimulated mast cells. *Eur. J. Immunol.* 37, 261-270.

Erickson JW and Cerione RA. (2004). Structural elements, mechanism, and evolutionary convergence of rho protein-guanine nucleotide exchange factor complexes. *Biochemistry* 43, 837-842.

Field KA, Apgar JR, Hong-Geller E, Siraganian RP, Baird B, Holowka D. (2000). Mutant RBL mast cells defective in Fc epsilon RI signaling and lipid raft biosynthesis are reconstituted by activated rho-family GTPases. *Mol. Biol. Cell* 11, 3661-3673.

Furuichi K, Rivera J, Isersky C. (1984). The fate of IgE bound to rat basophilic leukemia cells. III. relationship between antigen-induced endocytosis and serotonin release. *J. Immunol.* 133, 1513-1520.

Galli SJ, Maurer M, Lantz CS. (1999). Mast cells as sentinels of innate immunity. *Curr. Opin. Immunol.* 11, 53-59.

Gosse, J.A., Wagenknecht-Wiesner, A., Holowka, D., and Baird, B. (2005). Transmembrane sequences are determinants of immunoreceptor signaling. *J. Immunol.* 175, 2123–2131.

Hajnoczky G and Thomas AP. (1997). Minimal requirements for calcium oscillations driven by the IP3 receptor. *Embo. J.* 16, 3533-3543.

Hart MJ, Eva A, Evans T, Aaronson SA, Cerione RA. (1991). Catalysis of guanine nucleotide exchange on the CDC42Hs protein by the dbl oncogene product. *Nature* 354, 311-314.

Hasegawa, H., Kiyokawa, E., Tanaka, S., Nagashima, K., Gotoh,N., Shibuya, M., Kurata, T., and Matsuda, M. (1996). DOCK180, a major CRK-binding protein, alters cell morphology upon translocation to the cell membrane. *Mol. Cell. Biol.* 16, 1770−1776.

Holowka D, Calloway N, Cohen R, Gadi D, Lee J, Smith NL, Baird B. (2012). Roles for Ca(2+) mobilization and its regulation in mast cell functions. *Front. Immunol.* 3, 104.

Hong-Geller E, Cerione RA. (2000). Cdc42 and Rac stimulate exocytosis of secretory granules by activating the IP(3)/calcium pathway in RBL-2H3 mast cells. *J. Cell Biol.* 148, 481-494.

Hong-Geller E, Holowka D, Siraganian RP, Baird B, Cerione RA. (2001). Activated Cdc42/Rac reconstitutes Fcepsilon RI-mediated Ca2+ mobilization and degranulation in mutant RBL mast cells. *Proc. Natl. Acad. Sci. U.S.A.* 98, 1154-1159.

Johnson JL, Erickson JW, Cerione RA. (2012). C-terminal di-arginine motif of Cdc42 protein is essential for binding to phosphatidylinositol 4,5-bisphosphate-containing membranes and inducing cellular transformation. *J. Biol. Chem.* 287, 5764-5774.

Kim TD, Eddlestone GT, Mahmoud SF, Kuchtey J, Fewtrell C. (1997). Correlating Ca2+ responses and secretion in individual RBL-2H3 mucosal mast cells. *J. Biol. Chem.* 272:31225-31229.

Kulkarni, K., Yang, J., Zhang, Z., and Barford, D. (2011). Multiple factors confer specific Cdc42 and Rac protein activation by dedicator of cytokinesis (DOCK) nucleotide exchange factors. *J. Biol. Chem.* 286, 25341−25351.

Le Floc'h A, Tanaka Y, Bantilan NS, Voisinne G, Altan-Bonnet G, Fukui Y, Huse M. (2013). Annular PIP3 accumulation controls actin architecture and modulates cytotoxicity at the immunological synapse. *J. Exp. Med.* 210, 2721-2737.

Ma HT and Beaven MA. (2011). Regulators of Ca(2+) signaling in mast cells: Potential targets for treatment of mast cell-related diseases? *Adv. Exp. Med. Biol.* 716, 62-90.

Mazucato VM, Silveira E Souza AM, Nicoletti LM, Jamur MC, Oliver C. (2011). GD1b-derived gangliosides modulate FcepsilonRI endocytosis in mast cells. *J. Histochem. Cytochem.* 59, 428-440.

Meller N, Merlot S, Guda C. (2005). CZH proteins: A new family of rho-GEFs. *J. Cell Sci.* 118, 4937-4946.

Merrifield, C. J., Perrais, D. and Zenisek, D. (2005). Coupling between clathrin-coated-pit invagination, cortactin recruitment, and membrane scission observed in live cells. Cell 121, 593-606.

Metz M, Siebenhaar F, Maurer M. (2008). Mast cell functions in the innate skin immune system. *Immunobiology* 213, 251-260.

Meyer T and Stryer L. (1991). Calcium spiking. *Annu. Rev. Biophys. Biophys. Chem.* 20, 153-174.

Millard PJ, Ryan TA, Webb WW, Fewtrell C. (1989). Immunoglobulin E receptor cross-linking induces oscillations in intracellular free ionized calcium in individual tumor mast cells. *J. Biol. Chem.* 264, 19730-19739.

Miyamoto, Y., Yamauchi, J., Sanbe, A., and Tanoue, A. (2007). Dock6, a Dock-C subfamily guanine nucleotide exchanger, has the dual specificity for Rac1 and Cdc42 and regulates neurite outgrowth. *Exp. Cell Res.* 313, 791−804.

Nishikimi A, Kukimoto-Niino M, Yokoyama S, Fukui Y. (2013). Immune regulatory functions of DOCK family proteins in health and disease. *Exp. Cell Res.* 319, 2343-2349.

Oliver, C., Sahara, N., Kitani, S., Robbins, A.R., Mertz, L.M., and Siraganian, R.P. (1992). Binding of monoclonal antibody AA4 to gangliosides on rat basophilic leukemia cells produces changes similar to those seen with Fcε receptor activation. *J. Cell Biol.* 116, 635–646.

Parekh AB and Putney JW, Jr. (2005). Store-operated calcium channels. *Physiol. Rev.* 85, 757-810.

Posner, R. G., B. Lee, D. H. Conrad, D. Holowka, B. Baird, B. Goldstein (1992). Aggregation of IgE-receptor complexes on rat basophilic leukemia cells does not change the intrinsic affinity but can alter the kinetics of the ligand-IgE interaction. *Biochemistry* 31, 5350-5356.

Rhee SG. (2001). Regulation of phosphoinositide-specific phospholipase C. *Annu. Rev. Biochem.* 70, 281-312.

Santos Mde S, Naal RM, Baird B, Holowka D. (2013). Inhibitors of PI(4,5)P2 synthesis reveal dynamic regulation of IgE receptor signaling by phosphoinositides in RBL mast cells. *Mol. Pharmacol.* 83, 793-804.

Stauffer TP, Ahn S, Meyer T. (1998). Receptor-induced transient reduction in plasma membrane PtdIns(4,5)P2 concentration monitored in living cells. *Curr Biol* 8, 343-346.

Stracke, M.L., Basciano, L.K., and Siraganian, R.P. (1987). Binding properties and histamine release in variants of rat basophilic leukemia cells with changes in the IgE receptor. *Immunology Letters* 14, 287-292.

Takai S, Hasegawa H, Kiyokawa E, Yamada K, Kurata T, Matsuda M. (1996). Chromosomal mapping of the gene encoding DOCK180, a major crk-binding protein, to 10q26.13-q26.3 by fluorescence in situ hybridization. *Genomics* 35, 403-404.

Tian L, Hires SA, Mao T, Huber D, Chiappe ME, Chalasani SH, Petreanu L, Akerboom J, McKinney SA, Schreiter ER, et al. (2009). Imaging neural activity in worms, flies and mice with improved GCaMP calcium indicators. *Nat Methods* 6, 875-881.

Van den Bout I and Divecha N. (2009). PIP5K-driven PtdIns(4,5)P2 synthesis: Regulation and cellular functions. *J. Cell Sci.* 122, 3837-3850.

van Hennik PB, ten Klooster JP, Halstead JR, Voermans C, Anthony EC, Divecha N, Hordijk PL. (2003). The C-terminal domain of Rac1 contains two motifs that control targeting and signaling specificity. *J. Biol. Chem.* 278, 39166-39175.

Varnai P and Balla T. (1998). Visualization of phosphoinositides that bind pleckstrin homology domains: Calcium- and agonist-induced dynamic changes and relationship to myo-[3H]inositol-labeled phosphoinositide pools. *J Cell Biol* 143, 501-510.

Vig M and Kinet JP. (2009). Calcium signaling in immune cells. *Nat. Immunol.* 10, 21-27.

Vig M, Peinelt C, Beck A, Koomoa DL, Rabah D, Koblan-Huberson M, Kraft S, Turner H, Fleig A, Penner R, et al. (2006). CRACM1 is a plasma membrane protein essential for store-operated Ca2+ entry. *Science* 312, 1220-1223.

Watabe-Uchida, M., John, K. A., Janas, J. A., Newey, S. E., and Van Aelst, L. (2006). The Rac activator DOCK7 regulates neuronal polarity through local phosphorylation of stathmin/Op18. *Neuron* 51, 727−739.

Weernink PA, Meletiadis K, Hommeltenberg S, Hinz M, Ishihara H, Schmidt M, Jakobs KH. (2004). Activation of type I phosphatidylinositol 4-phosphate 5-kinase isoforms by the rho GTPases, RhoA, Rac1, and Cdc42. *J. Biol. Chem.* 279, 7840-7849.

Wollman R and Meyer T. (2012). Coordinated oscillations in cortical actin and Ca2+ correlate with cycles of vesicle secretion. *Nat. Cell Biol.* 14, 1261-1269.

Wu M, Wu X, De Camilli P. (2013). Calcium oscillations-coupled conversion of actin travelling waves to standing oscillations. *Proc. Natl. Acad. Sci. U.S.A.* 110, 1339-1344.

Yamauchi, J., Miyamoto, Y., Chan, J. R., and Tanoue, A. (2008). ErbB2 directly activates the exchange factor Dock7 to promote Schwann cell migration. *J. Cell. Biol.* 181, 351−365.

Zhou Y, Johnson JL, Cerione RA, Erickson JW. (2013). Prenylation and membrane localization of Cdc42 are essential for activation by DOCK7. Biochemistry 52, 4354-4363.

Chapter 3

PIP_3, Cdc42 and PKC play critical roles in antigen-stimulated PIP_2 synthesis, Ca^{2+} oscillations, and degranulation in RBL mast cells

3.1 ABSTRACT

Phosphatidylinositol 4,5-bisphosphate (PIP_2) is essential for many cellular processes, despite being a minor phospholipid component of the plasma membrane. As receptor stimulation often results in hydrolysis and depletion of PIP_2, a mechanism must exist to synthesize PIP_2 following receptor activation. Rho GTPases are implicated in PIP_2 synthesis, as well as in FcεRI mast cell degranulation, although the mechanisms by which they regulate these processes remain unclear. In this study we utilize RBL-2H3 mast cells, as well as a mutant RBL cell line, B6A4C1, that is deficient in antigen-stimulated Cdc42 activation and degranulation, to investigate the connection between Rho GTPase activation, PIP_2 synthesis, and degranulation. We find that antigen stimulation of RBL-2H3 cells results in increased PIP_2 levels and activation of Cdc42, which oscillates on and off the plasma membrane in response to stimulation. Increases in $PIP_{2,}$ and Cdc42 activation are not observed in antigen-stimulated B6A4C1 cells. Pharmacological inhibitors of Cdc42, PI3-kinase, and PKC strongly inhibit both antigen and thapsigargin-stimulated degranulation in RBL-2H3 cells. Cdc42 and PI3-kinase inhibition is bypassed by direct pharmacological activation of PKC. Antigen-stimulated PKC activation, as monitored by disassociation of MARCKS-ED-mRFP from the plasma membrane, is partially inhibited in B6A4C1 cells. Constitutively active Cdc42-G12V reconstitutes antigen-stimulated MARCKS dissociation from the plasma membrane. Finally, we demonstrate that the atypical Rho GTPase GEF, DOCK8, reconstitutes stimulated exocytosis in B6A4C1 cells, suggesting that it is through the DOCK GEF family that Cdc42 is activated to regulate PIP_2 synthesis. DOCK GEFs contain

PIP_3 binding domains, suggesting a novel hypothesis for why a PI3-kinase specific concentration of wortmannin inhibits degranulation in mast cells.

3.2 INTRODUCTION

Inositol lipids, constructed from a diacylglycerol (DAG) backbone linked to an inositol ring, and reversibly phosphorylated at positions 3, 4, and 5, transduce important signals from cellular receptors, and serve as the source of many second messengers (Tóth et al. 2016). These lipids are essential for many cellular functions, and misregulation leads to a variety of disease states, making their regulation an intense area of research (Di Paolo and Kim 2011; Di Paolo and De Camilli 2006). However, the rapid dynamics and low abundance of many inositol lipids makes studying their function and regulation difficult.

Phosphatidylinositol 4,5-bisphosphate (PIP_2) is one such phosphoinositide species, comprising less than 1% of all lipids found at the plasma membrane (Wenk et al. 2003; Ferrell and Huestis 1984). Despite its low abundance, PIP_2 is appreciated as a master regulator of cellular membranes and cellular signaling, in part, because it is important for endocytosis and exocytosis, and it acts as the substrate for phosphoinositide 3-kinases, as well as the substrate for phospholipase C (PLC) isoforms, which hydrolyze PIP_2 and generate Ca^{2+} mobilization in non-excitable cells (Raucher et al. 2000). Originally appreciated in G-protein coupled receptors, hydrolysis of PIP_2 occurs following stimulation of many different receptor types, including B-cell receptors, T-cell receptors, some neuronal receptors (Micheva, Holz, and Smith 2001), and many other immune cell specific receptors (Balla 2013). The high-affinity receptor for immunoglobulin E (IgE), FcεRI, highly expressed on the mast cell surface, is one such receptor, and antigen-mediated crosslinking of FcεRI/IgE complexes leads to a signaling cascade that

results in PIP_2 hydrolysis, Ca^{2+} mobilization, and exocytosis of secretory granules and recycling endosomes (Holowka et al. 2012).

An interesting aspect of Ca^{2+} mobilization in mast cells and many other cell types is the generation of sustained Ca^{2+} oscillations (Millard et al. 1988; Ryan, Millard, and Webb 1990). These oscillations result as the direct byproduct of PIP_2 hydrolysis, inositol 1,4,5- trisphosphate (IP_3) production, and Ca^{2+} release from the endoplasmic reticulum (ER) (Prince WT 1973; Woods, Cuthbertson, and Cobbold 1986). How sufficient PIP_2 is generated to produce sustained Ca^{2+} oscillations, despite its low abundance and constant receptor-stimulated hydrolysis, remains poorly understood. Rho GTPases Rho A, Rac1, and Cdc42 are interesting candidates for regulating receptor-stimulated PIP_2 synthesis, as their over-expression has been shown to increase PIP_2 synthesis by increasing the activity of type 1 phosphoinositide 5-kinase (PIP5-kinase) isoforms lα, lβ, and lγ (Chong et al. 1994; Weernink et al. 2004). Cdc42 is particularly interesting, as its over-expression has been shown to increase PIP_2 synthesis despite not directly interacting with PIP5-kinases, as Rho A and Rac1 have been demonstrated to do (Weernink et al. 2004)

To better understand the role of Cdc42 in receptor stimulated PIP_2 synthesis we compared RBL-2H3 mast cells with B6A4C1 cells, a chemically mutagenized RBL-2H3 cell line selected for deficiency in stimulated degranulation (Stracke et al. 1987; Oliver et al. 1992), and later characterized as deficient in receptor-stimulated Cdc42 activation (Wilkes et al. 2014). Over the course of this study, we determined that antigen stimulation results in an increase in PIP_2 levels in RBL-2H3 cells, whereas an increase in PIP_2 is not observed in stimulated B6A4C1 cells. To further characterize this difference we confirmed that receptor-mediated Cdc42 activation does not occur in B6A4C1 cells, and we now demonstrate that activation of protein kinase C

(PKC) is partially inhibited in this cell line. PKC activation can be reconstituted in these cells by expression of constitutively active Cdc42-G12V. PKC activation has previously been indicated to be important for PIP_2 production (Apgar 1995; Tóth et al. 2016), and this finding suggests an indirect mechanism by which Cdc42 may regulate receptor-mediated PIP_2 synthesis.

3.3 RESULTS

Antigen stimulation results in PIP_2 synthesis in RBL-2H3, but not in B6A4C1 cells.

Although it has long been recognized that RBL mast cell activation results in sustained Ca^{2+} oscillations, recent studies demonstrated that antigen-stimulation also results in oscillations of PIP_2 at the plasma membrane (Wollman and Meyer 2012; Wu, Wu, and De Camilli 2013). However, in contrast to Ca^{2+} oscillations, which typically appear within 15-45 seconds following stimulation, PIP_2 oscillations are frequently not observed until several minutes post stimulation. To determine if PIP_2 synthesis begins soon after antigen stimulation, or only at later time points when PIP_2 begins to oscillate, we expressed the PIP_2 marker, PH-PLCδ-EGFP, in RBL-2H3 cells, and monitored changes in stimulated PIP_2 levels using total internal reflection fluorescence (TIRF) microscopy. As shown in Figure 3.1A, and Supplementary Video 3.1, antigen-stimulation of RBL-2H3 cells results in the appearance of transient, bright puncta at the plasma membrane during the first several minutes of stimulation, which are not oscillatory at these time points. B6A4C1 cells, previously demonstrated to lack antigen-stimulated PIP_2 oscillations (Wilkes et al. 2014), also appear deficient in antigen-stimulated PIP_2 synthesis, as no new puncta are produced following stimulation during the same time period (Figure 3.1B). The total percentage of RBL-2H3 and B6A4C1 cells that exhibit antigen-stimulated PIP_2 synthesis as detected by this method is summarized in Figure 3.1C.

To quantify these observed differences by an independent method, we radiolabeled cells with [^{3}H]-inositol and compared antigen-stimulated [^{3}H]-PIP_2 synthesis between RBL-2H3 and B6A4C1 cells using an HPLC separation protocol. Antigen stimulation resulted in an ~ 43% increase in PIP_2 levels in RBL-2H3 cells, with no increase detected in B6A4C1 cells, as displayed in Figures 3.1D and E. These results confirm that B6A4C1 cells are not only deficient in antigen-stimulated degranulation and Cdc42 activation, but are also deficient in receptor-mediated PIP_2 synthesis.

DU40, BIM, and wortmannin inhibit antigen and thapsigargin-mediated RBL-2H3 degranulation. To further explore the connection between stimulated Cdc42 activation, PIP_2 synthesis, and degranulation, we next employed a pharmacological approach in RBL-2H3 cells. DU40, a geranylgeranyl transferase inhibitor (Peterson et al. 2006), prevents Rho GTPase localization to the plasma membrane, and inhibits antigen and thapsigargin-stimulated degranulation by ~70% and ~60% respectively, in a standard β-hexosaminidase degranulation assay (Figure 3.2A). However, addition of a PKC activating DAG analog, phorbol 12-myristate-13-acetate (PMA), bypasses this inhibition. A chemically inactive analog of DU40, SN, shows no significant degranulation inhibition (Figure 3.2A). As PKC activation by PMA bypasses DU40 inhibition we further evaluated the role that PKC may play in degranulation. PKC is known to be important for RBL signaling (Gadi et al. 2011; Ozawa et al. 1993) and certain isoforms have been shown to be effectors of Cdc42 (Cook et al. 2006; Coghlan, Chou, and Carpenter 2000). Consistent with previous literature (Martiny-Baron et al. 1993) the PKC inhibitor bisindolylmaleimide I (BIM), which is an active site inhibitor of all PKC isoforms,

Figure 3.1**. Antigen stimulation results in PIP_2 synthesis in RBL-2H3, but not B6A4C1 cells.** **A-B**: RBL-2H3 and B6A4C1 cells were electroporated with PH-PLCδ-EGFP, sensitized with IgE, stimulated with 200 ng/ml multivalent DNP-BSA and monitored using TIRF microscopy. **C**: Percentage of RBL-2H3 or B6A4C1 cells undergoing stimulated PIP_2 synthesis, as determined by formation of new PIP_2 puncta at the plasma membrane. Video was taken for 15 min for the RBL-2H3 cell. As stimulated PIP_2 synthesis was strongly observed within 3 min of stimulation, future videos were taken for 7-10 min. The B6A4C1 video here was taken for 7.5 min. Error bars indicate ± standard error of the mean of 6-8 independent experiments (n=10 cells for both cell lines) (** represents P-values <.01). **D and E**: RBL-2H3 and B6A4C1 cells were labeled with [^{3}H]-inositol, in inositol free medium for 24 hours, sensitized with IgE, and stimulated with 200 ng/ml DNP-BSA for 5 min at 37°. Perchloric acid was added to stop stimulation and precipitate lipids, following which cells were harvested and lipids were extracted and % total [3H]-inositol detected as phosphatidylinositol 4,5-bisphosphate (PIP_2) was quantified using HPLC. Unstimulated cells were then normalized to 100% and percent PIP_2 increase caused by antigen addition is displayed in **D** for RBL-2H3 cells and **E** for B6A4C1 cells. Error bars are ± standard deviation for 3 separate experiments.

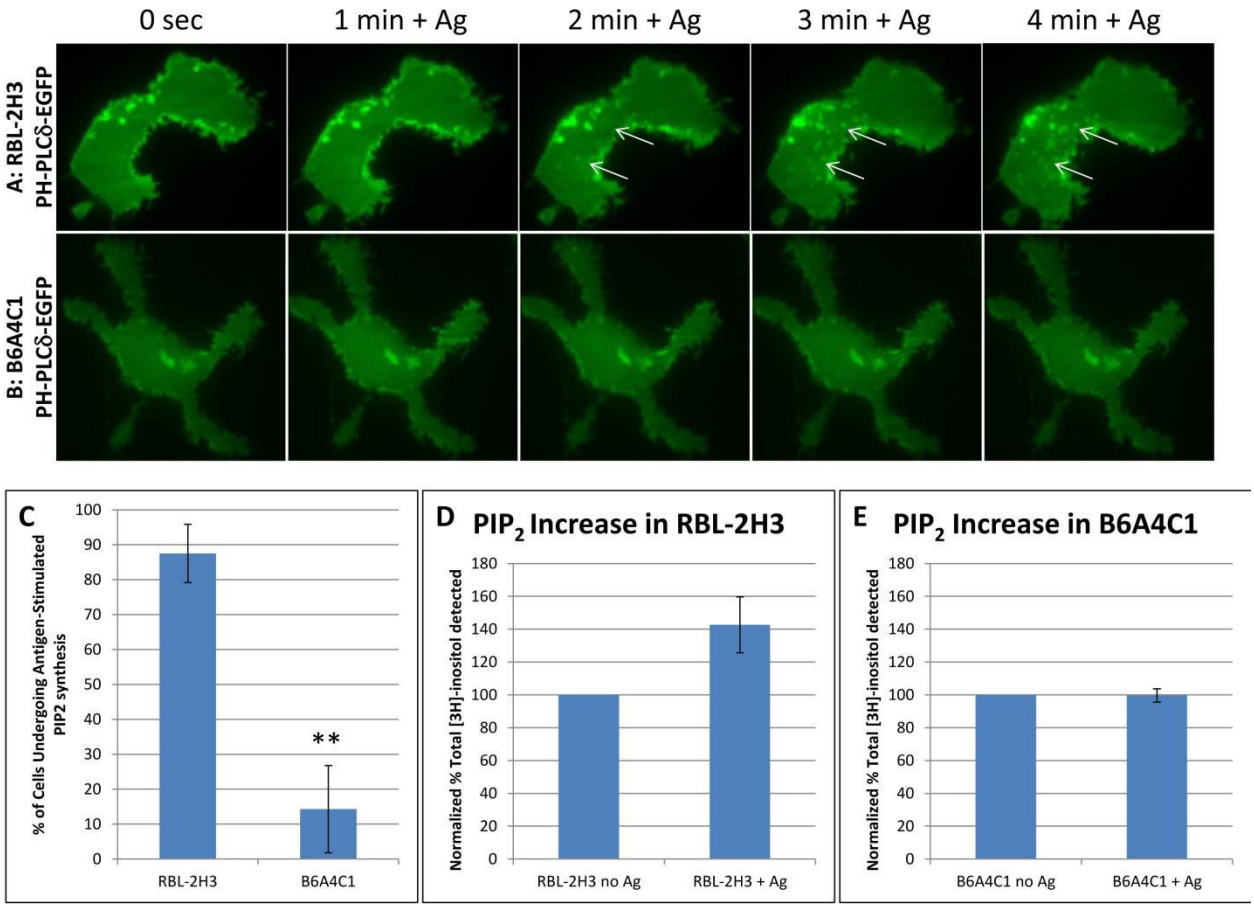
0 sec
1 min + Ag
2 min + Ag
3 min + Ag
4 min + Ag
A: RBL-2H3 PH-PLCδ-EGFP
B: B6A4C1 PH-PLCδ-EGFP
C
% of Cells Undergoing Antigen-Stimulated PIP2 synthesis
**
RBL-2H3
B6A4C1
D
PIP2 Increase in RBL-2H3
Normalized % Total [3H]-inositol detected
RBL-2H3 no Ag
RBL-2H3 + Ag
E
PIP2 Increase in B6A4C1
Normalized % Total [3H]-inositol detected
B6A4C1 no Ag
B6A4C1 + Ag

strongly inhibits antigen-stimulated degranulation by greater than 90% and thapsigargin-mediated degranulation by ~85% (Figure 3.2B). As expected, PMA does not overcome inhibition by BIM. PI3-kinases have also been previously shown to be important for RBL-2H3 signaling (Ching et al. 2001; Gilfillan and Tkaczyk 2006), although the exact mechanism by which they participate is unclear. Figure 3.2B demonstrates that 200 nM wortmannin, selective for PI3-kinase inhibition at this concentration, also inhibits antigen and thapsigargin-mediated degranulation, and this inhibition is also bypassed by addition of PMA, indicating PIP_3 is necessary for RBL mast cell degranulation upstream of PKC activation.

BIM enhances stimulated Ca^{2+} responses, but suppresses Ca^{2+} oscillations, whereas DU40 and wortmannin inhibit sustained Ca^{2+} oscillations. Rho GTPases have previously been shown to affect Ca^{2+} responses in mast cells (Hong-Geller et al. 2001; Field et al. 2000; Wilkes et al. 2014). We next investigated the effect of BIM, DU40, and wortmannin on antigen-stimulated Ca^{2+} responses to determine if their capacity to inhibit stimulated degranulation was a direct result of suppressing Ca^{2+} mobilization. RBL-2H3 cells were electroporated with the genetically encoded Ca^{2+} indicator, GCaMP3, and stimulated with antigen in the presence or absence of inhibitors and monitored via fluorimetry. An optimal dose of antigen leads to an initial peak in cytoplasmic Ca^{2+}, dominated by Ca^{2+} release from intracellular stores (R.S), as well as a more sustained phase following the initial peak that lasts for many minutes, indicative of store operated Ca^{2+} entry (SOCE), as displayed in Figure 3.3A. Despite its complete inhibition of degranulation, BIM shows no inhibition of Ca^{2+} responses, rather causing a small enhancement of the R.S. response and an ~40% enhancement of SOCE (Figure 3.3B, I, J) when compared to untreated cells. Wortmannin treatment inhibits the peak response and SOCE by

Figure 3.2. **DU40, BIM, and wortmannin inhibit antigen and thapsigargin-mediated RBL-2H3 degranulation**. Degranulation of RBL-2H3 cells treated with DU40 and SN (**A**), or BIM and wortmannin (**B**). RBL-2H3 cells were sensitized overnight with IgE. DU40 and SN were added at a concentration of 10μM for 24 hours prior to stimulation. BIM was added at a final concentration of 5μM, and wortmannin was added at 200nM concentration, for 5 min before stimulation. Cells were then stimulated with 200ng/ml DNP-BSA (Ag), 250nM Thapsigargin (Thaps), or 250nM Thapsigargin plus 80nM phorbol 12-myristate-13-acetate (PMA), or not stimulated to determine spontaneous degranulation (Spon) for 45 min at 37°, as indicated. Cellular supernatants were collected and analyzed for β-hexosaminidase release. Degranulation is expressed as a percent of the total β-hexosaminidase released by TX-100 lysis of cells plated under identical conditions.

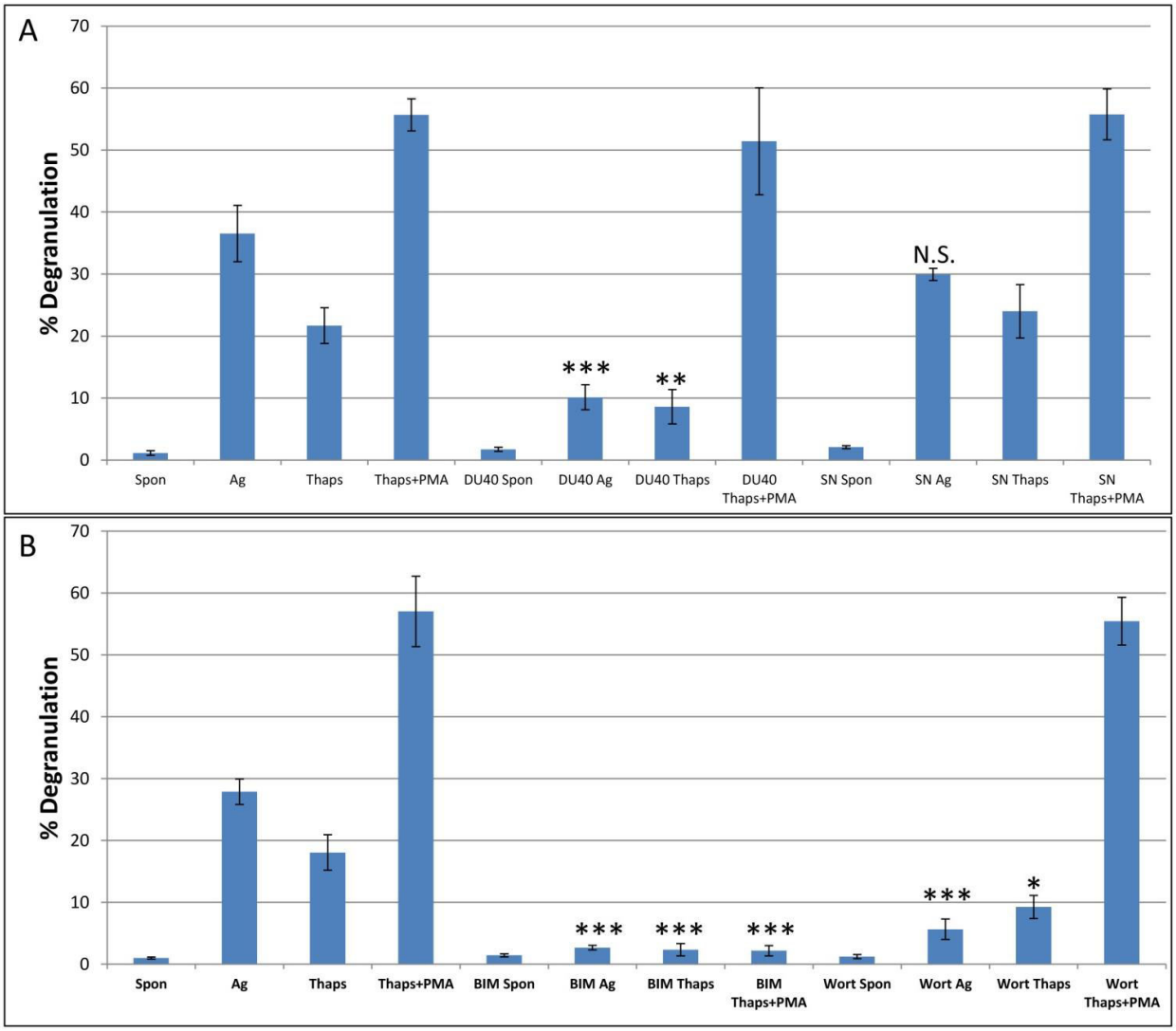
A
% Degranulation
70
60
50
40
30
20
10
0
***
**
N.S.
Spon
Ag
Thaps
Thaps+PMA
DU40 Spon
DU40 Ag
DU40 Thaps
DU40 Thaps+PMA
SN Spon
SN Ag
SN Thaps
SN Thaps+PMA
B
% Degranulation
70
60
50
40
30
20
10
0
***
***
***
***
*
Spon
Ag
Thaps
Thaps+PMA
BIM Spon
BIM Ag
BIM Thaps
BIM Thaps+PMA
Wort Spon
Wort Ag
Wort Thaps
Wort Thaps+PMA

~30% and 50% respectively (Figure 3.3C, I, J). DU40 shows no statistical significant inhibition of the peak response, but does show some small (~16%) inhibition of SOCE (Figure 3.3D, I, J).

To further evaluate these inhibitor's effect on Ca^{2+} responses, we again electroporated GCaMP3 into RBL-2H3 cells, and monitored stimulated Ca^{2+} oscillations, which are not discernable in bulk cell fluorimetry assays, on a cell by cell basis using confocal microscopy. A representative trace of stimulated Ca^{2+} oscillations in the absence of inhibitor is displayed in Figure 3.3E. Treatment with BIM completely inhibits all Ca^{2+} oscillations that follow the one or two initial oscillations due to R.S. (Figure 3.3F). Wortmannin does not inhibit the capacity of cells to oscillate, but, rather, sustained oscillations are consistently suppressed, beginning ~3 minutes following antigen stimulation (Figure 3.3G). DU40 also begins to inhibit late stage Ca^{2+} oscillations, although not as strongly as wortmannin (Figure 3.3H). The total number of Ca^{2+} oscillations were quantified and averaged over 30 cells from 3 separate experiments for all conditions, and results are summarized in Figure 3.3K. While the inhibitory effects of wortmannin on stimulated R.S. and SOCE are substantial and might be sufficient to explain its capacity to inhibit degranulation, Ca^{2+} results obtained using BIM and DU40 suggest that these inhibitors may inhibit a process independent of their effect on Ca^{2+}, as BIM enhances Ca^{2+} responses (although suppressing Ca^{2+} oscillations), and DU40 shows only modest inhibitory effects on Ca^{2+} signaling.

BIM, Wortmannin, and DU40 inhibit antigen stimulated PIP_2 synthesis in RBL-2H3 cells. BIM, wortmannin, and DU40 all inhibit thapsigargin-mediated degranulation (Figure 3.2), suggesting they have effects downstream of IP_3-dependent Ca^{2+} release from ER stores. Because of this, we evaluated whether the stimulated PIP_2 synthesis described in Figure 1 depends on Ca^{2+} mobilization and SOCE. RBL-2H3 cells were electroporated with the PIP_2 reporter,

Figure 3.3. **BIM enhances stimulated Ca^{2+} responses, but suppresses Ca^{2+} oscillations, whereas DU40 and wortmannin inhibit sustained Ca^{2+} oscillations.** Ca^{2+} responses of RBL-2H3 cells treated with BIM, DU40, and wortmannin. **A-D**: IgE-sensitized RBL-2H3 cells expressing GCaMP3 were stimulated in BSS with 200 ng/ml of DNP-BSA (Ag) at 100 sec. Cells were either untreated with inhibitor (**A**), treated for 5 min stimulation with 5μM BIM (**B**) or 200nM wortmannin (**C**), or treated for 24 hours with 10μM DU40, prior to stimulation. Initial fluorescent peak represents Ca^{2+} release from stores (R.S.), and the more sustained fluorescent increase represents store operated Ca^{2+} entry (SOCE). R.S was calculated at peak fluorescence following antigen addition, and SOCE was calculated at 150 seconds following this peak. **I and J**: Summary of 4 independent experiments monitoring changes in (**I**) peak GCaMP3 fluorescence due primarily to stimulated Ca^{2+} release from stores and (**J**) sustained SOCE after 2.5 min of stimulation. *Error bars* indicate ± s.d. for 3 separate experiments. **E-H**: RBL-2H3 cells were electroporated with GCaMP3, plated in MatTek dishes, sensitized with IgE, and treated with the various inhibitors identically as described in **A-D**. 200 ng/ml DNP-BSA was at ~t=20 seconds for all conditions. Representative responses of individual cells are shown. Summary of Ca2+ oscillations is described in **K**. Error bars indicate ± s.e.m. for 30 individual cells from 3 separate experiments for each condition shown (*** represents P-values <.001, ** represents P-values <0.01, * represents P-values <.05).

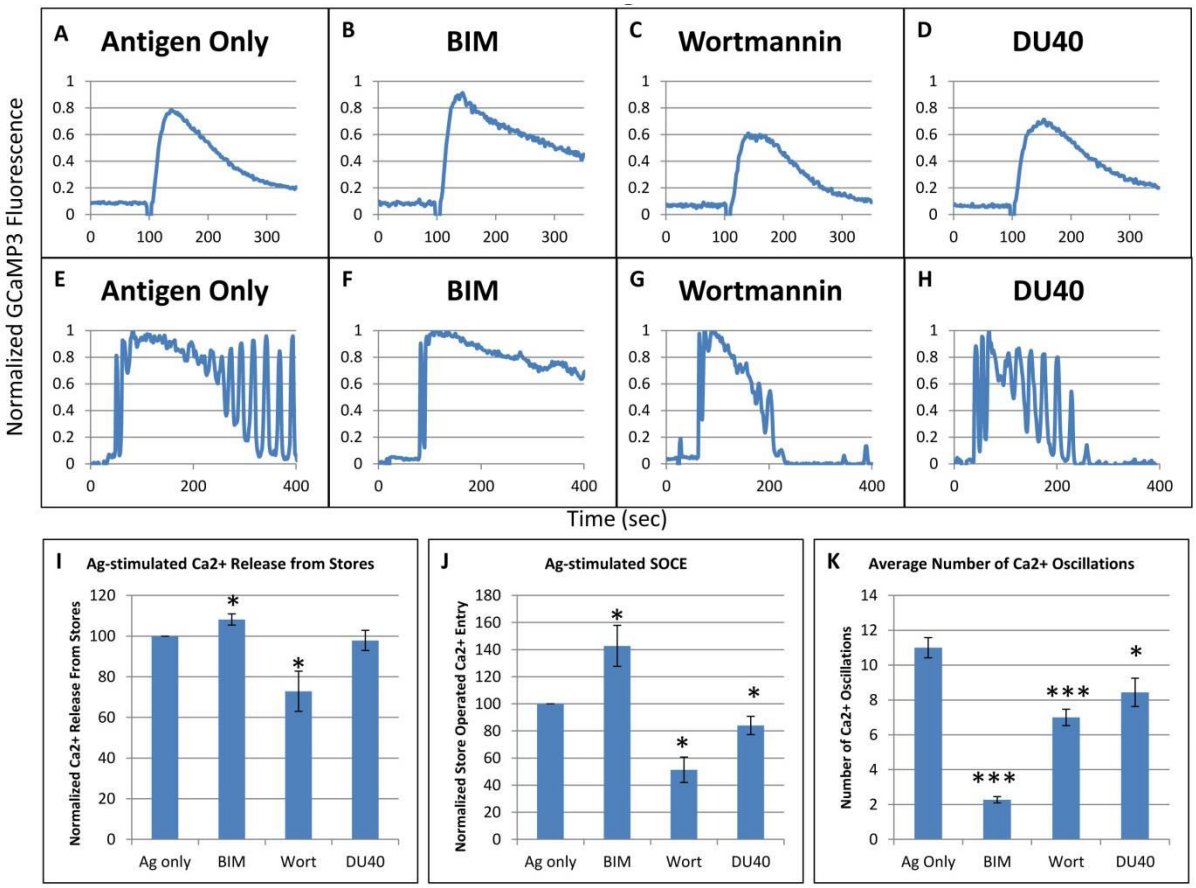
A Antigen Only
B BIM
C Wortmannin
D DU40
E Antigen Only
F BIM
G Wortmannin
H DU40
Normalized GCaMP3 Fluorescence
Time (sec)
I Ag-stimulated Ca2+ Release from Stores
Normalized Ca2+ Release From Stores
Ag only
BIM
Wort
DU40
J Ag-stimulated SOCE
Normalized Store Operated Ca2+ Entry
K Average Number of Ca2+ Oscillations
Number of Ca2+ Oscillations
Ag Only

PH-PLCδ-EGFP, allowed to recover overnight, and were then placed in Ca^{2+} free buffer, stimulated and monitored using TIRF. Even in the absence of extracellular Ca^{2+}, RBL-2H3 cells undergo stimulated PIP_2 synthesis as shown in Figure 3.4. We next evaluated the effects of BIM, wortmannin, and DU40 on stimulated PIP_2 synthesis using this method. As shown in Figure 3.4, all 3 of these inhibitors strongly suppress the number of cells undergoing antigen-stimulated PIP_2 synthesis, such that PIP_2 puncta formation was not observed in any of the cells treated with BIM, and wortmannin and DU40 inhibited this process in 80% and 82% of all cells, respectively.

Constitutively active Cdc42-G12V reconstitutes antigen-mediated PKC activation in B6A4C1 cells. As B6A4C1 cells are deficient in PIP_2 synthesis (Figure 1B, C, E), we investigated whether these cells are deficient in stimulated PKC activation. Upon activation, PKC is known to phosphorylate the protein myristoylated alanine-rich C-kinase substrate (MARCKS), which sequesters phosphatidylinositol 4-phosphate (PI4P) and PIP_2 at the plasma membrane in the absence of stimulated phosphoryation. RBL-2H3 and B6A4C1 cells were electroporated with the effector domain of MARCKS, fluorescently tagged with mRFP (MARCKS-ED-mRFP), which is sufficient for sequestering phosphoinositides at the plasma membrane in the absence of stimulated phosphorylation (Gadi et al. 2011). Cells were then stimulated and imaged using TIRF microscopy. In 85% of monitored RBL-2H3 cells, antigen stimulation results in displacement of MARCKS-ED-mRFP from the plasma membrane, resulting in decreased PM fluorescence. Following this initial displacement, MARCKS-ED-mRFP begins to oscillate on and off the membrane, as demonstrated in Figure 3.5A. In contrast, in 53% of all B6A4C1 cells observed, stimulation did not result in displacement of MARCKS-ED-mRFP from the membrane (Figure 3.5B, E), and the minor fluorescence decline observed is due to photobleaching. In the other 47% of stimulated B6A4C1 cells, MARCKS-ED-mRFP was

Figure 3.4. **BIM, wortmannin, and DU40 inhibit antigen stimulated PIP_2 synthesis in RBL-2H3 cells, which is a Ca^{2+} independent process.** Percentage of RBL-2H3 or B6A4C1 cells undergoing stimulated PIP_2 synthesis, as determined by formation of new PIP_2 puncta at the plasma membrane. RBL-2H3 were electroporated with PH-PLCδ-EGFP, sensitized with IgE, stimulated with 200 ng/ml multivalent DNP-BSA and monitored using TIRF microscopy. Cells were placed in Ca^{2+}-free BSS immediately prior to stimulation for no Ca^{2+} condition. Error bars indicate ± standard error of the mean of 6-8 independent experiments (n=10 cells for all conditions, except for DU40 where n=11) (*** represents P-values <.001. ** represents P-values <.01).

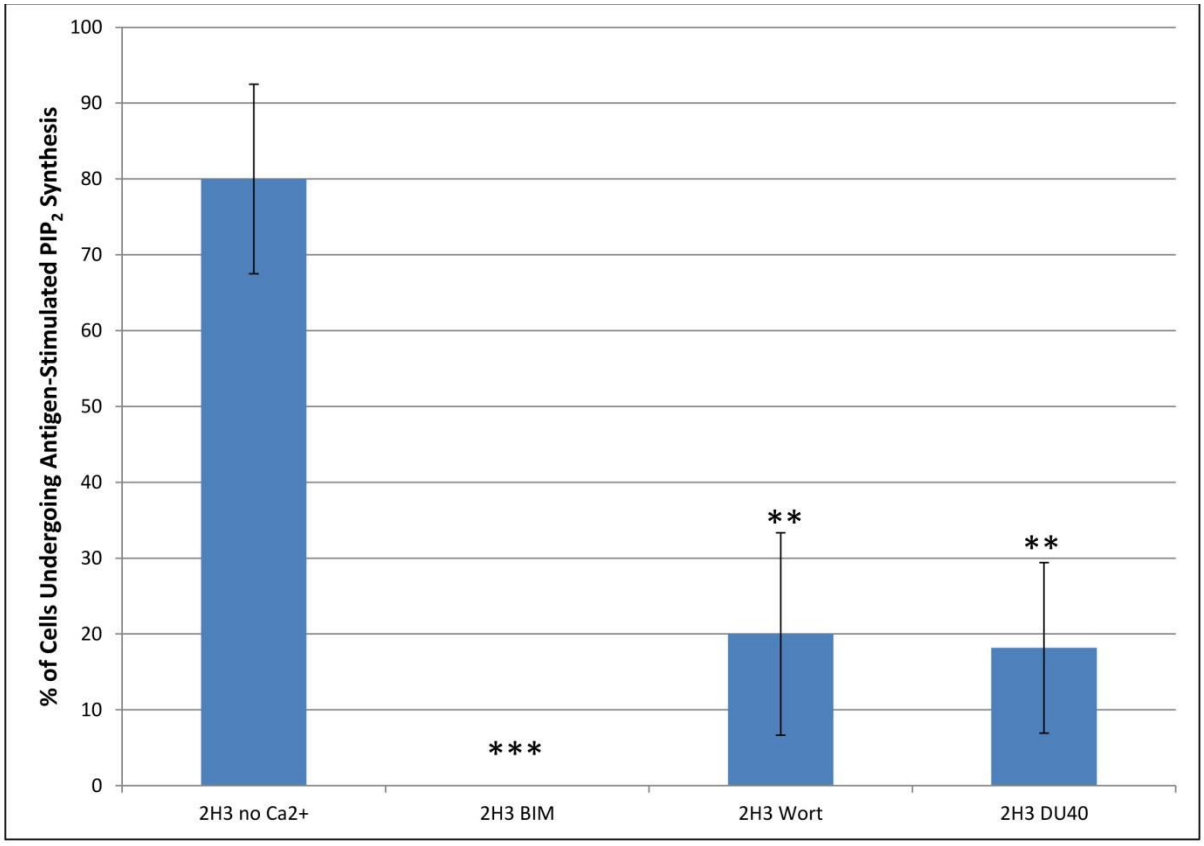
% of Cells Undergoing Antigen-Stimulated PIP2 Synthesis
100
90
80
70
60
50
40
30
20
10
0
***
**
**
2H3 no Ca2+
2H3 BIM
2H3 Wort
2H3 DU40

displaced, although subsequent oscillations were typically not observed (Figure 3.5C). Expression of the constitutively active mutant Cdc42-G12V increases the number of B6A4C1 cells that undergo stimulated MARCKS-ED-mRFP displacement from the plasma membrane to ~75% (Figure 3.5D, E). These results suggest that B6A4C1 cells are partially deficient in stimulated PKC activation, and Cdc42 may regulate degranulation and PIP_2 synthesis, in part, by regulating the activation of PKC.

Stimulated Cdc42 activation is an oscillatory process that is inhibited by wortmannin and is independent of extracellular Ca^{2+}. Wortmannin has previously been shown to reduce antigen-stimulated IP_3 production (Barker et al. 1995) and thapsigargin-stimulated degranulation (Cissel, Fraundorfer, and Beaven 1998) in RBL-2H3 cells, consistent with our results shown in Figures 3.2B and 3.3C, I, and J. Although mechanisms have been proposed to explain these effects, the inhibitory mechanism of wortmannin remains controversial. To determine if wortmannin treatment inhibits antigen-stimulated Cdc42 activation, we expressed a Crib Binding Domain-GFP construct (CBD-GFP), which binds to endogenous Cdc42 when the latter is activated, and we monitored stimulated changes in PM association of CBD-GFP in TIRF. Upon antigen stimulation, Cdc42 activation is observed in RBL-2H3 cells, as Cdc42 is recruited and activated at the plasma membrane as detected by CBD-GFP association. The activation and deactivation of Cdc42 occurs in a sustained, oscillatory manner as shown in Figure 3.6B. In the absence of antigen stimulation, no changes in the behavior of CBD-GFP are observed, as shown in Figure 3.6A. Stimulated Cdc42 oscillations are observed even in the absence of extracellular Ca^{2+}, as shown in Figure 3.6C. Activation of Cdc42 is not observed in B6A4C1 cells (Figure 3.6D). DU40 inhibits Cdc42 activation (Figure 3.6E), as does wortmannin (Figure 3.6F), suggesting it acts upstream of Cdc42 activation. These results are summarized in Figure 3.6G.

Figure 3.5. **Constitutively active Cdc42-G12V reconstitutes antigen-mediated PKC activation in B6A4C1 cells.** RBL-2H3 were electroporated with pcDNA and MARCKS-ED-mRFP (**A**). B6A4C1 cells were electroporated with MARCKS-ED-mRFP and pcDNA (**B, C**) or Cdc42-G12V (**D**), sensitized with IgE, and stimulated with 200ng/ml DNP-BSA at ~t=20 sec for all conditions. Cells were imaged using TIRF microscopy. **E**, Summary graph of % of cells with MARCKS-ED-mRFP displaced from the membrane following antigen stimulation. Error bars represent ± s.e.m from 15-20 independent experiments. For RBL-2H3 cells n=33, for B6A4C1 cells n=34, and for B6A4C1 cells expressing Cdc42-G12V n=17.

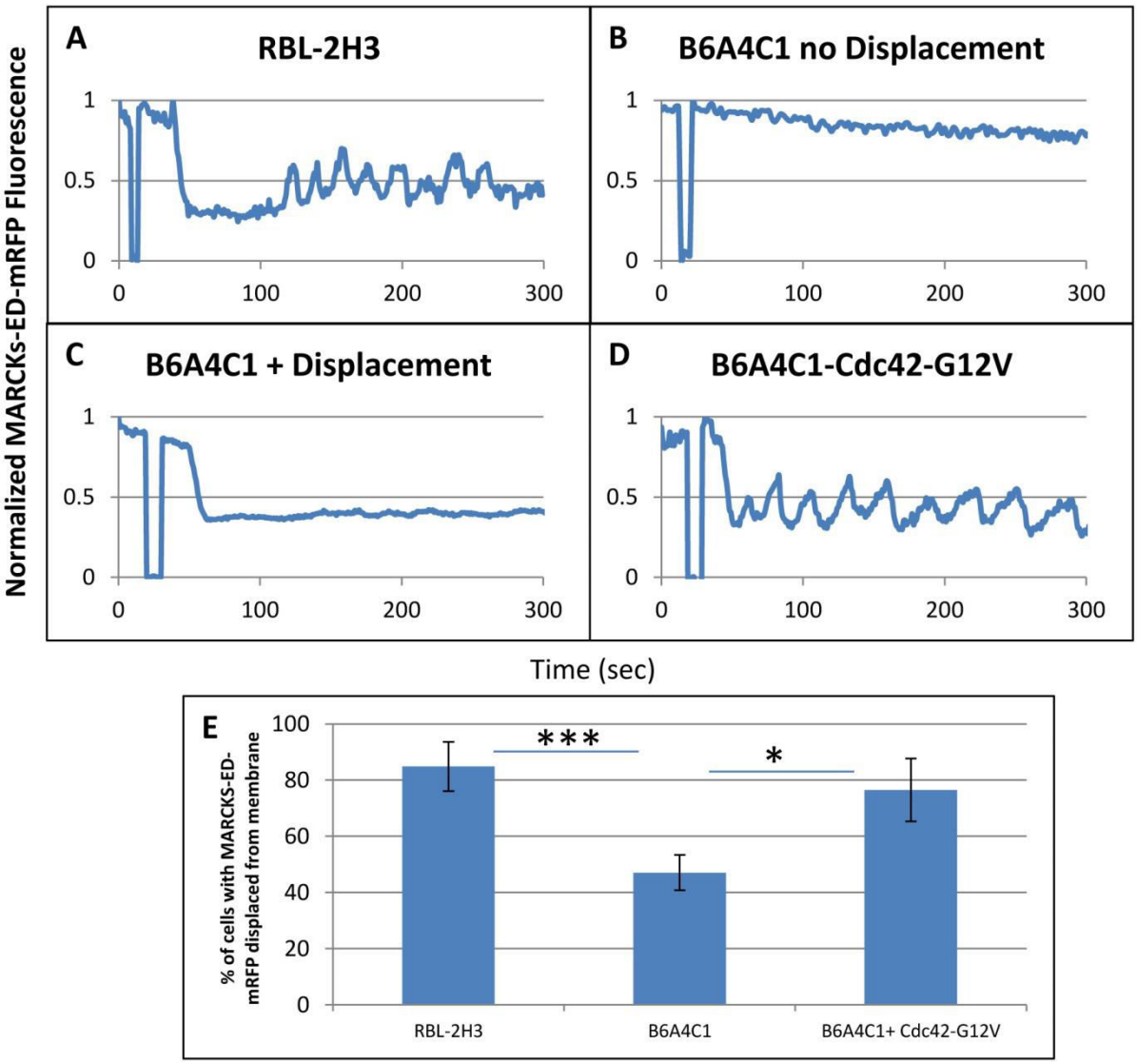
A
RBL-2H3
B
B6A4C1 no Displacement
C
B6A4C1 + Displacement
D
B6A4C1-Cdc42-G12V
Normalized MARCKs-ED-mRFP Fluorescence
1
0.5
0
0
100
200
300
Time (sec)

E
% of cells with MARCKS-ED-mRFP displaced from membrane
100
80
60
40
20
0
***
*
RBL-2H3
B6A4C1
B6A4C1+ Cdc42-G12V

VAMP8-mediated exocytosis is inhibited by BIM, is deficient in B6A4C1 cells, and reconstituted by DOCK8. Recent studies point to a role for the atypical Rho GTPase DOCK GEF family in mast cell signaling (Wilkes et al. 2014; Ogawa et al. 2014). These GEFs contain a DHR-1 domain which binds to phosphatidylinositol 3,4,5-trisphosphate (PIP_3), essential for DOCK localization to the plasma membrane, as well as a DHR-2 domain necessary for activation of both Cdc42 and Rac1 (Côté and Vuori 2007). As B6A4C1 cells are deficient in antigen-stimulated Cdc42 activation and probably Rac1 activation (Hong-Geller et al.), it is possible that the primary defect of these cells is the absence of a GEF capable of activating both Cdc42 and Rac1. Although we have previously shown that DOCK7, which is capable of activating Cdc42 and Rac, reconstitutes Ca^{2+} oscillations in B6A4C1 cells, we have never demonstrated the capacity of any GEF, Dbl or DOCK, to reconstitute stimulated exocytosis in mutant B6A4C1 cells. Using VAMP8-pHluorin as a marker for recycling endosomes, which are exocytosed upon antigen stimulation, we investigated whether DOCK8, recently shown in a shRNA mast cell screen to be a potential regulator of degranulation (Bambouskova et al. 2016), could reconstitute stimulated exocytosis in B6A4C1 cells. In RBL-2H3 cells, antigen stimulates VAMP8-pHluorin exocytosis. This process manifests as an increase in fluorescence, as the pHluorin tag, initially quenched in the acidic environment of the recycling endosome, becomes dequenched upon encountering the neutral pH environment of the extracellular space, as shown in Figure 3.7A. As B6A4C1 cells are partially defective in PKC activation, we explored whether BIM inhibited VAMP8-mediated exocytosis in RBL-2H3 cells. As shown in Figure 3.7B, BIM strongly inhibits this exocytic response. B6A4C1 cells do not undergo stimulated VAMP8-pHluorin exocytosis (Figure 3.7C). However, expression of DOCK8 in B6A4C1 cells fully reconstitutes antigen-stimulated VAMP8-phluorin exocytosis, as described in Figure 3.7D.

Figure 3.6. **Stimulated Cdc42 activation is an oscillatory process inhibited by wortmannin and is independent of extracellular Ca^{2+}. A-F:** RBL-2H3 and B6A4C1 cells were electroporated with a Crib-Binding-Domain-GFP (CBD-GFP) construct, sensitized with IgE, and stimulated with 200 ng/mL DNP-BSA at ~t=20 sec for all conditions, except for **A** where no DNP-BSA was added, to monitor spontaneous changes in Cdc42 activation in TIRF. **C**, cells were placed in Ca^{2+} free BSS prior to stimulation. **E,** RBL-2H3 cells were treated with 10μM DU40 for 24 hours prior to stimulation. **F**, RBL-2H3 cells were treated with 200 nM wortmannin for 5 minutes prior to DNP-BSA addition. **G**, summary of results from 7-10 different independent experiments. Error bars represent ± s.e.m from 10-14 cells for each condition quantified (RBL-2H3, B6A4C1, RBL-2H3 + Wort n=14 cells; RBL-2H3 no Ca^{2+}, RBL-2H3 + DU40 n=10 cells). (*** represents P-values <.001).

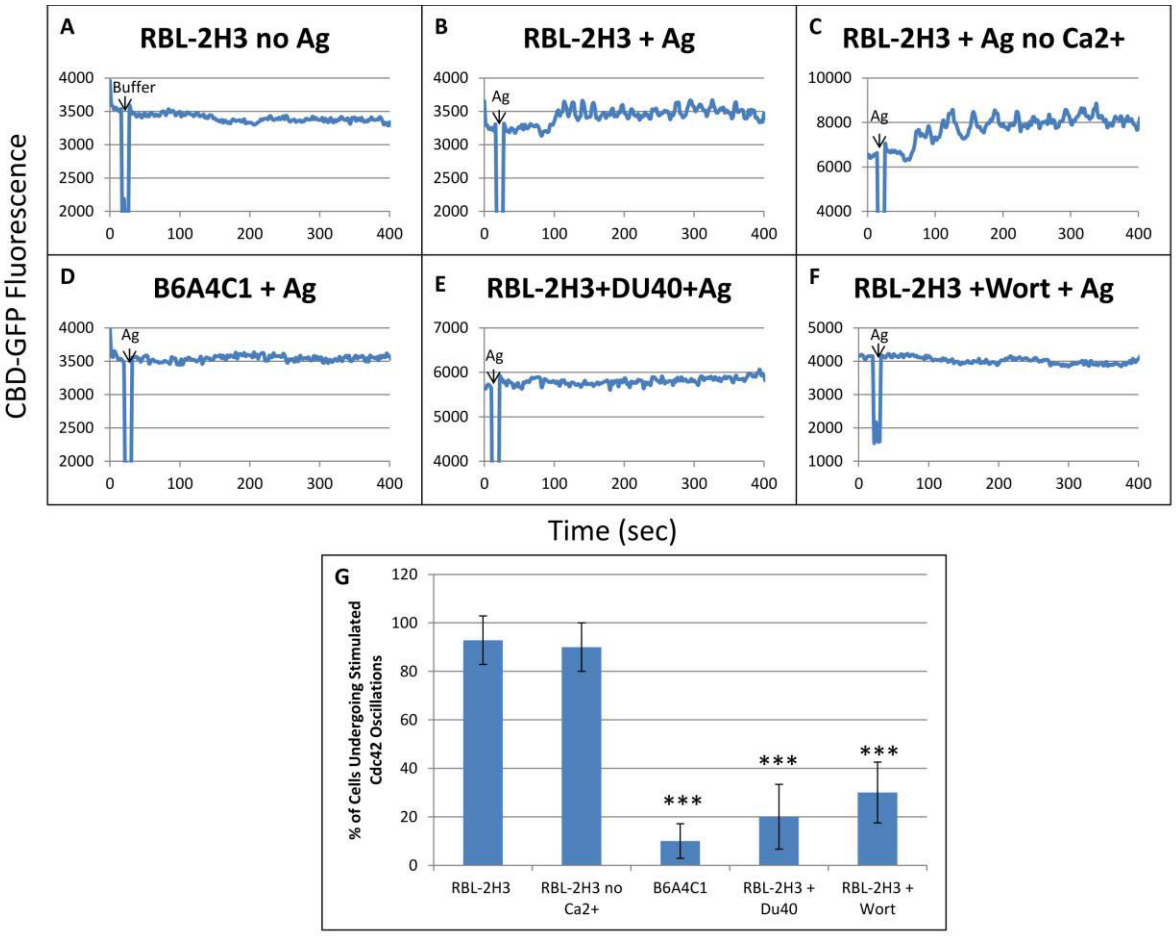
A
RBL-2H3 no Ag
Buffer
B
RBL-2H3 + Ag
Ag
C
RBL-2H3 + Ag no Ca2+
Ag
D
B6A4C1 + Ag
Ag
E
RBL-2H3+DU40+Ag
Ag
F
RBL-2H3 +Wort + Ag
Ag
CBD-GFP Fluorescence
Time (sec)
G
% of Cells Undergoing Stimulated Cdc42 Oscillations
RBL-2H3
RBL-2H3 no Ca2+
B6A4C1
RBL-2H3 + Du40
RBL-2H3 + Wort
***
***
***

However, the catalytically inactive mutant DOCK8 V/A, with a valine essential for GEF activity mutated to an alanine, did not reconstitute VAMP8-mediated exocytosis in B6A4C1 cells (Figure 3.7E). A summary of these responses, averaged over 50-60 cells for each of these conditions is summarized in Figure 3.7F.

3.4 DISCUSSION

Our findings reveal roles for PIP_3, Cdc42, and PKC in regulating antigen-stimulated PIP_2 synthesis and, as a result, for sustained Ca^{2+} oscillations and degranulation in RBL mast cells. A schematic depicting our main findings is shown in Figure 3.8. RBL-2H3 cells undergo stimulated PIP_2 synthesis, as determined by live cell TIRF microscopy and by HPLC fractionation following [^{3}H]-inositol radiolabeling and stimulation of RBL-2H3 cells. B6A4C1 cells have previously been characterized as deficient in antigen-stimulated Cdc42 activation and degranulation, although the connection between these two deficiencies was unclear. Here we identify antigen-stimulated PIP_2 synthesis as a novel deficiency in this mutant RBL cell line, suggesting, for the wild type RBL-2H3 cells, a clear connection between receptor-mediated Cdc42 activation, PIP_2 synthesis and degranulation.

To further elucidate the signaling pathways that connect these cellular events, we pharmacologically inhibited Cdc42, along with Rho A and Rac1, using the geranylgeranyl transferase inhibitor DU40, in RBL-2H3 cells. Previous studies have demonstrated that antigen-stimulation results in activation of both Cdc42 and Rac1, with Cdc42 activation occurring upstream of PKC activation, as BIM does not inhibit Cdc42 activation (El-Sibai and Backer 2007). Constitutively active Cdc42 and Rac1 have both been shown to reconstitute degranulation in B6A4C1 cells (Hong-Geller et al. 2001), suggesting they have some overlapping functions in

Figure 3.7. **VAMP8-mediated exocytosis is inhibited by BIM, is deficient in B6A4C1 cells, and reconstituted by DOCK8.** Representative traces taken from fields of 5-6 RBL-2H3 cells expressing VAMP8-pHluorin (**A-B**) and B6A4C1 cells expressing VAMP8-pHluorin and pcDNA (**C**), DOCK8 (**D**), or DOCK8 V/A (E). Cells were sensitized with IgE and stimulated in BSS with 200 ng/ml DNP-BSA at 20 sec. 50 mM NH_4Cl was added at ~400 sec to neutralize the cellular environment and dequench VAMP8-pHluorin to determine total amount of VAMP8-pHluorin expressed, enabling the calculation of percent exocytosis values. For RBL-2H3 cells treated in the presence of BIM (**B**), 5μM BIM was added 5 minutes prior to DNP-BSA addition. **F**: Summary of three independent experiments monitoring changes in VAMP8-pHluorin fluorescence due to DNP-BSA stimulation. Error bars indicate ± s.e.m for 55-60 cells for each condition tested (*** represents P-values <0.001)

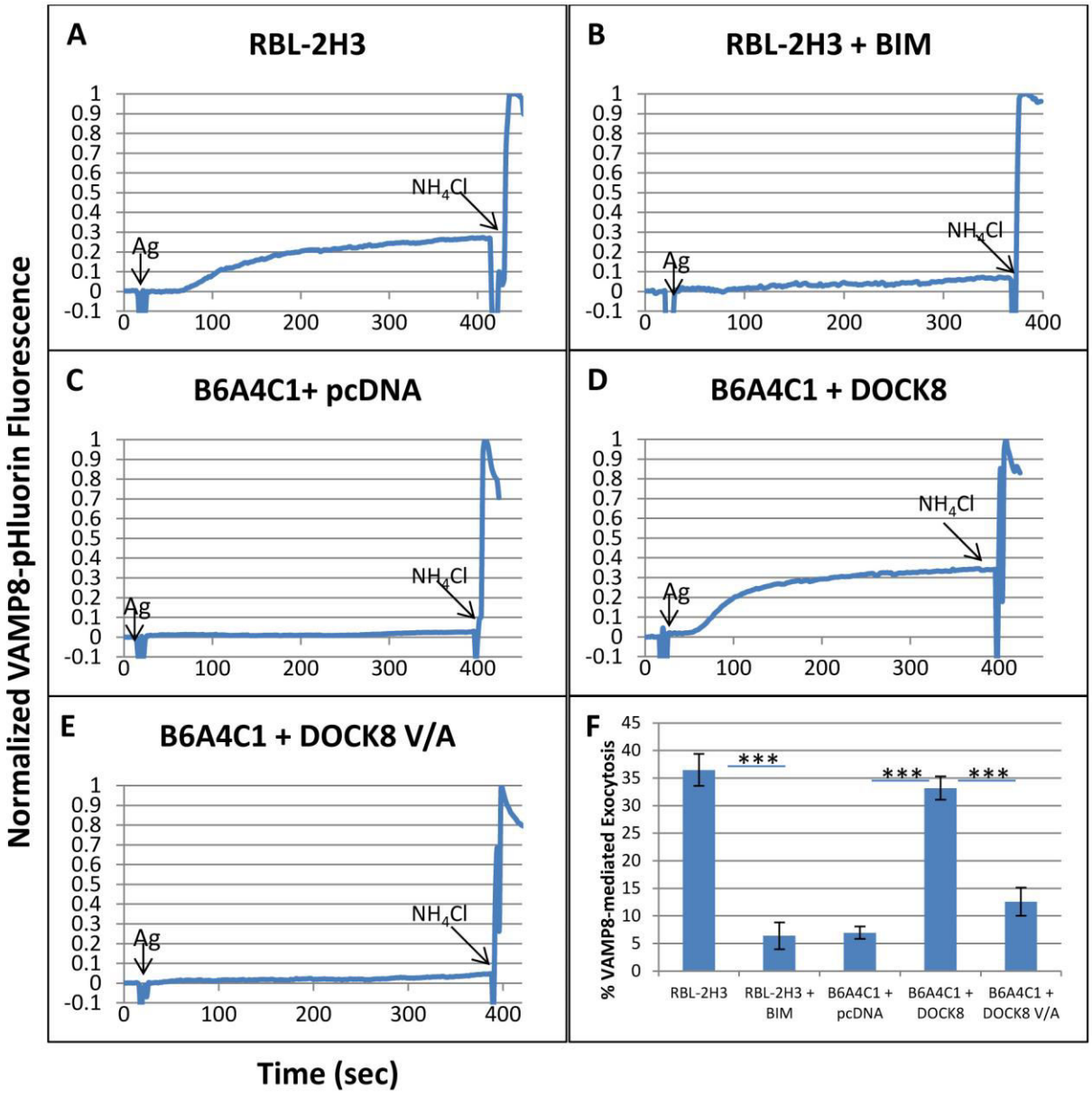
A
RBL-2H3
B
RBL-2H3 + BIM
C
B6A4C1+ pcDNA
D
B6A4C1 + DOCK8
E
B6A4C1 + DOCK8 V/A
F
Ag
NH4Cl
Normalized VAMP8-pHluorin Fluorescence
Time (sec)
% VAMP8-mediated Exocytosis
***
RBL-2H3
RBL-2H3 + BIM
B6A4C1 + pcDNA
B6A4C1 + DOCK8
B6A4C1 + DOCK8 V/A

RBL signaling. However, Rac1 does not reconstitute all defects in these mutant cells, despite reconstituting degranulation (Field et al. 2000). Recognizing that Rac1 activity may compensate for Cdc42 inhibition alone, we opted for a pharmacological approach that inhibited both Cdc42 and Rac1.

Using this approach we observed that DU40 treatment strongly inhibits antigen and thapsigargin-mediated degranulation, although this inhibition can be bypassed by direct activation of PKC with PMA, a trend also observed with wortmannin treatment. As a result, the effect of BIM, a PKC inhibitor, was evaluated and shown to strongly inhibit degranulation. Degranulation depends on Ca^{2+} mobilization, however, BIM actually enhances stimulated SOCE, suggesting the mechanism of inhibition is different. PKC activation has been shown to phosphorylate Orai1 and suppress SOCE; knockdown or inhibition of PKC conversely enhanced SOCE (Kawasaki et al. 2010), potentially explaining why we observe this enhancement. Our finding that BIM suppresses Ca^{2+} oscillations provides strong evidence that PKC is regulating PIP_2 availability, as PIP_2 hydrolysis is necessary to generate Ca^{2+} oscillations. Our findings that wortmannin and DU40 also inhibit sustained Ca^{2+} oscillations suggest that these inhibitors also affect PIP_2 levels. In a recent study conducted in RBL cells, stimulation by a leukotriene via a G-protein coupled receptor shows that reducing PIP_2 levels directly suppresses sustained Ca^{2+} oscillations (Alswied and Parekh 2015), consistent with our interpretation of our current results. Alswied and Parekh's findings also support the idea that studying stimulated Ca^{2+} oscillations is a useful, albeit indirect, readout of PIP_2 availability, and it can provide novel mechanistic insights not gleaned from more typical fluorimetry Ca^{2+} assays, which obscure oscillations in individual cells. We next showed that BIM, DU40, and wortmannin all strongly inhibit receptor-stimulated PIP_2 synthesis in RBL-2H3 cells using TIRF microscopy and PLCδ PH-EGFP to

Figure 3.8. **Summary depicting DOCK GEFs and Cdc42 signaling through PKC to increase PIP_2 levels necessary for sustained Ca^{2+} oscillations and degranulation.** Antigen stimulation results in the activation of Cdc42 and PKC, leading to increased levels of PI4P and PIP_2, necessary steps for exocytosis, PIP_2 resynthesis, and sustained PIP_2 hydrolysis. Wortmannin, in addition to inhibiting PLCγ1, potentially inhibits mast cell signaling by disrupting DOCK GEF DHR1 interactions with PIP_3, preventing DOCK translocation to the plasma membrane, and preventing Cdc42 activation by DOCK GEF DHR2, Ca^{2+} oscillations, and degranulation. The dotted black arrow pointing to PIP5K, representing PIP5K activation, is an important step in this pathway that is poorly understood and needs further investigation, although Rho GTPases are strong candidates for regulating this event, as described in text. Adapted from Wilkes et al., 2014.

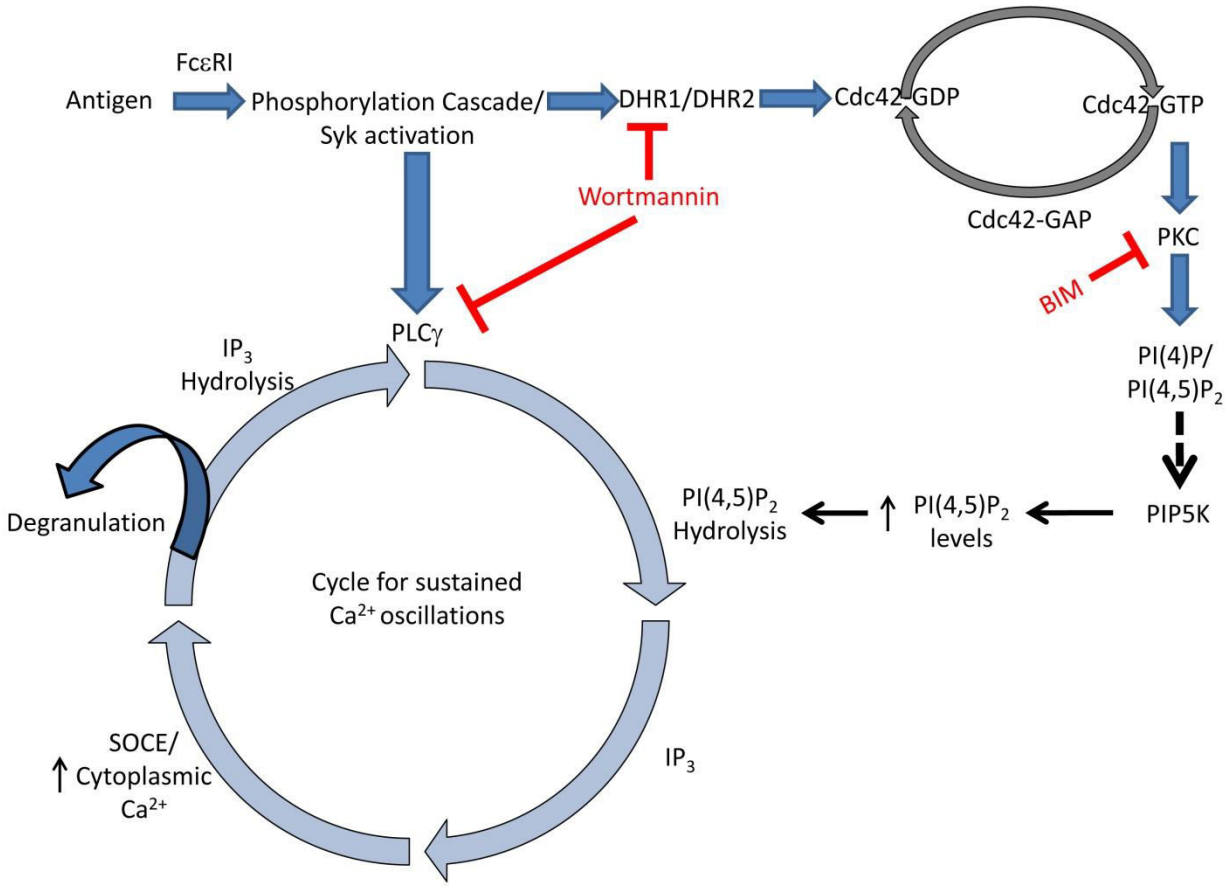
FcεRI
Antigen
Phosphorylation Cascade/
Syk activation
DHR1/DHR2
Cdc42-GDP
Cdc42-GTP
Cdc42-GAP
Wortmannin
PKC
BIM
PLCγ
IP3
Hydrolysis
PI(4)P/
PI(4,5)P2
Degranulation
PI(4,5)P2
Hydrolysis
PI(4,5)P2
levels
PIP5K
Cycle for sustained
Ca2+ oscillations
SOCE/
Cytoplasmic
Ca2+
IP3

monitor PIP_2 levels at the plasma membrane. BIM showed strongest inhibition of these three compounds, consistent with it being the most potent inhibitor of Ca^{2+} oscillations and degranulation. To explore whether Cdc42 might signal through PKC to regulate PIP_2 synthesis, we demonstrated that B6A4C1 cells are partially deficient in PKC activation, as MARCKS-ED-mRFP was not displaced from the plasma membrane in >50% of cells observed. Cdc42-G12V reconstituted this defect when expressed in B6A4C1 cells, providing evidence that Cdc42 signals, at least in part, through PKC activation in this signaling pathway.

PKC consists of a family of at least 10 different Thr/Ser kinases that are typically divided into three categories, conventional (or classical), novel, and atypical (Gadi et al. 2011; Newton 2010; Nishizuka 1995). DAG is necessary for the activation of both conventional and novel PKC isoforms through binding to a C1 domain. Conventional isoforms require the presence of Ca^{2+} for activation through a C2 domain, although Ca^{2+} is not necessary for activation of novel isoforms. Atypical isoforms require neither Ca^{2+} nor DAG for activation. RBL-2H3 cells have been shown to express PKC isoforms α, β, δ, ε, and ζ (Kumada et al. 1995). PKC isoforms α, β and β1 (conventional) and δ (novel) have all been shown to play a role in mast cell signaling (Ozawa et al. 1993; Nechushtan et al. 2000; Abdel-Raheem et al. 2005), however, it is possible other isoforms, yet to be investigated, also participate.

PKC activation is thought to be essential for mast cell degranulation, in part, because it phosphorylates the protein MARCKS at the plasma membrane in RBL cells and this in turn releases sequestered PIP_2 to be available for exocytosis (Gadi et al. 2011). However, in addition to increasing available PIP_2 for this purpose, we now hypothesize that MARCKS phosphorylation is likely a critical event for synthesis of PIP_2, from substrate, following its hydrolysis. MARCKS sequesters not only PIP_2, but also the more abundant phospholipid PI4P,

at the plasma membrane (McLaughlin and Murray 2005). MARCKS displacement by PKC makes PI4P available for phosphorylation, a necessary step in the resynthesis of PIP_2. Our hypothesis is consistent with results from other studies that indicate that PKC regulates PIP_2 synthesis (Field et al. 2000; Tóth et al. 2016), although, until recently, it has been unclear how PKC regulates this important cellular event.

As many isoforms of PKC exist, it is possible that overlapping functions explain why we see inhibition of PKC activation in only 53% of B6A4C1 cells. The conventional PKC isoform α (Cook et al. 2006), and atypical isoforms λ and ζ (Coghlan, Chou, and Carpenter 2000) have been shown to be effectors of Cdc42. Future studies are necessary to identify the PKC isoform, or isoforms, that Cdc42 interacts with in RBL signaling. 47% of B6A4C1 cells did undergo displacement of MARCKS-ED-mRFP following antigen stimulation. However, consistent with our findings that B6A4C1 cells are deficient in PIP_2 synthesis, subsequent MARCKS-ED-mRFP oscillations were typically not observed following MARCKS displacement in these cells. This suggests that additional defects preventing receptor-stimulated PIP_2 synthesis may exist in B6A4C1 cells, and that Cdc42 activation may also directly regulate PIP5-kinases, in addition to PKC activation, to regulate PIP_2 synthesis. Future studies will be necessary to further explore this possibility.

Our finding that pretreatment with wortmannin inhibits antigen-stimulated Ca^{2+} release from stores and SOCE is consistent with previous studies that show wortmannin reduces IP_3 production and PLCγ1 activation (Ching et al. 2001; Gilfillan and Tkaczyk 2006; Barker et al. 1995; Sil et al. 2007), although it is likely that the dose of DNP-BSA used determines the extent of this inhibitory effect. We now propose a novel hypothesis that wortmannin acts to inhibit DOCK GEF signaling by preventing DOCK DHR-1 domains from interacting with PIP_3 at the

plasma membrane. Our discovery that DOCK8, capable of activating both Cdc42 and Rac1, fully reconstitutes stimulated VAMP8-mediated exocytosis in B6A4C1 cells, whereas the catalytically inactive mutant DOCK8 V/A does not, supports the idea that DOCK GEFs play a critical role in RBL-2H3 signaling, consistent with previous evidence (Wilkes et al. 2014; Ogawa et al. 2014). Our results do not demonstrate that DOCK8 is the defective GEF in B6A4C1 cells, but rather it is likely that DOCK8, or a closely related DOCK GEF isoform, is necessary for antigen-stimulated signaling in mast cells. Future studies will further characterize the roles of specific DOCK GEFs in these cells and identify differences between these proteins in RBL-2H3 and B6A4C1 cells.

In conclusion, the resynthesis of PIP_2 following its receptor-mediated hydrolysis, is an important signaling event. This study provides strong evidence that Cdc42 activation is critical for receptor-stimulated PIP_2 synthesis, an event necessary for sustained Ca^{2+} oscillations and degranulation. Cdc42 activates PKC, and inhibition of this process suppresses Ca^{2+} oscillations and strongly inhibits degranulation, although the exact PKC isoform involved is yet to be identified. Activation of Cdc42 and PKC are also critical for increasing the accessible PIP_2 necessary for exocytic events. DOCK8 reconstitutes stimulated exocytosis in B6A4C1 cells, adding to the growing understanding that DOCK GEFs play an important role in mast cell signaling. Whether DOCK GEFs play a more general role in regulating PIP_2 synthesis requires further investigation.

3.5 MATERIALS AND METHODS

Cell Culture: RBL-2H3 and B6A4C1 cells were cultured as monolayers in minimal essential medium with Earle's salts (Invitrogen Corp., Carlsbad, CA), 20% fetal bovine serum (Atlanta

Biologicals, Atlanta, GA), and 10 μg/ml gentamicin sulfate (Invitrogen) as previously described (Gosse et al. 2005)

Reagents and Chemicals: Thapsigargin, Bisindolylmaleimide I, wortmannin, phorbol 1,2-dibutyrate, and phorbol 12-myristate-13-acetate were purchased from Sigma-Aldrich (St. Louis, MO). DU40 and SN were generous gifts from Dr. Patrick Casey (Duke-National University of Singapore Medical School, Singapore).

Expression Plasmids: The genetically encoded calcium indicator, GCaMP3, previously described (Tian et al., 2009), was purchased from Addgene (plasmid #22692). VAMP8-pHluorin-fusion was created as previously described (Wilkes et al. 2014). PH-PLCδ-EGFP (Varrnai & Balla 1998) was a gift from Dr. Tamas Balla (National Institutes of Health). DOCK8-YFP, and DOCK8-V/A-YFP, were gifts from Dr. Daniel Billadeau (Mayo Clinic Cancer Center, Rochester, MN). Crib-Binding-Domain-GFP was a gift from Dr. Min Wu (National University of Singapore, Mechanobiology Institute) and Dr. Pietro De Camilli (Yale University School of Medicine, New Haven, NY).

Transfection: Both RBL-2H3 and B6A4C1 cell lines were transfected by electroporation under identical conditions for fluorimetry-based Ca^{2+} and exocytosis experiments, and for imaging-based Ca^{2+} and PIP_2 synthesis experiments. Cells were harvested three to five days after passage and ~ 5 x 10^6 cells were electroporated in 0.5 ml of cold electroporation buffer (137 mM NaCl, 2.7 mM KCl, 1 mM $MgCl_2$, 1 mg/ml glucose, 20 mM HEPES (pH 7.4) using 10 μg of GCaMP3 for Ca^{2+} experiments, 5 μg of VAMP8-pHluorin for exocytosis measurements, or 10 μg PH-PLCδ-EGFP for PIP_2 measurements, at 280 V and 950 μF using Gene Pulser X (Bio-Rad). For fluorimetry-based Ca^{2+} experiments (Figure 3), cells were then plated in 100 mm dishes. For Ca^{2+} oscillation, PIP_2 synthesis, MARCKS-ED-mRFP, and VAMP8-pHluorin experiments,

electroporated cells were resuspended in 6 mls of medium and plated in three different MatTek dishes (2 ml/dish) (MatTek Corporation, Ashland, MA). For all experiments, cells were allowed to recover for 24 hours and sensitized overnight with 0.5 μg/ml anti-2,4-dinitrophenyl (DNP) IgE (Posner et al. 1992) during this recovery time.

PH-PLCδ-EGFP Measurements: ~ 5 x 10^6 RBL-2H3 or B6A4C1 cells were electroporated with 10 μg PH-PLCδ-EGFP then treated with 0.1 μM phorbol 1,2-dibutyrate for 1-2 hours, which reduces the number of pre-existing PIP_2 domains at the plasma membrane of cells. Cells were allowed to recover for approximately 24 hours, washed into buffered saline solution (BSS: 135 mM NaCl, 5 mM KCl, 1 mM $MgCl_2$, 1.8 mM $CaCl_2$ 5.6 mM D(+) glucose, 20 mM HEPES, pH 7.4), and PH-PLCδ-EGFP fluorescence was monitored initially for twenty seconds, then 200 ng/ml DNP-BSA was added and PH-PLCδ-EGFP fluorescence was observed for 7-10 minutes using a 100X oil objective on a Zeiss Elyra super resolution microscope. Stimulated PIP_2 synthesis was analyzed by monitoring appearance of new puncta following antigen addition. Lateral movements of PIP_2 puncta were not counted as new PIP_2 synthesis. Antigen stimulated-puncta were also distinguished from pre-existing PIP_2 puncta by the following criteria: new PIP_2 puncta typically diffused rapidly or were hydrolyzed following DNP-BSA addition, and their presence was more transient than preexisting-PIP_2 puncta undergoing lateral or minor vertical movements (See supplementary video 1). Antigen-stimulated synthesis of PIP_2 puncta was more readily observed in cells strongly expressing PH-PLCδ-EGFP, so bright, fluorescent cells were analyzed for all conditions tested.

[^{3}H]-inositol labeling: RBL-2H3 and B6A4C1 cells were plated in 100 mm dishes at a density of 1 x 10^^{6} cells for 24 hours, then washed with and placed in inositol-free DMEM (Invitrogen) medium and radiolabeled with inositol, Myo,-[2-3H(N)] (Perkin Elmer, NET114A005MC) for

24 hours. Cells were then washed two times with BSS, stimulated with 200 ng/ml DNP-BSA, and incubated for 5 minutes at 37°. Cells were then precipitated in 4.5% perchloric acid and lysates were washed in 100mM EDTA. The phospholipids contained within each cell precipitate were deacylated by treatment with methylamine.1 ml of methylamine reagent (10.7% methylamine, 45.7% methanol, 11.4% 1-butanol) was added to each cell precipitate, incubated for 30 min at room temperature, and then incubated in a 53°C heat block for 1 hour. Unreacted methylamine was then removed in vacuo, and the dried pellet was resuspended in 300 μl sterile water. After a second sequence of drying in vacuo, and resuspension in 300 μl sterile water, an equal volume of 1-butanol/ethylether/formic acid ethyl ester (20:4:1) was added. The samples were vortexed for 5 min and centrifuged for 2 min. The aqueous phase containing the [^{3}H]glycero-phosphoinositides was transferred to new tubes and the extraction repeated once more with 1-butanol/ethylether/formic acid ethyl ester (20:4:1). Finally, the aqueous phase was collected and dried in vacuo. Samples were then resuspended in sterile water and 5 million counts of each sample were separated by HPLC (Shimadzu) using a partisphere SAX column (GE healthcare) and measured by a 610TR radiomatic detector (PerkinElmer), as previously described (Manford et al. 2012; Rudge, Anderson, and Emr 2004).

Degranulation: RBL-2H3 cells were sensitized with IgE and plated in triplicate at a density of 5 × 10^5/well and incubated overnight. DU40 and SN were added at a concentration of 10 μM for 24 hours prior to stimulation. The next day BIM and wortmannin were added to cells at a concentration of 5 μM and 200 nM, respectively, for 5 minutes, then all cells were washed three times with BSS and β-hexosaminidase release in response to 200 ng/ml DNP-BSA, 250 nM thapsigargin, and 250 nM thapsigargin + 80 nM PMA was assessed as described previously (Naal et al. 2004).

Ca^{2+} Measurements: Cytoplasmic Ca^{2+} levels were measured using an SLM 8100C steady-state fluorimeter (SLM Instruments, Urbana, IL). Cells previously electroporated with GCaMP3 were allowed to recover as described above, harvested using PBS/EDTA, and resuspended in 1.8 ml BSS. Cells were then incubated and stirred at 37ºC for 5 minutes, and GCaMP3 levels were monitored (excitation 490 nm, emission 520 nm). BIM and wortmannin inhibitors were then added for ~5 minutes, and cells were then stimulated with 200 ng/ml DNP-BSA to monitor Ca^{2+} release from stores and SOCE. Cells were then lysed by 0.1% Triton X-100 to obtain the maximum value of GCaMP3 fluorescence, then 5 mM EGTA was added to determine background fluorescence, and this differential was used to normalize Ca^{2+} responses. Ca^{2+} release from stores was quantified at the fluorescence peak immediately following antigen addition. SOCE was quantified 150 s after DNP-BSA addition.

For imaging analysis of Ca^{2+}oscillations, cells expressing GCaMP3 were washed into BSS and incubated for 5 minutes at 37ºC within a confined heating chamber prior to live cell imaging. GCaMP3 fluorescence was monitored for twenty seconds prior to addition of 200 ng/ml DNP-BSA, and Ca^{2+} oscillations were monitored over a time interval of ~400 sec using a 40X H_2O, heated objective on a Zeiss 710 confocal microscope. GCaMP3 was excited using the 488-nm line of a krypton/argon laser and viewed with a 502-551 nm band-pass filter.

Offline image analysis was conducted using ImageJ (National Institutes of Health). Changes in GCaMP3 fluorescence were normalized by dividing the maximum GCaMP3 fluorescence value by the initial fluorescence basal level monitored before DNP-BSA addition. Transient increases in GCaMP3 fluorescence were scored as oscillations if the transient peak was at least half of the maximum GCaMP3 fluorescence peak response observed for an individual cell. Statistical analysis of Ca^{2+} oscillations was conducted by counting and averaging the

number of oscillatory peaks over a 400 second time interval, beginning immediately following the initial calcium transient.

MARCKS-ED-mRFP Measurements: RBL-2H3 and B6A4C1 cells were electroporated as described above with 20 μg of MARCKS-ED-mRFP and B6A4C1 cells were also electroporated with 10 μg of pcDNA or Cdc42-G12V and plated and sensitized overnight in MatTek dishes. Cells were then stimulated with 200 ng/ml DNP-BSA, and monitored for 7-10 minutes using the Zeiss Elyra super resolution microscope.

CBD-GFP Measurements: RBL-2H3 and B6A4C1 cells were electroporated with 10 μg of CBD-GFP. DU40 was added to cells 24 hours prior to stimulation at 10 μM concentration. Wortmannin was added at a 200 nM concentration 5 min prior to stimulation. RBL-2H3 cells monitored in the absence of extracellular Ca^{2+} were washed and placed in Ca^{2+}-free BSS immediately prior to imaging. Cells were then stimulated with 200 ng/ml DNP-BSA and monitored for 7-10 minutes using the Zeiss Elyra super resolution microscope.

VAM8-Exocytosis Measurements: Antigen-stimulated exocytosis was monitored as time-dependent increases in VAMP8-pHluorin fluorescence using a Zeiss 710 confocal microscope. RBL-2H3 cells were electroporated with VAMP8-pHluorin and B6A4C1 cells were electroporated with VAMP8-pHluorin and 10 μg DOCK8, plated in MatTek dishes, and then sensitized with IgE and allowed to recover for 24 hours, as described above. Cells were incubated at 37ºC for 5 min and in indicated cases, 5 μM BIM DNP-BSA was added for this time period. Cells were then stimulated with 200 ng/ml DNP-BSA and increases in VAMP8-pHluorin fluorescence levels were monitored over a ~400 second time interval. 50 mM NH_4Cl was then added to rapidly neutralize the acidic environment of endosomes, resulting in a dequenching of VAMP8-pHluorin and revealing total values for VAMP8-pHluorin fluorescence.

Statistical Analyses: Statistical analysis was performed with Prism software (Graphpad) and Microsoft Excel. All bar graphs display mean ± SEM unless otherwise noted. The statistical significance of all figures was determined by a One-Way ANOVA (Analysis of Variance) followed by Tukey's post test. Level of significance is denoted as follows: $*P < 0.05$, $**P < 0.01$, $***P < 0.001$.

ACKNOWLEDGEMENTS

We thank Dr. Jon Erickson (Cornell University) for helpful discussions and Carol Bayles for maintaining the Cornell Imaging Facility. We also thank Dr. Chris Stefan (University College London, United Kingdom) for analyzing our [^{3}H]-phosphoinositide samples. This work was supported by the National Science Foundation Graduate Research Fellowship under Grant No. NSF DGE-1144153 (MMW), and was also supported through grants R01 AI022499 and R01 GM117552 from the National Institutes of Health.

REFERENCES

Abdel-Raheem, Ihab T, Izumi Hide, Yuhki Yanase, Yukari Shigemoto-Mogami, Norio Sakai, Yasuhito Shirai, Naoaki Saito, et al. 2005. "Protein Kinase C-Alpha Mediates TNF Release Process in RBL-2H3 Mast Cells." *British Journal of Pharmacology* 145 (4): 415–23. doi:10.1038/sj.bjp.0706207.

Alswied, Abdullah, and Anant B. Parekh. 2015. "Ca2+ Influx through Store-Operated Calcium Channels Replenishes the Functional Phosphatidylinositol 4,5-Bisphosphate Pool Used by Cysteinyl Leukotriene Type I Receptors." *Journal of Biological Chemistry* 290 (49): 29555–66. doi:10.1074/jbc.M115.678292.

Apgar, J R. 1995. "Activation of Protein Kinase C in Rat Basophilic Leukemia Cells Stimulates Increased Production of Phosphatidylinositol 4-Phosphate and Phosphatidylinositol 4,5-Bisphosphate: Correlation with Actin Polymerization." *Mol Biol Cell* 6 (1): 97–108. http://www.ncbi.nlm.nih.gov/pubmed/7749199\nhttp://www.ncbi.nlm.nih.gov/pmc/articles/PMC275817/pdf/mbc00021-0104.pdf.

Balla, T. 2013. "Phosphoinositides: Tiny Lipids with Giant Impact on Cell Regulation." *Physiological Reviews* 93 (3): 1019–1137. doi:10.1152/physrev.00028.2012.

Bambouskova, Monika, Iva Polakovicova, Ivana Halova, Gautam Goel, Lubica Draberova, Viktor Bugajev, Aivi Doan, et al. 2016. "New Regulatory Roles of Galectin-3 in High-Affinity IgE Receptor" 36 (9): 1366–82. doi:10.1128/MCB.00064-16.Address.

Barker, S A, K K Caldwell, A Hall, A M Martinez, J R Pfeiffer, J M Oliver, and B S Wilson. 1995. "Wortmannin Blocks Lipid and Protein Kinase Activities Associated with PI 3-Kinase and Inhibits a Subset of Responses Induced by Fc Epsilon R1 Cross-Linking." *Mol Biol Cell* 6 (9): 1145–58. http://www.ncbi.nlm.nih.gov/pubmed/8534912\nhttp://www.ncbi.nlm.nih.gov/pmc/articles/PMC301273/pdf/mbc00078-0063.pdf.

Ching, Tsui Ting, Ao Lin Hsu, Amy J. Johnson, and Ching Shih Chen. 2001. "Phosphoinositide 3-Kinase Facilitates Antigen-Stimulated Ca2+ Influx in RBL-2H3 Mast Cells via a Phosphatidylinositol 3,4,5-Trisphosphate-Sensitive Ca2+ Entry Mechanism." *Journal of Biological Chemistry* 276 (18): 14814–20. doi:10.1074/jbc.M009851200.

Chong, L D, a Traynor-Kaplan, G M Bokoch, and M a Schwartz. 1994. "The Small GTP-Binding Protein Rho Regulates a Phosphatidylinositol 4-Phosphate 5-Kinase in Mammalian Cells." *Cell* 79 (3): 507–13. doi:10.1016/0092-8674(94)90259-3.

Cissel, D S, P F Fraundorfer, and M a Beaven. 1998. "Thapsigargin-Induced Secretion Is Dependent on Activation of a Cholera Toxin-Sensitive and Phosphatidylinositol-3-Kinase-Regulated Phospholipase D in a Mast Cell Line." *The Journal of Pharmacology and Experimental Therapeutics* 285 (1): 110–18. http://www.ncbi.nlm.nih.gov/pubmed/9536000.

Coghlan, M P, M M Chou, and C L Carpenter. 2000. "Atypical Protein Kinases Clambda and -Zeta Associate with the GTP-Binding Protein Cdc42 and Mediate Stress Fiber Loss."

Molecular and Cellular Biology 20 (8): 2880–89. http://www.pubmedcentral.nih.gov/articlerender.fcgi?artid=85517&tool=pmcentrez&rendertype=abstract.

Cook, Anthony C, Cojen Ho, Jennifer L Kershner, Steve a Malinowski, Heath Moldveen, Brigid a Stagliano, and Simon J Slater. 2006. "Competitive Binding of Protein Kinase Calpha to Membranes and Rho GTPases." *Biochemistry* 45 (48): 14452–65. doi:10.1021/bi0612420.

Côté, Jean François, and Kristiina Vuori. 2007. "GEF What? Dock180 and Related Proteins Help Rac to Polarize Cells in New Ways." *Trends in Cell Biology*. doi:10.1016/j.tcb.2007.05.001.

Di Paolo, Gilbert, and Pietro De Camilli. 2006. "Phosphoinositides in Cell Regulation and Membrane Dynamics." *Nature* 443 (7112): 651–57. doi:10.1038/nature05185.

Di Paolo, Gilbert, and Tae-Wan Kim. 2011. "Linking Lipids to Alzheimer's Disease: Cholesterol and Beyond." *Nature Reviews. Neuroscience* 12 (5): 284–96. doi:10.1038/nrn3012.

El-Sibai, Mirvat, and Jonathan M. Backer. 2007. "Phospholipase C?? Negatively Regulates Rac/Cdc42 Activation in Antigen-Stimulated Mast Cells." *European Journal of Immunology* 37 (1): 261–70. doi:10.1002/eji.200635875.

Ferrell, J E, and W H Huestis. 1984. "Phosphoinositide Metabolism and the Morphology of Human Erythrocytes." *The Journal of Cell Biology* 98 (6): 1992–98.

Field, K a, J R Apgar, E Hong-Geller, R P Siraganian, B Baird, and D Holowka. 2000. "Mutant RBL Mast Cells Defective in Fc Epsilon RI Signaling and Lipid Raft Biosynthesis Are Reconstituted by Activated Rho-Family GTPases." *Molecular Biology of the Cell* 11 (10): 3661–73. http://www.pubmedcentral.nih.gov/articlerender.fcgi?artid=15022&tool=pmcentrez&rendertype=abstract.

Gadi, Deepti, Alice Wagenknecht-Wiesner, David Holowka, and Barbara Baird. 2011. "Sequestration of Phosphoinositides by Mutated MARCKS Effector Domain Inhibits Stimulated Ca(2+) Mobilization and Degranulation in Mast Cells." *Molecular Biology of the Cell* 22 (24): 4908–17. doi:10.1091/mbc.E11-07-0614.

Gilfillan, Alasdair M, and Christine Tkaczyk. 2006. "Integrated Signalling Pathways for Mast-Cell Activation." *Nature Reviews. Immunology* 6 (3): 218–30. doi:10.1038/nri1782.

Gosse, JA Julie a, Alice Wagenknecht-Wiesner, David Holowka, Barbara Baird, and David Holowka. 2005. "Transmembrane Sequences Are Determinants of Immunoreceptor Signaling." *The Journal of Immunology* 175 (4): 2123–31. doi:175/4/2123 [pii].

Holowka, David, Nathaniel Calloway, Roy Cohen, Deepti Gadi, Jinmin Lee, Norah L Smith, and Barbara Baird. 2012. "Roles for Ca2+ Mobilization in Mast Cell Functions." *Frontiers in Immunology* 3: 104. doi:10.3389/fimmu.2012.00104.

Hong-Geller, E, D Holowka, R P Siraganian, B Baird, and R a Cerione. 2001. "Activated Cdc42/Rac Reconstitutes Fcepsilon RI-Mediated Ca2+ Mobilization and Degranulation in Mutant RBL Mast Cells." *Proceedings of the National Academy of Sciences of the United*

States of America 98 (3): 1154–59. doi:10.1073/pnas.98.3.1154.

Kawasaki, Takumi, Takehiko Ueyama, Ingo Lange, Stefan Feske, and Naoaki Saito. 2010. "Protein Kinase C-Induced Phosphorylation of Orai1 Regulates the Intracellular Ca2+ Level via the Store-Operated Ca2+ Channel." *Journal of Biological Chemistry* 285 (33): 25720–30. doi:10.1074/jbc.M109.022996.

Kumada, T, S Nakashima, Y Nakamura, H Miyata, and Y Nozawa. 1995. "Antigen-Mediated Phospholipase D Activation in Rat Basophilic Leukemia (RBL-2H3) Cells: Possible Involvement of Calcium/calmodulin." *Biochim Biophys Acta* 1258 (2): 107–14. http://www.ncbi.nlm.nih.gov/pubmed/7548173.

Manford, Andrew G., Christopher J. Stefan, Helen L. Yuan, Jason A. MacGurn, and Scott D. Emr. 2012. "ER-to-Plasma Membrane Tethering Proteins Regulate Cell Signaling and ER Morphology." *Developmental Cell* 23 (6): 1129–40. doi:10.1016/j.devcel.2012.11.004.

Martiny-Baron, G, M G Kazanietz, H Mischak, P M Blumberg, G Kochs, H Hug, D Marme, and C Schachtele. 1993. "Selective Inhibition of Protein Kinase C Isozymes by the Indolocarbazole Go 6976." *J. Biol. Chem.* 268 (13): 9194–97. http://www.jbc.org/content/268/13/9194.abstract.

McLaughlin, Stuart, and Diana Murray. 2005. "Plasma Membrane Phosphoinositide Organization by Protein Electrostatics." *Nature* 438 (December): 605–11. doi:10.1038/nature04398.

Micheva, Kristina D., Ronald W. Holz, and Stephen J. Smith. 2001. "Regulation of Presynaptic Phosphatidylinositol 4,5-Biphosphate by Neuronal Activity." *Journal of Cell Biology* 154 (2): 355–68. doi:10.1083/jcb.200102098.

Millard, P J, D Gross, W W Webb, and C Fewtrell. 1988. "Imaging Asynchronous Changes in Intracellular Ca2+ in Individual Stimulated Tumor Mast Cells." *Proceedings of the National Academy of Sciences of the United States of America* 85 (6): 1854–58. doi:10.1073/pnas.85.6.1854.

Naal, Rose Mary Z G, Joel Tabb, David Holowka, and Barbara Baird. 2004. "In Situ Measurement of Degranulation as a Biosensor Based on RBL-2H3 Mast Cells." *Biosensors and Bioelectronics* 20 (4): 790–95. doi:10.1016/j.bios.2004.03.017.

Nechushtan, H, M Leitges, C Cohen, G Kay, and E Razin. 2000. "Inhibition of Degranulation and Interleukin-6 Production in Mast Cells Derived from Mice Deficient in Protein Kinase Cbeta." *Blood* 95 (5): 1752–57. http://www.ncbi.nlm.nih.gov/cgi-bin/Entrez/referer?http://www.bloodjournal.org/cgi/content/abstract/95/5/1752\nhttp://www.bloodjournal.org/cgi/content/full/95/5/1752\nhttp://www.bloodjournal.org/cgi/content/abstract/95/5/1752.

Newton, Alexandra C. 2010. "Protein Kinase C: Poised to Signal." *American Journal of Physiology. Endocrinology and Metabolism* 298 (3): E395–402. doi:10.1152/ajpendo.00477.2009.

Nishizuka, Y. 1995. “Protein Kinase C and Lipid Signaling for Sustained Cellular Responses.” *The FASEB Journal : Official Publication of the Federation of American Societies for Experimental Biology* 9 (7): 484–96.

Ogawa, Kana, Yoshihiko Tanaka, Takehito Uruno, Xuefeng Duan, Yosuke Harada, Fumiyuki Sanematsu, Kazuhiko Yamamura, et al. 2014. “DOCK5 Functions as a Key Signaling Adaptor That Links FcεRI Signals to Microtubule Dynamics during Mast Cell Degranulation.” *The Journal of Experimental Medicine* 211 (7): 1407–19. doi:10.1084/jem.20131926.

Oliver, Constance, Noriyuki Sahara, Seiichi Kitani, April R. Robbins, Lawrence M. Mertz, and Reuben P. Siraganian. 1992. “Binding of Monoclonal Antibody AA4 to Gangliosides on Rat Basophilic Leukemia Cells Produces Changes Similar to Those Seen with Fee Receptor Activation.” *Journal of Cell Biology* 116 (3): 635–46.

Ozawa, Koichiro, Koji Yamada, Marcelo G. Kazanietz, Peter M. Blumberg, and Michael A. Beaven. 1993. “Different Isozymes of Protein Kinase C Mediate Feedback Inhibition of Phospholipase C and Stimulatory Signals for Exocytosis in Rat RBL-2H3 Cells.” *Journal of Biological Chemistry* 268 (4): 2280–83.

Peterson, Yuri K., Patrick Kelly, Carolyn A. Weinbaum, and Patrick J. Casey. 2006. “A Novel Protein Geranylgeranyltransferase-I Inhibitor with High Potency, Selectivity, and Cellular Activity.” *Journal of Biological Chemistry* 281 (18): 12445–50. doi:10.1074/jbc.M600168200.

Posner, R G, B Lee, D H Conrad, D Holowka, B Baird, and B Goldstein. 1992. “Aggregation of IgE-Receptor Complexes on Rat Basophilic Leukemia Cells Does Not Change the Intrinsic Affinity but Can Alter the Kinetics of the Ligand-IgE Interaction.” *Biochemistry* 31 (23): 5350–56.

Prince WT, Berridge MJ. 1973. “The Role of Calcium in the Action of 5-Hydroxytryptamine and Cyclic AMP on Salivary Glands.” *J Exp Biol*, no. 58: 367–84.

Raucher, D, T Stauffer, W Chen, K Shen, S Guo, J D York, M P Sheetz, and T Meyer. 2000. “Phosphatidylinositol 4,5-Bisphosphate Functions as a Second Messenger That Regulates Cytoskeleton-Plasma Membrane Adhesion.” *Cell* 100 (2): 221–28. doi:10.1016/S0092-8674(00)81560-3.

Rudge, Simon A, Deborah M Anderson, and Scott D Emr. 2004. “Vacuole Size Control: Regulation of PtdIns(3,5)P2 Levels by the Vacuole-Associated Vac14-Fig4 Complex, a PtdIns(3,5)P2-Specific Phosphatase.” *Molecular Biology of the Cell* 15 (1): 24–36. doi:10.1091/mbc.E03-05-0297.

Ryan, T. A., P. J. Millard, and W. W. Webb. 1990. “Imaging [Ca2+]i Dynamics during Signal Transduction.” *Cell Calcium* 11 (2-3): 145–55. doi:10.1016/0143-4160(90)90067-5.

Sil, Dwaipayan, Jong Bum Lee, Dan Luo, David Holowka, and Barbara Baird. 2007. “Trivalent Ligands with Rigid DNA Spacers Reveal Structural Requirements for IgE Receptor Signaling in RBL Mast Cells.” *ACS Chemical Biology* 2 (10): 674–84.

doi:10.1021/cb7001472.

Stracke, M, L Basciano, and R Siraganian. 1987. “Binding Properties and Histamine Release in Variants of Rat Basophilic Leukemia Cells with Changes in the IgE Receptor.” *Immunology Letters* 14 (4): 287–92. doi:10.1016/0165-2478(87)90006-X.

Tóth, József T., Gergo Gulyás, Dániel J. Tóth, András Balla, Gerald R V Hammond, László Hunyady, Tamás Balla, and Péter Várnai. 2016. “BRET-Monitoring of the Dynamic Changes of Inositol Lipid Pools in Living Cells Reveals a PKC-Dependent PtdIns4P Increase upon EGF and M3 Receptor Activation.” *Biochimica et Biophysica Acta - Molecular and Cell Biology of Lipids* 1861 (3): 177–87. doi:10.1016/j.bbalip.2015.12.005.

Varnai, Peter, and Tamas Balla. 1998. “Visualization of Phosphoinositides That Bind Pleckstrin Homology Domains: Calcium- and Agonist-Induced Dynamic Changes and Relationship to Myo-[3H]inositol-Labeled Phosphoinositide Pools.” *Journal of Cell Biology* 143 (2): 501–10. doi:10.1083/jcb.143.2.501.

Weernink, Paschal A Oude, Konstantinos Meletiadis, Silvia Hommeltenberg, Matthias Hinz, Hisamitsu Ishihara, Martina Schmidt, and Karl H. Jakobs. 2004. “Activation of Type I Phosphatidylinositol 4-Phosphate 5-Kinase Isoforms by the Rho GTPases, RhoA, Rac1, and Cdc42.” *Journal of Biological Chemistry* 279 (9): 7840–49. doi:10.1074/jbc.M312737200.

Wenk, Markus R, Louise Lucast, Gilbert Di Paolo, Anthony J Romanelli, Sharon F Suchy, Robert L Nussbaum, Gary W Cline, Gerald I Shulman, Walter McMurray, and Pietro De Camilli. 2003. “Phosphoinositide Profiling in Complex Lipid Mixtures Using Electrospray Ionization Mass Spectrometry.” *Nature Biotechnology* 21 (7): 813–17. doi:10.1038/nbt837.

Wilkes, Marcus M, Joshua D Wilson, Barbara Baird, and David Holowka. 2014. “Activation of Cdc42 Is Necessary for Sustained Oscillations of Ca2+ and PIP2 Stimulated by Antigen in RBL Mast Cells.” *Biology Open* 3 (8): 700–710. doi:10.1242/bio.20148862.

Wollman, R, and T Meyer. 2012. “Coordinated Oscillations in Cortical Actin and Ca2+ Correlate with Cycles of Vesicle Secretion.” *Nature Cell Biology* 14 (12): 1261–69. doi:10.1038/ncb2614.

Woods, Niall M, K. S. Roy Cuthbertson, and Peter H Cobbold. 1986. “Repetitive Transient Rises in Cytoplasmic Free Calcium in Hormone-Stimulated Hepatocytes.” *Nature* 319 (6054): 600–602. doi:10.1038/319600a0.

Wu, M, X Wu, and P De Camilli. 2013. “Calcium Oscillations-Coupled Conversion of Actin Travelling Waves to Standing Oscillations.” *Proc Natl Acad Sci U S A* 110 (4): 1339–44. doi:10.1073/pnas.1221538110.

Chapter 4

Physiological and Pathological Functions of Alpha-Synuclein in a Mammalian Cell Model

4.1 ABSTRACT

The intrinsically disordered protein alpha-synuclein (a-syn) is genetically and pathologically linked to Parkinson's disease (PD). In a highly aggregated form a-syn is the major constituent of Lewy bodies, the pathological hallmark of PD, and single-point mutations or changes in expression levels of a-syn often lead to early onset or sporadic forms of the disease. The physiological role of a-syn is thought to be disrupted in patients with PD. However, despite intensive research, the normal function of a-syn in healthy neurons remains to be defined. Utilizing RBL-2H3 mast cells as a mammalian model system we investigated the capacity of transfected a-syn to modulate stimulated processes of exocytosis and endocytosis. Exocytosis can be stimulated by the multivalent antigen DNP-BSA, or by the SERCA inhibitor thapsigargin, and monitored using the recycling endosomal marker VAMP8-pHluorin. Here we demonstrate that low expression levels of human a-syn inhibit exocytosis in these cells. Inhibition occurs with both Wt and with several mutants of a-syn, after stimulation by either DNP-BSA or thapsigargin, revealing inhibition downstream of IP3-initiated Ca^{2+} mobilization. A-syn loses capacity to inhibit exocytosis when expressed at higher levels, suggesting that aggregation reduces the inhibitory species for this process. Conversely, we find that stimulated endocytosis of fluorescently labeled immunoglobulin E is inhibited when a-syn is expressed only at the higher levels in RBL-2H3 cells. Expression of a-syn at low levels in PC-12 cells, a dopamine releasing cell line, also inhibits stimulated exocytosis. Together, our results show that transfected a-syn interferes with stimulated endosomal trafficking, depending on expression levels within cells. The phenotype we have characterized in these model systems points to disruption of normal cellular function caused by dysregulation of a-syn expression, such as may occur in PD.

4.2 INTRODUCTION

Parkinson's disease (PD) is the most common neurodegenerative movement disorder (Irwin, Lee, and Trojanowski 2013). With increased risk of diagnosis after age 60, PD onset strongly correlates with age, affecting ~1-2% of the population over age 65 (Langston 2006). Clinically, PD symptoms (tremors, rigidity, bradykinesia, postural dysfunction) are associated with death of dopaminergic neurons in the substantia nigra, coupled with the presence of abnormal protein aggregates, known as Lewy bodies, in surviving neurons (Sulzer 2007; Langston 2006). The primary component of these intraneuronal aggregates is the presynaptic protein alpha-synuclein (a-syn) (Spillantini 1999).

A-syn is a 140 amino acid protein with ill-defined function found predominantly in neurons, although its expression is also detected in other cell types (Barbour et al. 2008). In addition to being the primary component of Lewy bodies, a-syn has been genetically linked to autosomal dominant familial PD, often causing early disease onset (Polymeropoulos et al. 1997; Petrucci, Ginevrino, and Valente 2016). Despite this genetic link, autosomal dominant familial PD is not common, accounting for less than 10% of all PD cases (Schulte and Gasser 2011). However, elevated levels of a-syn are observed in many patients who develop sporadic, not genetic, forms of PD, suggesting a critical role for this protein in the majority of PD cases (Chiba-Falek, Lopez, and Nussbaum 2006; Murphy et al. 2014). A recent genome wide-association study has also identified the gene which encodes for a-syn, SNCA, as one of the strongest risk loci for sporadic forms of PD (Nalls et al. 2014). As a result, a-syn has been the focus of intense research with the aim of understanding the relationship between a-syn function, aggregation, and PD pathology. Despite over two decades of research this connection is still poorly understood.

Neurons release neurotransmitters at presynaptic terminals, often thousands of times per minute, and evidence points to this location as a prime target for initiation of neurodegeneration

(Kramer and Schulz-Schaeffer 2007). Several studies implicate a critical role for a-syn in regulation of synaptic vesicle trafficking and homeostasis (Snead and Eliezer 2014). Understanding mechanistically if, and how, a-syn regulates synaptic vesicle trafficking is necessary for improving our understanding of PD onset and pathology. Recycling endosomes are essential for synaptic vesicle exocytosis and endocytosis (Hoopmann et al. 2010). In this study we utilize the SNARE protein Vesicle-Associated Membrane Protein 8 (VAMP8), a marker for recycling endosomes (Marshall et al. 2015; van Ijzendoorn 2006; Wilson et al. 2016), to monitor stimulated recycling endosomal trafficking in mammalian RBL-2H3 cells, which serve as a model for secretory cells. RBL-2H3 responses are stimulated via antigen-mediated crosslinking of the high affinity receptor (FcεRI) for immunoglobulin E (IgE), which results in exocytosis of both secretory lysosomes (degranulation) and recycling endosomes (Holowka et al. 2012; Naal et al. 2003). These exocytic processes can also be triggered by thapsigargin, which inhibits the sarco/endoplasmic reticulum Ca^{2+}-ATPase (SERCA) pump and thereby circumvents receptor-mediated signaling to cause an increase in cytoplasmic Ca^{2+}.

Over the course of these studies we discovered that expressing low concentrations of human Wt a-syn, or human a-syn mutants genetically linked to PD, inhibits exocytosis of recycling endosomes stimulated by either antigen or thapsigargin in RBL cells. Interestingly, expression of high concentrations of a-syn causes not only loss of this inhibition, but enhancement of stimulated exocytosis compared to control cells. In addition, we found that high concentrations of human a-syn partially inhibit stimulated endocytosis of antigen-crosslinked IgE-FcεRI in RBL-2H3 cells, and inhibition of this process is not detected when human a-syn is expressed at lower concentrations. We further found that the capacity to inhibit stimulated exocytosis depends on membrane interaction mediated by the N-terminus of a-syn, whereas inhibition of endocytosis at high concentrations of a-syn depends on the acidic C-terminus.

4.3 Results

Wt, A53T, and E46K human a-syn inhibit antigen-stimulated exocytosis of recycling endosomes, but not exocytosis of secretory granules/lysosomes. RBL-2H3 is a model cell line often used to study stimulated mast cell responses. The hapten 2,4-dinitrophenyl multiply conjugated to bovine serum albumin (DNP-BSA) is often used as an antigen to stimulate RBL-2H3 cells that are sensitized with anti-DNP IgE. DNP-BSA crosslinks IgE/FcεRI on the cell surface to initiate a signaling cascade, triggering Ca^{2+} release from intracellular stores, store operated Ca^{2+} entry from the extracellular medium, and consequent exocytosis of secretory lysosomes and recycling endosomes. Using this cell line we investigated the possible role for a-syn in regulating stimulated exocytosis. RBL-2H3 cells were co-transfected with human a-syn and the reporter VAMP8-pHluorin, with fluorescence that is quenched when localized to the acidic environment of the recycling endosome. VAMP8-pHluorin fluorescence increases markedly after trafficking to, and exocytosis at, the plasma membrane, thereby encountering the neutral pH environment of the extracellular medium. This change in fluorescence allows analysis and quantification of stimulated exocytosis in live cells.

As shown in Figures 4.1A and C, cells expressing an empty pcDNA vector, together with VAMP8-pHluorin, and stimulated with a low dosage of DNP-BSA (1 ng/ml) results in increased fluorescence at the plasma membrane. However, human Wt a-syn co-expressed with VAMP8-pHluorin strongly inhibits this stimulated exocytosis (Figures 4.1B and D). We found that human a-syn mutants A53T and E46K, genetically linked to PD, also inhibit stimulated exocytic responses (Figures 4.1E and F, respectively). Quantification of many replicates of these experiments is summarized in Figure 4.1G. All human a-syn constructs inhibit stimulated, but not spontaneous, exocytic responses. When spontaneous values are subtracted Wt a-syn (67% inhibition), A53T (85% inhibition), and E46K (81% inhibition) all strongly inhibit stimulated exocytosis of recycling

endosomes. The calculated difference in percent inhibition among Wt, A53T, and E46K a-syn is not statistically significant.

As activation of RBL-2H3 cells results in exocytosis of both secretory granules/lysosomes and recycling endosomes we next investigated whether, under identical conditions, human a-syn inhibits both of these exocytic processes, or if the inhibition is specific for stimulated recycling endosomal trafficking. Using Vesicle-Associated Membrane Protein 7 (VAMP7) as a secretory granule marker (Hibi, Hirashima, and Nakanishi 2000; Wernersson and Pejler 2014) we observed that human Wt a-syn does not significantly inhibit antigen-mediated degranulation (Figure 4.1H), potentially suggesting that under these conditions, inhibition appears to be specific to recycling endosomal trafficking, although a-syn may inhibit stimulated degranulation under other conditions.

To determine if the inhibitory effect of Wt human a-syn is maintained at a higher dose of DNP-BSA we next set up a sensitivity assay, stimulating RBL-2H3 cells first with a low dosage of antigen (1ng/ml DNP-BSA), followed by a higher dose (200 ng/ml DNP-BSA). Under these conditions RBL-2H3 cells expressing Wt human a-syn inhibited stimulated exocytosis at the low dose of antigen, but inhibition was lost at the higher dose (**I**). RBL-2H3 cells expressing only pcDNA and VAMP8-pHluorin show normal stimulated exocytosis (**J**). That RBL-2H3 cells are able to undergo full, stimulated exocytosis at a higher dosage of antigen, suggests that the inhibition observed by expressing Wt human a-syn is not a toxic effect, but represents a physiological function of a-syn, that is overcome under certain conditions.

All known familial human PD a-syn mutants inhibit thapsigargin-mediated recycling endosomal trafficking, when expressed at lower concentrations. PD patients often have elevated levels of a-syn (Chiba-Falek, Lopez, and Nussbaum 2006; Murphy et al. 2014), and fibrillation and aggregation of a-syn is thought to depend on concentration (Wood et al. 1999). We expressed human Wt a-syn at concentrations lower than those for Figure 4.1, to test whether this affected inhibition of

stimulated recycling endosomal exocytosis. We stimulated cells with thapsigargin, as a previous study suggests that a-syn inhibition of dopamine exocytosis occurs downstream of stimulated Ca^{2+} responses (Larsen et al. 2006). Figure 4.2A demonstrates that thapsigargin also stimulates VAMP8-mediated recycling endosomal exocytosis, although at a rate slower than that stimulated by DNP-BSA. This difference may be because thapsigargin activates protein kinase C, an essential step in stimulated exocytosis, more slowly than DNP-BSA (Gadi et al. 2011). Expressed at the lower concentrations (Figure 4.1), Wt, A53T, and E46K human a-syn all maintain the capacity to inhibit stimulated exocytosis of recycling endosomes (Figures 4.2B-D). We tested two recently discovered autosomal dominant familial PD-linked a-syn mutants, H50Q (Supplemental Figure 4.1) and G51D (Figure 4.2E), and these also inhibit thapsigargin-mediated exocytosis.

Previous studies reported that the disordered C-terminus of a-syn mediates interactions with proteins involved in exocytosis (Fan et al. 2004; Chutna et al. 2014; Breda et al. 2015), including Rab 11 which participates in stimulated RBL-2H3 exocytosis (Wilson et al, 2016), These results suggest a role for the C-terminus in mediating the inhibition we observe (Figures 4.2 B-E). However, we found that truncated a-syn 1-102 (C-terminal residues 103-140 deleted) also inhibits thapsigargin-mediated exocytosis of recycling endosomes (Figure 4.2F). We also tested Wt a-syn tagged with mRFP on its C-terminus (Wt-syn-mRFP). As a-syn is a small protein (~14 kDa) a fluorescent tag the size of mRFP (~27 kDa) may disrupt its physiological function. However, Wt-syn-mRFP maintains full capacity to inhibit stimulated exocytosis (Supplemental Figure 4.2), further supporting the idea that the C-terminus is not involved in this inhibition.

The N-terminus of a-syn has been shown to be necessary for membrane binding (Burre, Sharma, and Sudhof 2012), and we evaluated whether this is involved in the inhibition we observe. The genetically linked mutant A30P has weakened membrane affinity (Bodner et al. 2010), but this mutant still shows inhibition under our conditions (Figure 4.2G). To further reduce a-syn membrane

Figure 4.1. **Wt, A53T, and E46K human a-syn inhibit antigen-stimulated exocytosis of recycling endosomes, but not exocytosis of secretory granules/lysosomes.** RBL-2H3 cells expressing VAMP8-pHluorin and pcDNA (**A**) and VAMP8-pHluorin and human Wt a-syn (**B**) were sensitized with anti-DNP IgE and stimulated with 1ng/ml DNP-BSA at 20 sec. 50 mM NH_4Cl was added at ~300 sec to neutralize the cellular environment and dequench VAMP8-pHluorin.. Increased fluorescence around the perimeter of cells represents DNP-BSA induced VAMP8-mediated exocytosis. **C-F**: Representative traces integrated from multiple fields of 5-6 cells, similar to those shown in **A** and **B**, showing average change in fluorescence levels following DNP-BSA addition. **G and H**: Summary of three independent experiments monitoring changes in either VAMP8-pHluorin fluorescence (**G**) or VAMP7-pHluorin (**H**) fluorescence, in individual cells, due to DNP-BSA stimulation. Error bars indicate ± s.e.m (*** represents P-values <0.001, N.S. indicates values are not significantly different). **I-J**: RBL-2H3 cells expressing VAMP8-pHluorin and Wt human a-syn (**I**) or pcDNA (**J**) were sensitized with anti-DNP IgE and stimulated with 1ng/ml DNP-BSA at 20 sec, and 200ng/ml DNP-BSA at 360 seconds. 50 mM NH_4Cl was added at 550 seconds.

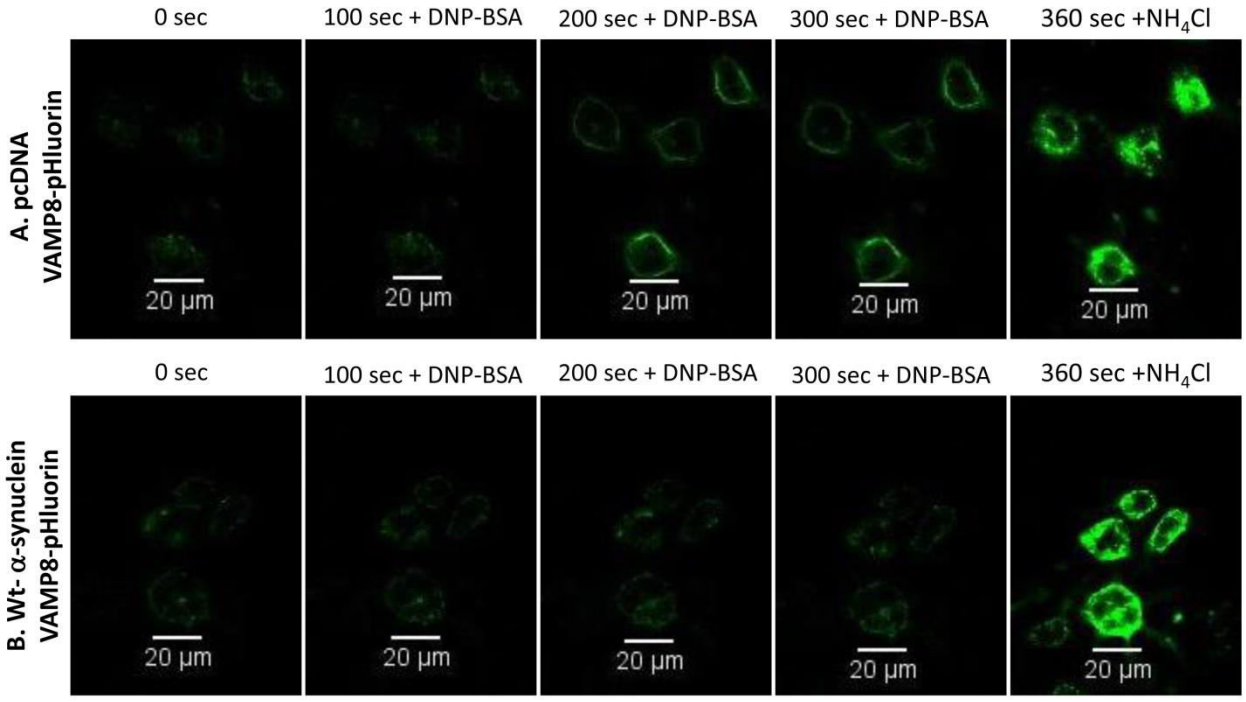
0 sec
100 sec + DNP-BSA
200 sec + DNP-BSA
300 sec + DNP-BSA
360 sec +NH4Cl
A. pcDNA VAMP8-pHluorin
B. Wt- α-synuclein VAMP8-pHluorin
20 µm

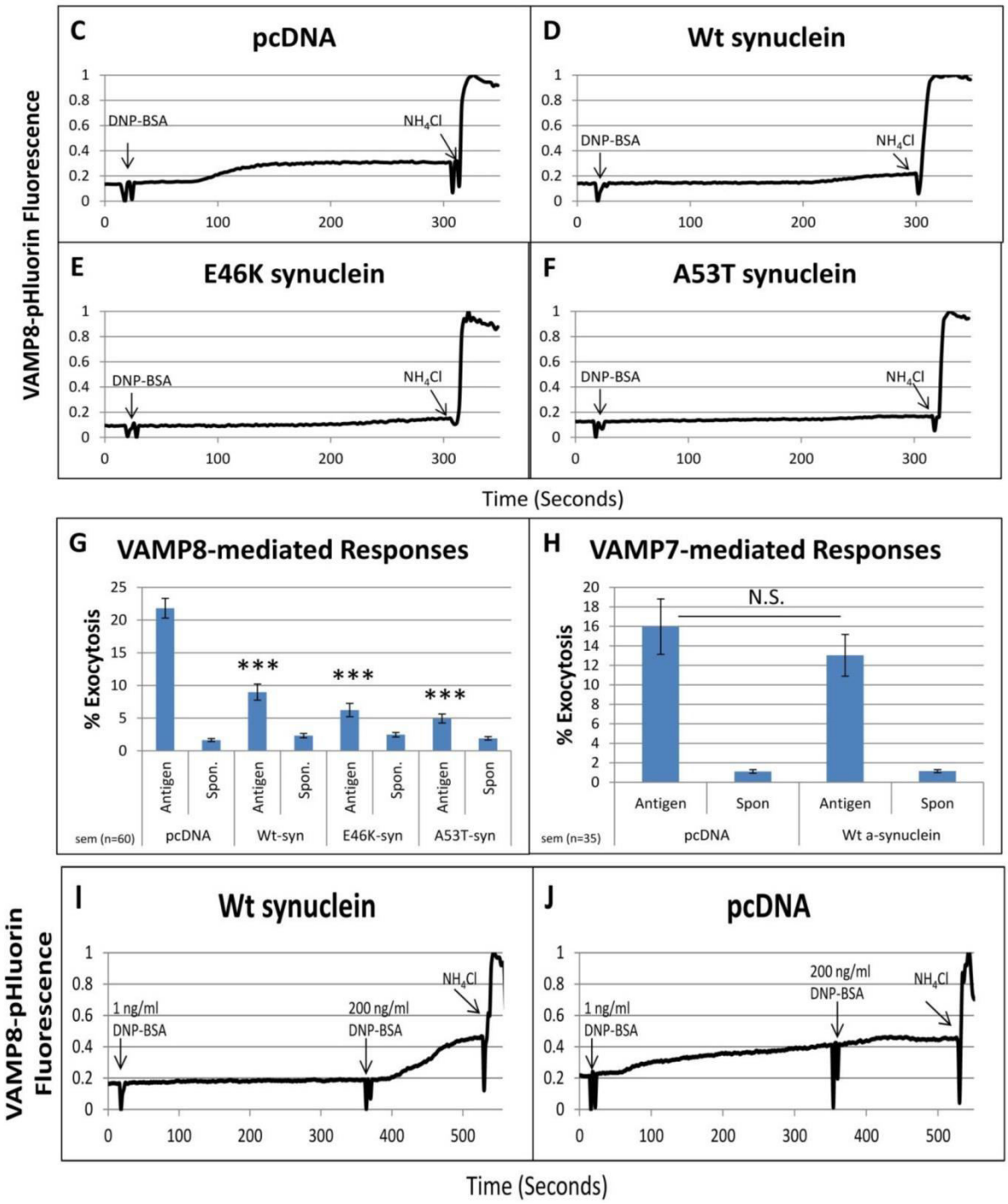
C
pcDNA
D
Wt synuclein
E
E46K synuclein
F
A53T synuclein
DNP-BSA
NH4Cl
VAMP8-pHluorin Fluorescence
Time (Seconds)
G
VAMP8-mediated Responses
% Exocytosis
Antigen
Spon.
pcDNA
Wt-syn
E46K-syn
A53T-syn
sem (n=60)
***
H
VAMP7-mediated Responses
N.S.
Spon
Wt a-synuclein
sem (n=35)
I
Wt synuclein
1 ng/ml
DNP-BSA
200 ng/ml
DNP-BSA
J
pcDNA

binding affinity we introduced a valine to proline mutation at residue 70 within the A30P mutant (A30P/V70P). The V70P mutation was previously shown to prevent membrane binding when introduced with another alanine to proline mutant (A11P/V70P) (Burré, Sharma, and Südhof 2015; Burre, Sharma, and Sudhof 2012). Expression of the A30P/V70P mutant did not inhibit thapsigargin-mediated exocytosis in our assay (Figure 4.2H), suggesting that membrane binding is essential for the inhibition we observe. A summary of inhibition caused by all human a-syn mutants we tested is shown in Figure 4.2I and in Supplemental Figure S4.1C.

High expression of human a-syn results in loss of inhibition and an enhanced response. We evaluated the concentration dependence of human a-syn effects on exocytosis of stimulated recycling endosomes. We transfected cells with the same amount of VAMP8-pHluorin as in Figure 4.2, together with five times the amount of pcDNA or human a-syn. Surprisingly, cells expressing pcDNA at this high concentration do not undergo exocytosis stimulated by thapsigargin (Figure 4.3A), and the mechanism for this inhibition is not clear. In contrast, RBL-2H3 cells expressing high concentrations of Wt, A53T, G51D, and 1-102 human a-syn show robust thapsigargin-stimulated exocytosis, suggesting these forms of a-syn at this higher expression level have lost the capacity to inhibit stimulated responses (Figures 4.3C-3F). However, not only are these responses significantly higher than the pcDNA control (Figure 4.3A), they also show consistent enhancement over the thapsigargin-stimulated exocytic response observed at low expression levels of pcDNA (Figure 4.2A).

Data collected for cells transfected with low concentrations (Figure 4.2) and high concentrations (Figure 4.3) of different a-syn constructs were typically collected on the same day, with pcDNA expressed at low concentrations always used as a positive control. As a result, direct comparison between averaged % exocytosis from pcDNA expressed at low concentrations, and the

Figure 4.2. **Wt and familial PD human a-syn mutants inhibit thapsigargin-stimulated exocytosis of recycling endosomes.** RBL-2H3 cells were co-transfected with VAMP8-pHluorin and low concentrations of the following: pcDNA (**A**), Wt a-syn (**B**); familial PD a-syn mutants A53T (**C**), E46K (**D**), G51D (**E**), A30P (**G**); structural a-syn mutants with either a truncated C-terminus, 1-102 (**F**), or a double proline mutant that prevents membrane binding, A30P/V70P (**H**). All conditions were stimulated with thapsigargin (250 nM) at t=20 sec, followed by addition of 50 mM NH_4Cl at t= ~400 sec to neutralize the cellular environment. The representative traces of stimulated exocytic responses shown in **A-H** are average fluorescence levels over time integrated from microscopic fields containing 5-6 cells (similar to images shown in Figure 4.1A and 4.1B). (**I**) Summary of 3-4 independent experiments monitoring changes in VAMP8-pHluorin fluorescence, in individual cells, are displayed as percent exocytosis values for all conditions tested. Error bars indicate ± s.e.m for 55 individual cells for each condition shown (*** represents P-values <0.001).

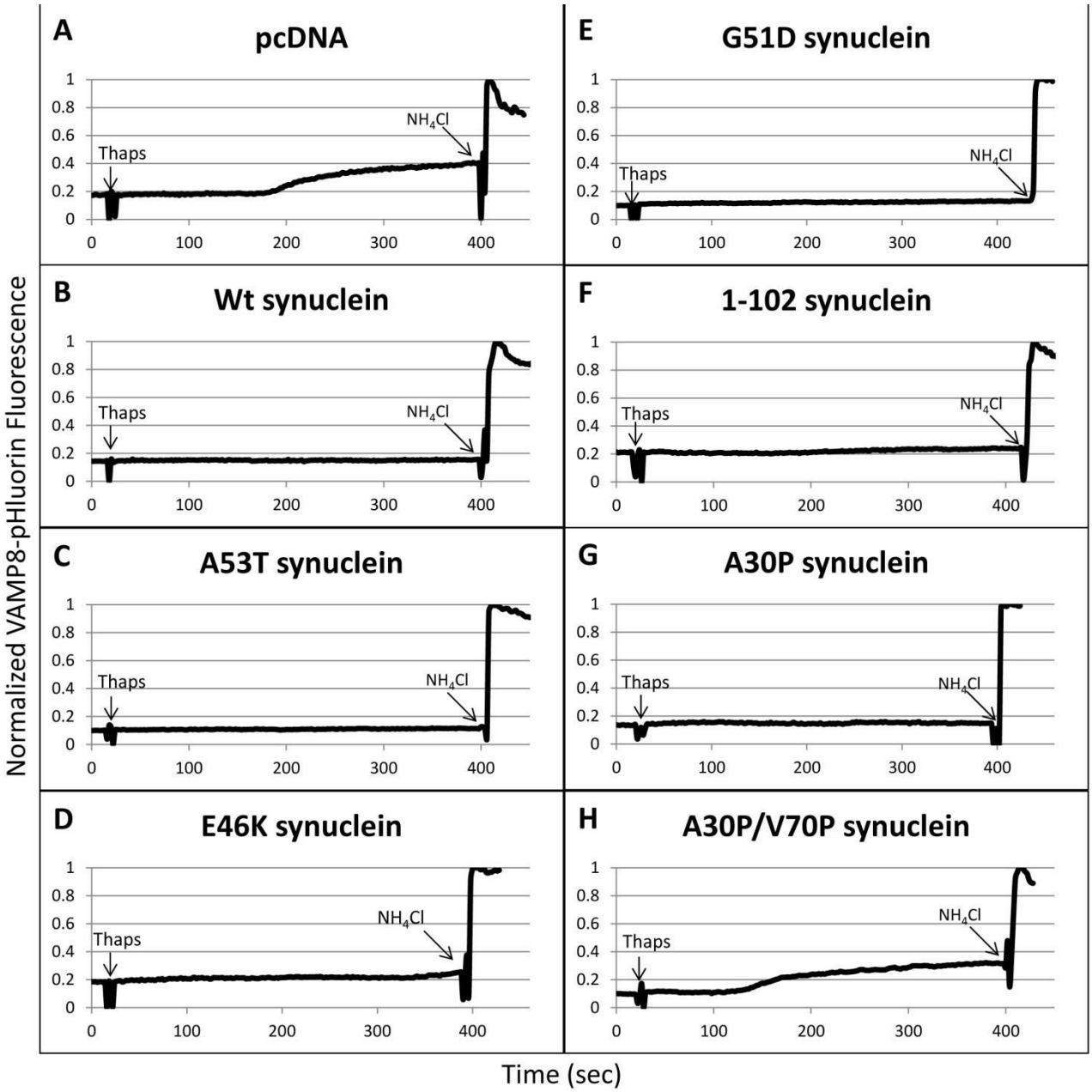
A
pcDNA
B
Wt synuclein
C
A53T synuclein
D
E46K synuclein
E
G51D synuclein
F
1-102 synuclein
G
A30P synuclein
H
A30P/V70P synuclein
Thaps
NH4Cl
Normalized VAMP8-pHluorin Fluorescence
Time (sec)

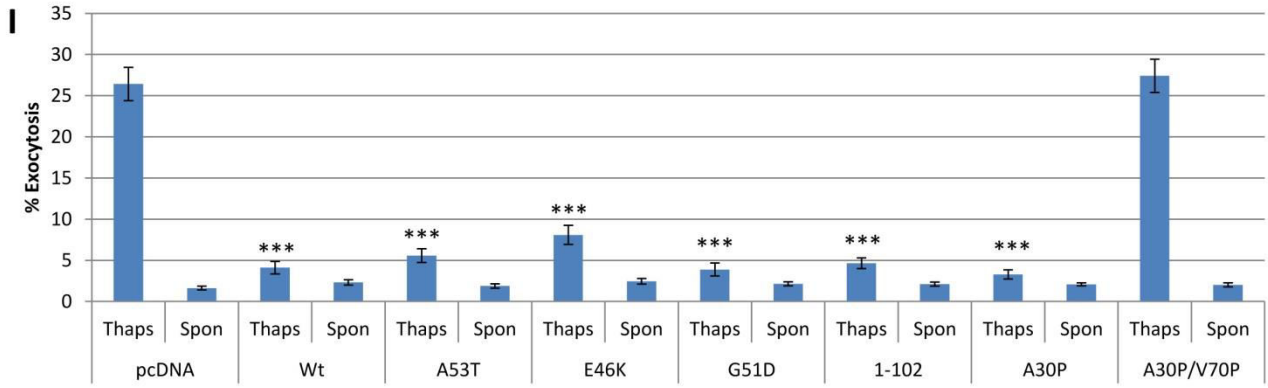
I
% Exocytosis
Thaps
Spon
pcDNA
Wt
A53T
E46K
G51D
1-102
A30P
A30P/V70P
***

various a-syn constructs tested at high concentrations, can be directly compared. Comparing the average exocytosis response stimulated by thapsigargin in cells transfected with pcDNA at low levels (Figure 4.2I; 26.4% exocytosis), with the average values in Figure 4.3G, show that expression at high levels of Wt (35.9% exocytosis), A53T (31.5% exocytosis), G51D (34.8% exocytosis), and 1-102 (37.6% exocytosis) cause enhancement by 36%, 19%, 32%, and 42% respectively. This enhancement of thapsigargin-stimulated exocytosis of recycling endosomes may represent a gain of function occurring only at high concentrations of the expressed human a-syn. Enhancing effects at these high expression levels are especially striking when compared to cells transfected with pcDNA transfected at the same concentration, which show no stimulated response (Figure 4.3A). Wt-syn-mRFP also loses the capacity to inhibit exocytosis when expressed at higher concentrations (Supp. Figure S4.2). Consistent with the enhancement observed when Wt, A53T, G51D, and 1-102 a-syn are expressed at high levels, Wt-syn-mRFP expressed at high concentration shows an ~20% increase in stimulated exocytosis when compared to mRFP expressed at high concentrations (Supp Figure 4.2E).

In contrast to Wt and other mutants tested at high expression levels (Figure 4.3C-F), A30P a-syn does not exhibit loss of inhibition under these conditions (Figure 4.3B and G). A30P has been shown to undergo slower fibrilization kinetics when compared to Wt and other mutant forms of a-syn (Lemkau et al. 2012), which may explain this difference from loss of inhibition observed for Wt, A53T, and G51D. In our experiments RBL-2H3 cells express a-syn for only 24 hours before being stimulated; suggesting more time may be necessary for fibrils and aggregates to form following A30P a-syn expression. To test this hypothesis A30P and VAMP8-pHluorin were expressed for 40 hours, and under these conditions A30P no longer inhibits stimulated exocytosis, although it does not appear to enhance exocytosis (compared to pcDNA control) to the same extent as Wt, A53T, and G51D a-syn (Supplementary Figure S4.3).

Low and high concentration levels of expressed human a-syn can be imaged and quantified using fluorescence microscopy and flow cytometry. Because of the concentration dependence we observed in Figures 4.2 and 4.3 we further investigated a-syn expression levels, recognizing that the relationship between transfected DNA and expressed protein does not always correlate (Maier, Güell, and Serrano 2009). Using conditions identical to those in Figures 4.2 and 4.3, RBL-2H3 cells were electroporated with VAMP8-pHluorin and with either low or high concentrations of pcDNA or human a-syn. After 24 hours cells were fixed and labeled with a monoclonal a-syn primary antibody, followed by labeling with an Alexa-647-labeled secondary antibody. We detected no a-syn labeling in pcDNA expressing cells (Figure 4.4A and 4.4B). However, at low expression levels, Wt a-syn labeling was clearly visible (Figure 4.4C), and this fluorescence was substantially brighter for Wt a-syn expressed at high concentrations (Figure 4.4D). Figure 4.4C and D also demonstrate that VAMP8-pHluorin is a good reporter for positively transfected cells, as >90% of all cells expressing VAMP8-pHluorin also express a-syn.

To quantify differences in expression levels, electroporated cells were harvested, fixed, labeled, and then analyzed using flow cytometry. VAMP8-pHluorin expressing cells were gated, and Alexa-647 fluorescence levels from these positively transfected cells were quantified. Figure 4.4E displays a representative histogram comparing Alexa-647 fluorescence levels, measured from only VAMP8-pHluorin expressing cells, comparing samples expressing either low or high concentrations of pcDNA or human Wt a-syn. This histogram confirms differences in human a-syn expression levels, with the higher human Wt a-syn transfection concentration exhibiting an ~4 fold increase in mean Alexa-647 fluorescence when compared to the lower human Wt a-syn transfection concentration. Figure 4.4F shows mean Alexa-647 fluorescence values from control or a-syn mutants analyzed in Figures 4.2 and 4.3; low concentrations of H50Q and E46K human a-syn are quantified in supplementary Figure S4.1.

Figure 4.3. **High expression of human a-syn results in loss of inhibition and enhanced exocytosis.** RBL-2H3 cells co-transfected with VAMP8-pHluorin and high concentrations of pcDNA (**A**), A30P (**B**), Wt (**C**), A53T (**D**), G51D (**E**), or 1-102 (**F**) human a-syn. All conditions were stimulated identical to experiments in Figure 4.2, with addition of thapsigargin (250 nM) at t=20 sec, followed by addition of 50 mM NH_4Cl at ~t=400 sec to neutralize the cellular environment. Results from 3 independent experiments for each condition are summarized and represented as percent exocytosis in **G**. Error bars indicate ± s.e.m for 55 individual cells for each condition shown (*** represents P-values <0.001).

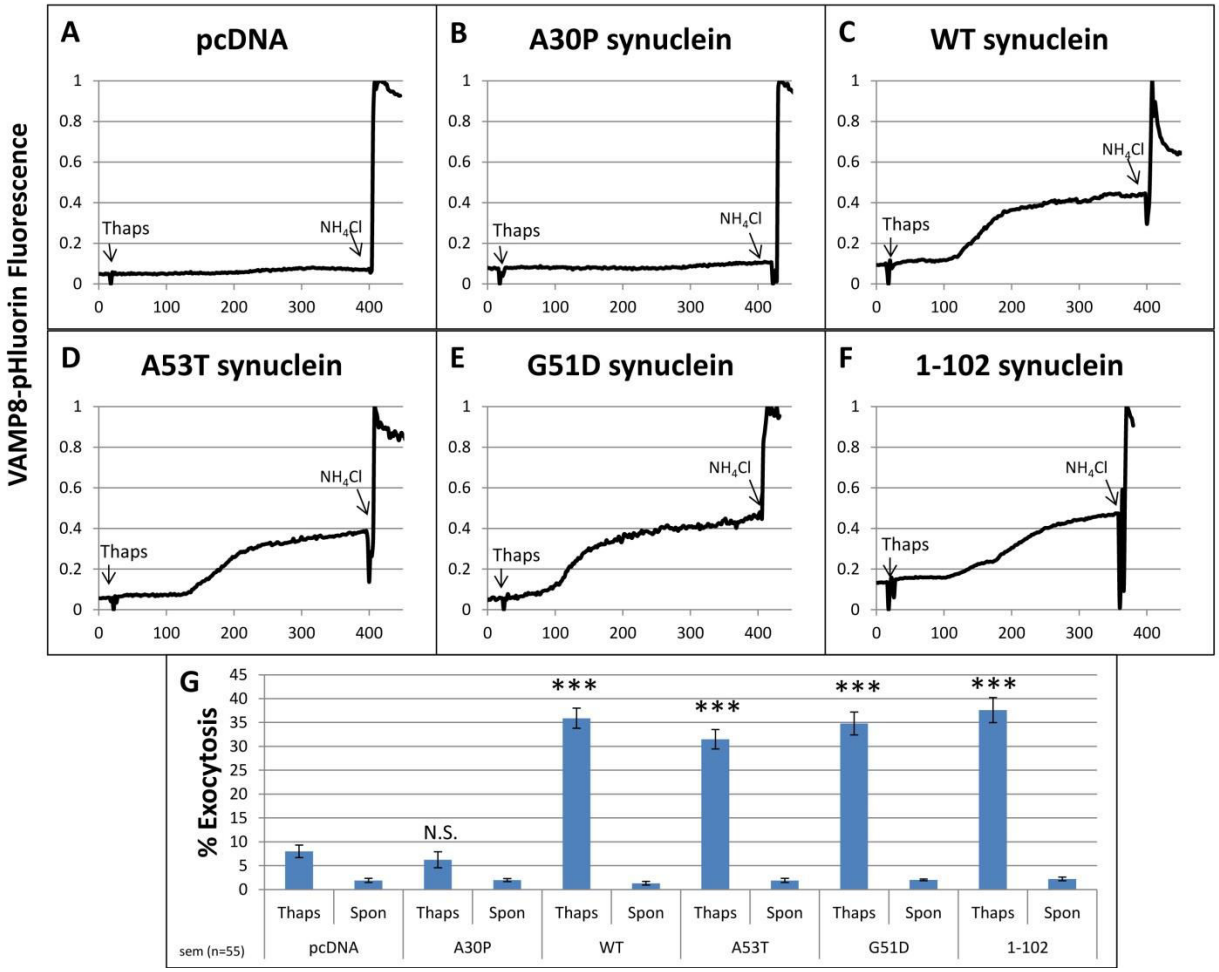
VAMP8-pHluorin Fluorescence
A
pcDNA
B
A30P synuclein
C
WT synuclein
D
A53T synuclein
E
G51D synuclein
F
1-102 synuclein
Thaps
NH4Cl
G
% Exocytosis
N.S.
***
Thaps
Spon
sem (n=55)
pcDNA
A30P
WT
A53T
G51D
1-102

Low expression of human a-syn inhibits stimulated exocytosis of recycling endosomes in PC-12 cells. Dopamine releasing neurons are particularly susceptible to damage in PD patients, with 60-80% of dopamine-containing neurons from the substantia nigra lost in PD patients (Cheng, Ulane, and Burke 2010). Therefore, we investigated whether trends observed in RBL-2H3 cells were more general. PC-12 is a dopamine secreting chromaffin cell line often used as a model for neuronal signaling. We expressed VAMP8-pHluorin and pcDNA or human a-syn in PC-12 cells, which were then stimulated with thapsigargin and phorbol 12-myristate-13-acetate (PMA), which was necessary to stimulate exocytosis in this cell line. Stimulated cells expressing VAMP8-pHluorin and pcDNA showed an ~25% exocytic response (Figure 4.5A). We found strong inhibition by human Wt a-syn expressed at low concentrations, corresponding to an average inhibition of ~71% when spontaneous values are subtracted (Figures 4.5B, 4.5C).

Stimulated endocytosis is inhibited by higher concentrations of human a-syn, depending on the C-terminus. Although several studies have implicated a-syn as an important regulator of synaptic vesicle trafficking, most of these have focused on endocytosis, rather than exocytosis (Busch et al. 2014; Vargas et al. 2014). Therefore, we evaluated whether a-syn affects stimulated endocytosis in RBL-2H3 cells, and its possible concentration dependence. Cells were transfected with mRFP as a reporter for positively transfected cells, together with either pcDNA or human a-syn constructs at high or low concentrations. Cells were then labeled with IgE conjugated to fluorescein isothiocyanate (FITC-IgE), which displays bright fluorescence at the plasma membrane upon binding to the FcεRI receptor. Antigen crosslinking causes FITC-IgE/FcεRI to be endocytosed, and the FITC fluorescence becomes quenched as it moves from the neutral pH environment of the extracellular space to the more acidic environment of the endosome. Transfected cells were placed in a flow cytometer and stimulated with an anti-IgE antibody, which causes quenching of FITC-IgE due to endocytosis, as shown in Figures 4.6A-D. Averaged data corresponding to Figures 4.6 A-D

Figure 4.4. **Low and high concentration levels of expressed human a-syn can be imaged and quantified using fluorescence microscopy and flow cytometry. A-D:** Representative confocal images of a-syn expression levels in RBL-2H3 cells (scale bar equals 20 μm). Cell co-expressing VAMP8-pHluorin and low concentrations of pcDNA (**A**) or Wt human a-syn (**C**), or high concentrations of pcDNA (**B**) or human Wt a-syn (**D**) were fixed and labeled with a primary monoclonal a-syn antibody, followed by labeling with an Alexa-647 secondary antibody, and imaged with confocal microscopy. Cells expressing the conditions described in **A-D** were harvested, fixed, labeled with a monoclonal a-syn antibody, labeled with an Alexa-647 secondary antibody and analyzed using flow cytometry. Alexa-647 fluorescence was then measured in RBL-2H3 cells expressing VAMP8-pHluorin, so that only positively transfected cells were quantified. A representative histogram of Alexa-647 fluorescence from VAMP8-pHluorin expressing cells is shown in **E,** with 5,000-6,000 VAMP8-pHluorin expressing cells analyzed for each condition. **F**, quantified results are averaged and summarized for all conditions tested at both high and low concentration in Figures 4.2 and 4.3. Error bars indicate coefficient of variance for 3 independent experiments, with between 15,000 and 20,000 total VAMP8-pHluorin expressing cells analyzed for each condition shown.

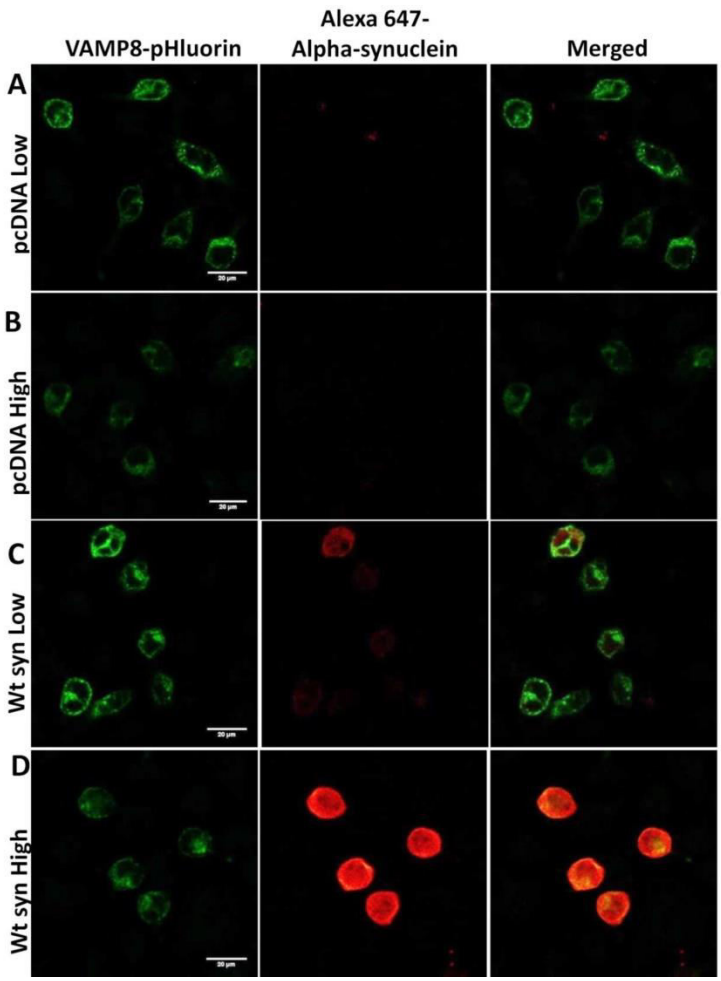
VAMP8-pHluorin
Alexa 647-
Alpha-synuclein
Merged
A
pcDNA Low
B
pcDNA High
C
Wt syn Low
D
Wt syn High

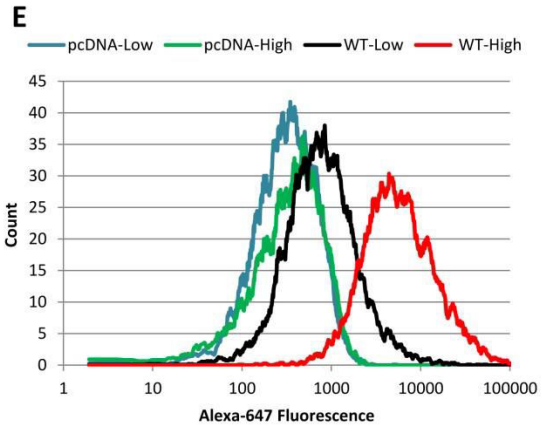
E
pcDNA-Low
pcDNA-High
WT-Low
WT-High
Count
Alexa-647 Fluorescence

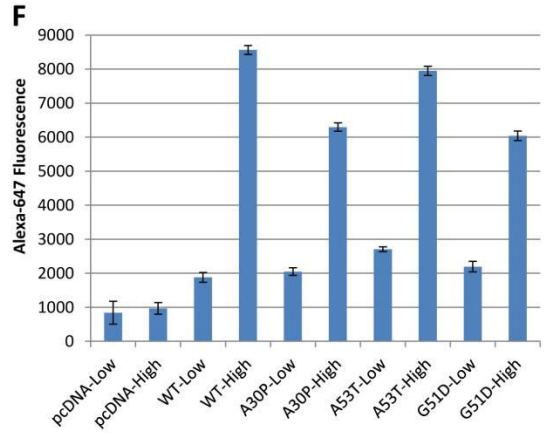
F
Alexa-647 Fluorescence
pcDNA-Low
pcDNA-High
WT-Low
WT-High
A30P-Low
A30P-High
A53T-Low
A53T-High
G51D-Low
G51D-High

are summarized in Figure 4.6E. We found that human Wt a-syn expressed at low concentrations showed only minor inhibition of stimulated FITC-IgE endocytosis that was not statistically significant (Figure 4.6A).In contrast, expression of human Wt a-syn at high concentrations shows increased inhibition of stimulated FITC-IgE endocytosis (Figure 4.6B), suggesting concentration dependence. Unlike the case with exocytosis (Figure 4.3) A30P expressed at high concentrations caused inhibition of stimulated endocytosis similar to that caused by Wt a-syn (Figure 4.6C). To investigate whether this inhibition is related to the aggregation state of a-syn, we tested the 1-102 mutant, which lacks the C-terminus and is also known to form aggregates rapidly (Murray et al. 2003). The 1-102 mutant did not inhibit stimulated endocytosis (Figure 4.6D), suggesting an effect of aggregation alone is not sufficient for this observed inhibition, but a functional C-terminus participates. We found that Wt-syn-mRFP, which is C-terminally tagged, also fails to inhibit stimulated endocytosis (data not shown), supporting the view that the unperturbed C-terminus of a-syn is involved in inhibition of stimulated endocytosis.

4.4 Discussion

For over two decades a-syn and its associated synucleinopathies have been intensively studied, yet the normal cellular function of this protein, as well as how disruption of this function relates to onset of PD, remain poorly understood. Our studies reveal that exogenous expression of human a-syn inhibits antigen- and thapsigargin-stimulated exocytosis in RBL-2H3 cells (Figure 4.1 and 4.2), as well as stimulated exocytosis in PC-12 cells (Figure 4.5). This inhibition appears to be specific to stimulated recycling endosomal exocytosis (Figure 4.1G-H) (Wilson et al. 2016), which is of interest as abnormal endocytic trafficking is observed in many neurodegenerative disorders, including PD (Wang et al. 2014). Our findings also add to a growing body of literature showing that

Figure 4.5. **Low expression of human a-syn inhibits stimulated exocytosis of recycling endosomes in PC-12 cells.** Traces of stimulated exocytosis averaged from 5-6 individual PC-12 cells expressing VAMP8-pHluorin and either pcDNA (**A**), or Wt human a-syn (**B**). 80 nM phorbol 12-myristate-13-acetate (PMA) was added at t=20 sec to activate protein kinase C, 250 nM thapsigargin was added at t=300 sec to stimulate exocytosis, and 50mM NH_4Cl was added at t=600 sec to neutralize the cells and determine total VAMP8-pHluorin expressed. **C**, average stimulated percent exocytosis determined from 3 independent experiments, with error bars representing ± s.e.m for 25 individual cells for each condition shown (*** represents P-values <0.001).

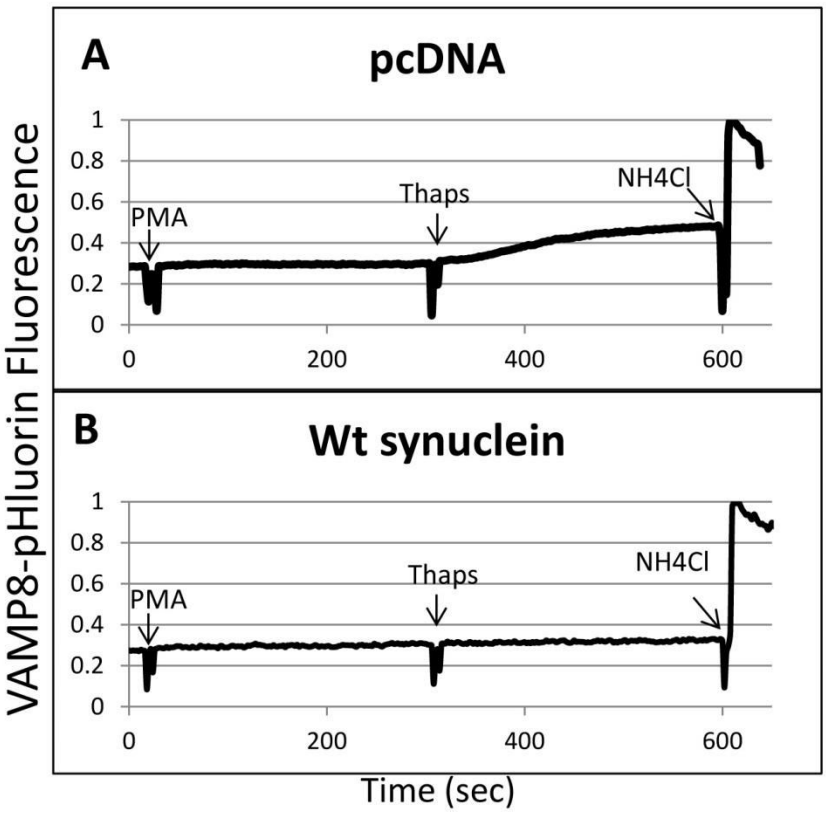
A
pcDNA
B
Wt synuclein
VAMP8-pHluorin Fluorescence
PMA
Thaps
NH4Cl
0
0.2
0.4
0.6
0.8
1
0
200
400
600
Time (sec)

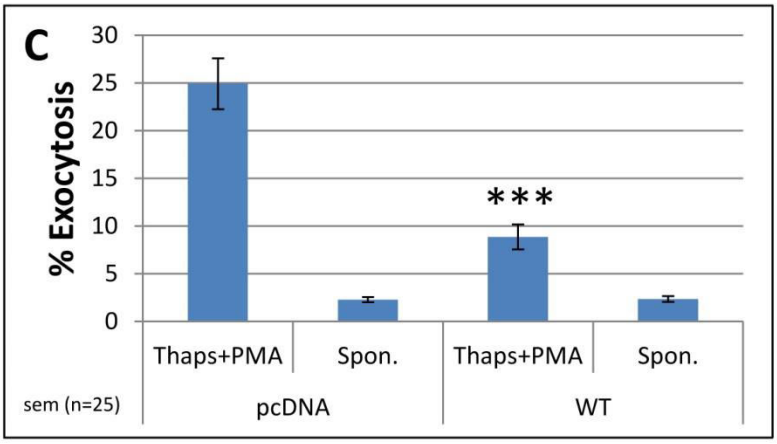
C
% Exocytosis
0
5
10
15
20
25
30
***
Thaps+PMA
Spon.
Thaps+PMA
Spon.
pcDNA
WT
sem (n=25)

a-syn regulates stimulated, as well as homeostatic, endocytic trafficking (Cooper et al. 2006; Thayanidhi et al. 2010; Busch et al. 2014; Xu et al. 2016).

Although addition of 1ng/ml DNP-BSA stimulates exocytosis in RBL-2H3 cells (Figure 4.1J), this concentration of antigen is lower than what is commonly used to stimulate maximal degranulation in mast cells (Wilkes et al. 2014; Shelby et al. 2013). Although it is unclear why exogenous expression of human a-syn inhibits antigen-stimulated exocytosis only at a low (1 ng/ml) but not high (200 ng/ml) concentration of DNP-BSA, several possible explanations exist. First, it is possible that 1 ng/ml DNP-BSA stimulates a stronger recycling endosomal response compared to a secretory lysosomal response. This explanation is supported by the ~36% overall increase in percent recycling endosomal exocytosis in Figure 4.1G (21.8%) vs secretory lysosomal degranulation in 4.1H (15.9%). 200 ng/ml DNP-BSA is often used as an optimal antigen dose to stimulate maximum degranulation in our experiments, and it is possible that a-syn inhibition of recycling endosomal exocytosis is masked at this higher concentration of antigen, which may favor degranulation.

Another possible explanation regards the stabilization, and subsequent break down, of the syntaxin-1, SNAP-25, and synaptobrevin-2 SNARE complex, the formation of which is necessary for synaptic vesicle fusion. A-syn has been shown to stabilize this complex (Burré et al. 2010), and it is possible that addition of a low concentration of human a-syn to a rat cell line containing no, or extremely low amounts of, a-syn, not detectable by the monoclonal a-syn antibody used in our experiments (Figure 4.4A-D), stabilizes the SNARE complex to the point that its disassociation is prevented at 1ng/ml DNP-BSA antigen. However the higher 200 ng/ml DNP-BSA concentration may overcome this stabilization, resulting in a normal exocytic response. Although it remains unclear why a-syn inhibits at lower but not higher doses of antigen, this result demonstrates that the inhibitory effect we observe is not toxic to RBL-2H3 cells. Lack of toxicity suggests that this

Figure 4.6. **Higher concentrations of human a-syn inhibit stimulated endocytosis, depending on the C-terminus.** RBL-2H3 cells were co-transfected with mRFP, to mark positively transfected cells, and low concentrations of pcDNA or Wt human a-syn (**A**), or high concentrations of pcDNA and human Wt a-syn (**B**), A30P (**C**), or 1-102 (**D**). Cells were labeled with fluorescein isothiocyanate conjugated to anti-DNP IgE (FITC-IgE), incubated at 37°, and stimulated with anti-IgE antibody**.** Stimulation results in endocytosis of FITC-IgE, which becomes quenched as it moves from the neutral pH environment of the extracellular space to the acidic environment of the recycling endosome. End point fluorescence values were normalized to 100% for pcDNA control cells, and % endocytosis for a-syn conditions was then calculated relative to this internally normalized 100% pcDNA value. These results are summarized in **E**. Error bars represent ± s.d. from 3 independent experiments. (** represents P-values <0.01, * represents P-values <.05, N.S. means not statistically significant).

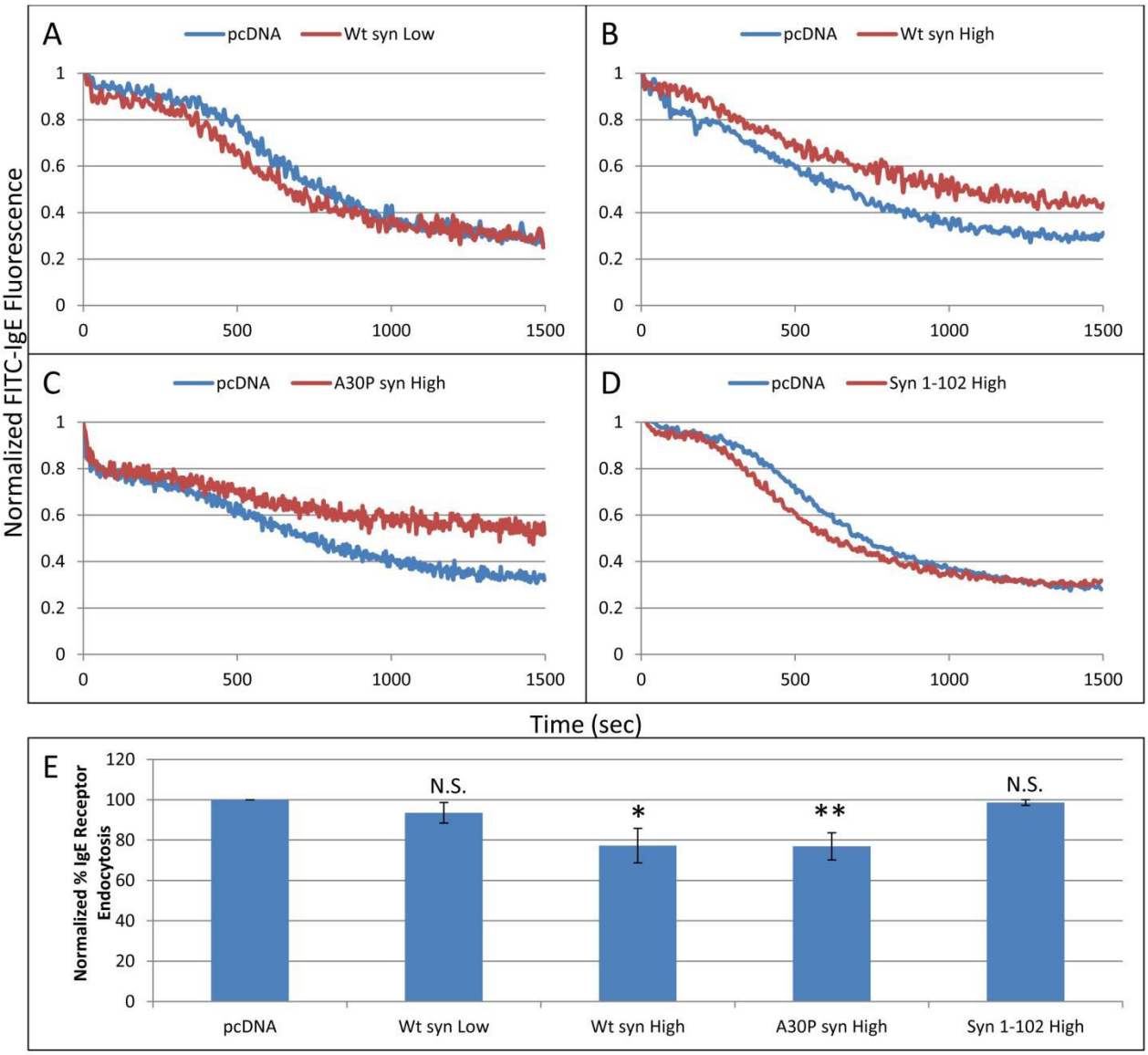
A
pcDNA
Wt syn Low
B
pcDNA
Wt syn High
C
pcDNA
A30P syn High
D
pcDNA
Syn 1-102 High
Normalized FITC-IgE Fluorescence
Time (sec)
0
0.2
0.4
0.6
0.8
1
0
500
1000
1500

E
Normalized % IgE Receptor Endocytosis
0
20
40
60
80
100
120
N.S.
*
**
N.S.
pcDNA
Wt syn Low
Wt syn High
A30P syn High
Syn 1-102 High

inhibitory phenotype may represent a physiological function of a-syn, detectable because of our unique, experimental conditions, which introduce human a-syn into cells containing little, or no, endogenous a-syn.

The concentration of a-syn within cells is known to be a critical factor in the capacity of human a-syn to aggregate and develop into toxic species (Narkiewicz, Giachin, and Legname 2014). Our results show clear evidence that the function of human a-syn in RBL-2H3 cells strongly depends on concentration and membrane binding (Figure 4.2H-I). In contrast to the inhibition observed at lower concentrations of exogenously expressed human a-syn, higher concentrations show no inhibitory effects, even enhancing the percent stimulated exocytosis (Figure 4.3). Higher concentrations of a-syn are typically correlated with genetic and sporadic PD, and high concentrations are associated with aggregation into Lewy bodies (Kim 2013). At present we lack a clear readout to determine if human a-syn is aggregating when expressed at higher concentrations. However, a schematic depicting our interpretation of our concentration-dependent results is displayed in Figure 4.7, suggesting that higher concentrations of a-syn begin to aggregate, displace monomeric a-syn from the plasma membrane, and prevent inhibition of recycling endosomal exocytosis.

Our study also finds that a-syn affects stimulated endocytosis of IgE/FcεRI in RBL-2H3 cells (Figure 4.6). Our finding that low expression levels of human a-syn have no detectable impact on stimulated endocytosis, whereas high expression levels do, further demonstrates that the function of human a-syn depends on concentration in RBL cells. In addition, reduced endocytosis, coupled with enhanced exocytosis, would also result in a bigger apparent exocytosis, as observed in our experiments. The inhibition of stimulated IgE/FcεRI endocytosis most likely represents an effect on stimulated secretory granule endocytosis, although this inhibition may also affect recycling endosome endocytosis. Future experiments will aim to directly test the effects of overexpressed a-

Figure 4.7. **Potential functions of human alpha-syn**.

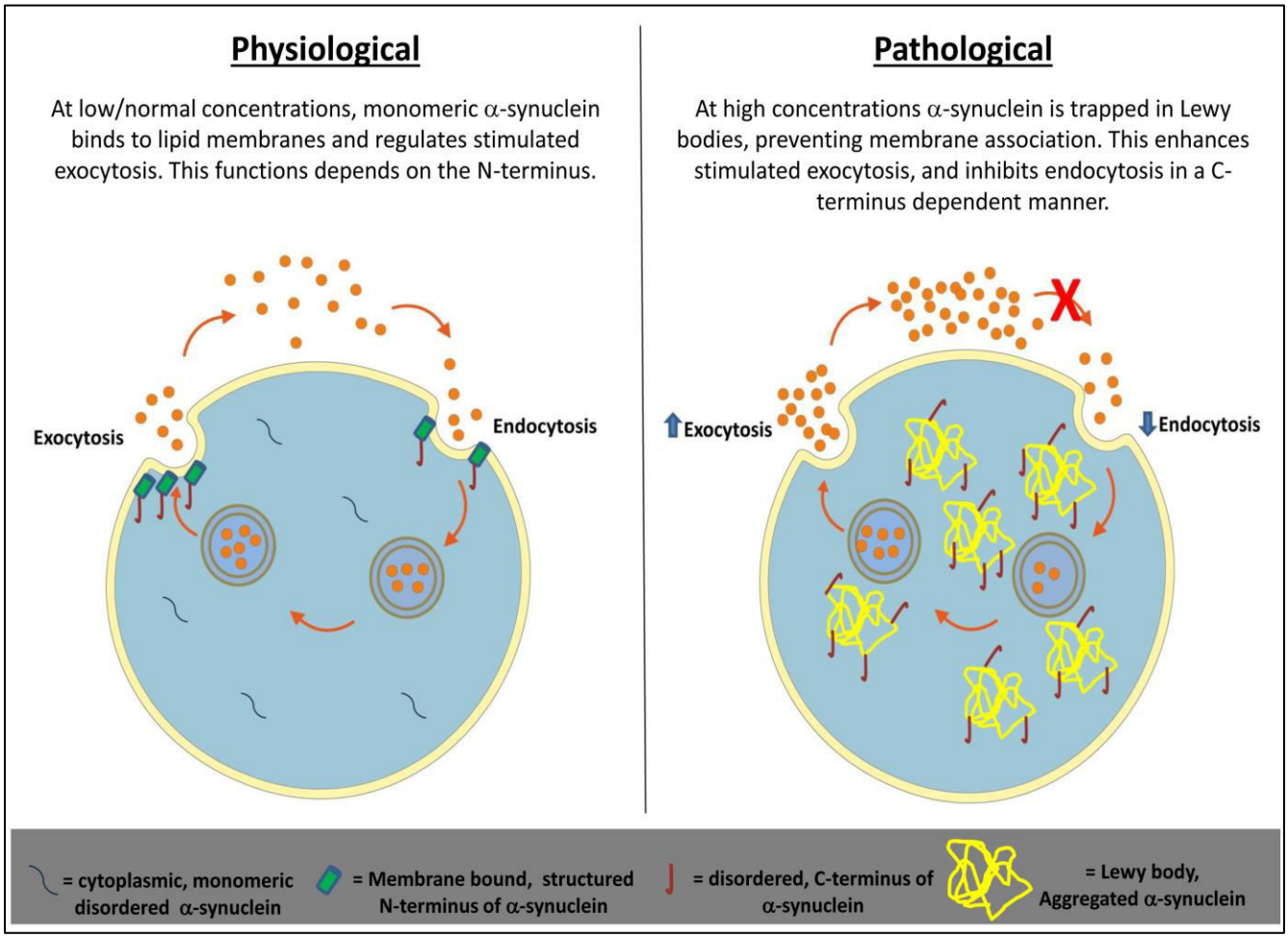

syn on stimulated recycling endosome endocytosis. Previous studies report that expression of high levels of human a-syn prevents neurotransmitter release due to inhibition of synaptic vesicle recycling, following exocytosis. This reduces the number of readily releasable synaptic vesicles and therefore the size of the synaptic vesicle recycling pool (Gaugler et al. 2012; Nemani et al. 2010; Lundblad et al. 2012; Scott and Roy 2012; Busch et al. 2014; Xu et al. 2016). Our studies support this hypothesis, as increased human a-syn levels partially impair stimulated endocytosis in our system. However, our data suggest that a reduced synaptic vesicle pool may also be observed because stimulated exocytosis has initially been enhanced. Under conditions where human a-syn is highly expressed, as in our experimental setup, an initial enhancement of stimulated endosomal exocytosis, coupled by partial inhibition of subsequent endocytosis, would also result in a reduced synaptic vesicle pool in the cytoplasm over time, as depicted in Figure 4.7.

In conclusion, using RBL-2H3 cells as a model system to study the function of a protein known to play a critical role in neurological processes, has allowed us to identify human a-syn as a regulator of stimulated recycling endosomal exocytosis and IgE/FcεRI endocytosis, processes thought to be highly susceptible to neurodegeneration due to aging. We found that human a-syn inhibits stimulated exocytosis and endocytosis, inversely, in a concentration dependent manner. Future experiments will aim to validate our results in neurons, with the goal of further clarifying the physiological function of human a-syn in healthy and dysregulated neuronal cells.

4.5 Materials and Methods

Cell Culture: RBL-2H3 cells were cultured as monolayers in minimal essential medium (Invitrogen Corp., Carlsbad, CA) with 20% fetal bovine serum (Atlanta Biologicals, Atlanta, GA) and 10 μg/ml gentamicin sulfate (Invitrogen) as previously described (Gosse et al. 2005). PC-12 cells were cultured in Dulbecco's modified eagle medium (Invitrogen Corp., Carlsbad, CA) with 10% fetal bovine serum and 10 μg/ml gentamicin.

Reagents and Chemicals: Thapsigargin and phorbol 12-myristate-13-acetate were purchased from Sigma-Aldrich (St. Louis, MO).

Expression Plasmids: DNA plasmids Wt a-syn, A53T a-syn, and E46K a-syn were generously provided by Dr. David Eliezer (Weill Cornell Medical College, NYC, NY). All other a-syn mutants were created by site directed mutagenesis using Phusion High-Fidelity DNA Polymerase (New England Biolabs). VAMP8-pHluorin was created as previously described (Wilson et al. 2016; Wilkes et al. 2014). To create the Wt-syn-mRFP construct, the cDNA encoding human Wt a-syn was introduced into a clontech vector containing mRFP sequence, using Hind III and Kpn I restriction sites.

Transfection: Both RBL-2H3 and PC-12 cell lines were transfected by electroporation under identical conditions for stimulated exocytosis experiments. Cells were harvested three to five days after passage and ~ 5 x 10^6 cells were electroporated in 0.5 ml of cold electroporation buffer (137 mM NaCl, 2.7 mM KCl, 1 mM $MgCl_2$, 1 mg/ml glucose, 20 mM HEPES (pH 7.4) using 5 μg of reporter plasmid DNA (VAMP8-pHluorin, VAMP7-pHluorin, or mRFP) together with 5 μg of effector plasmid DNA (pcDNA 3.0, Wt, A53T, E46K, A30P, G51D, H50Q, 1-102, A30P/V70P) for "low" concentration experiments or 25 μg of effector plasmid for "high" concentration experiments.

For experiments in Figure 4.1, 5 μg of VAMP8-pHluorin or VAMP7-pHluorin was electroporated with 12.5 μg of Wt, A53T, or E46K a-syn. mRFP and Wt-syn-mRFP were expressed in a Clontech vector which was found to express more efficiently than the pcDNA 3.0 vector that untagged a-syn constructs were cloned into. For these constructs we expressed 1.5 μg of mRFP or Wt-syn-mRFP for "low" and 10 μg of mRFP or Wt-syn-mRFP a-syn for "high" concentration experiments with 5 μg of VAMP8-pHluorin. We found that 10 μg of empty Clontech vector does not inhibit exocytosis when expressed at higher concentrations, unlike pcDNA 3.0.

For all conditions cells were electroporated at 280 V and 950 μF using Gene Pulser X (Bio-Rad). Following electroporation, cells were immediately resuspended in 6 ml of medium and plated in three different MatTek dishes (2 ml/dish) (MatTek Corporation, Ashland, MA). Cells in Figure 4.1 were sensitized with 0.5 μg/ml anti-2,4-dinitrophenyl (DNP) IgE overnight after being plated in MatTek dishes (Posner et al. 1992). For all experiments, cells were allowed to recover for 24 hours. For experiments in Supplementary Figure S4.3, RBL-2H3 cells were electroporated with 10 μg of VAMP8-pHluorin and 25 μg of A30P or pcDNA 3.0 and were allowed to recover for 40 hours before imaging.

Stimulated Exocytosis Assays: 24 hours after electroporation cells were washed once with buffered saline solution (BSS: 135 mM NaCl, 5 mM KCl, 1 mM $MgCl_2$, 1.8 mM $CaCl_2$ 5.6 mM D(+) glucose, 20 mM HEPES, pH 7.4) and then placed in BSS and incubated for 5 minutes at 37ºC within a confined heating chamber prior to live cell imaging. For RBL-2H3 cells VAMP8-pHluorin or VAMP7-pHluorin fluorescence was monitored for twenty seconds prior to addition of either 1 ng/ml DNP-BSA, or 250nM thapsigargin, followed by the addition of 50 mM NH_4Cl 6-8 min after stimulation. For our sensitivity assay described in Figure 4.1 I and J, cells were first stimulated with 1 ng/ml DNP-BSA and then, after ~340 seconds, stimulated with 200 ng/ml DNP-BSA. PC-12 cells

were stimulated with 100 nM PMA at 20 sec, and 250 nM thapsigargin at 300 sec. Cells were monitored using a 40X H_20 heated objective on a Zeiss 710 confocal microscope. VAMP8-pHluorin and VAMP7-pHluorin was excited using the 488-nm line of a krypton/argon laser and viewed with a 502-551 nm band-pass filter.

Offline image analysis was conducted using ImageJ (National Institutes of Health). Changes in VAMP7-pHluorin or VAMP8-pHluorin fluorescence were normalized to a 0-1 scale using the following equation: (value-minimum)/(maximum-minimum) with value being the measured pHluorin fluorescence at a given time point, minimum being the lowest monitored fluorescent value, and maximum being the value observed following NH_4Cl addition. Percent exocytosis is calculated by the following equation: ((stimulated fluorescence-basal fluorescence)/(NH4Cl fluorescence-basal fluorescence)*100). Data normalized in this manner is presented in Figure 4.1 C-F; Figure 4.2 A-H; Figure 4.3 A-F; Figure 4.5 A-B.

Immunofluorescence: For immunofluorescence imaging cells were electroporated as described above, plated in MatTek dishes, allowed to recover for ~24 hours then fixed with 4% paraformaldehyde + 0.1% glutaraldehyde. Fixed cells were then labeled with an a-syn monoclonal primary antibody (BD Biosciences # 610787) followed by labeling with goat-anti mouse Alexa 647 IgG1 secondary antibody in PBS with 10 mg/ml BSA and imaged on a Zeiss 710 confocal microscope using a 40x H_20 objective.

Flow Cytometry and Immunofluorescence. Samples were electroporated as described above except that following electroporation, cells were plated in 60 mm dishes. After 24 hours cells were harvested using PBS/EDTA, washed and centrifuged in BSS, and then fixed with 4% paraformaldehyde + 0.1% glutaraldehyde. Samples were then labeled with a-syn monoclonal primary antibody (BD Biosciences) followed by labeling with a goat-anti mouse Alexa 647 IgG1

secondary antibody in PBS with 10 mg/ml BSA. Samples were analyzed using a BD FACSAria Fusion Fluorescence Activated Cell Sorter, and data were analyzed using FCS Express 5 Flow Research software. Analysis was gated to include single cells on the basis of forward and side light-scatter, and cells were then gated to identify positively transfected cells (VAMP8-pHluorin or mRFP). For quantification of expression levels (Figure 4.4) Alexa-647 fluorescence was measured only for VAMP8-pHluorin expressing cells. For endocytosis experiments mRFP expressing cells were gated and quenching of FITC-IgE was monitored from that subset of cells.

Endocytosis: RBL-2H3 cells were co-transfected via electroporation with 5 μg of mRFP, to identify positively transfected cells, and 5 μg of pcDNA or 5 μg Wt a-syn (for low concentrations). For high concentrations, RBL-2H3 cells were electroporated with 5 μg of mRFP and 25 μg of pcDNA or 25 μg of Wt a-syn, A30P a-syn, or 1-102 a-syn. Cells were allowed to recover for ~24 hours and were then harvested, placed in suspension, and sensitized with 3μg/ml FITC-IgE for 45 min at 37°C. Sensitized cells were then placed in the BD FACSAria Fusion Fluorescence Activated Cell Sorter at 37°C, and IgE/FcεRI complexes were crosslinked by addition of anti-IgE antibody at t = 0 sec. Acidification of internalized complexes was monitored by FITC-IgE fluorescence quenching, monitored from cells positively expressing mRFP. Data were collected for ~1500 seconds, following which they were analyzed using FCS Express 5 Flow Research software and Microsoft Excel.

Statistical Analyses: Statistical analysis was performed with Prism software (Graphpad) and Microsoft Excel. Statistical significance was determined by a One-Way ANOVA (Analysis of Variance) followed by Tukey's post test. Level of significance is denoted as follows: $*P < 0.05$, $**P < 0.01$, $***P < 0.001$.

ACKNOWLEDGEMENTS

I thank Dr. David Eliezer for initiating this collaboration, for frequent assistance with interpretation of results, and for guidance in evaluating specific a-syn mutants, and planning experiments. I also thank Drs Jacqueline Burre and Manu Sharma (Weill Cornell Medical College) for helpful discussions and Carol Bayles for maintaining the Cornell Imaging Facility. This work was supported by grants to the Cornell University Biotechnology Resource Center (NIH S10RR025502), the National Science Foundation Graduate Research Fellowship under Grant No. NSF DGE-1144153 (MMW), and the National Institute of General Medical Sciences grant R01 GM117552. I thank and acknowledge the assistance of my fellow graduate student Meraj Ramezani, who cloned human a-syn constructs A30P, G51D, H50Q, 1-102, A30P/V70P, and who created the Wt-syn-mRFP construct. Meraj also performed all of the endocytosis assays described in Chapter 4.

Supplementary Figure 4.1. **H50Q human a-syn also inhibits stimulated recycling endosome exocytosis. A-C:** RBL-2H3 cells transfected with VAMP8-pHluorin and pcDNA or H50Q and stimulated with thapsigargin. **D**, quantification of low concentrations of H50Q and E46K a-syn analyzed by flow cytometry (compare to Figure 4.4F). Supp. Figure 4.1A and pcDNA response for 4.1C and 4.1D are identical to pcDNA responses shown in Figure 4.2A, 4.2I, and 4.4F and are included to show the control compared to H50Q stimulated response, or control vs H50Q and E46K expression levels.

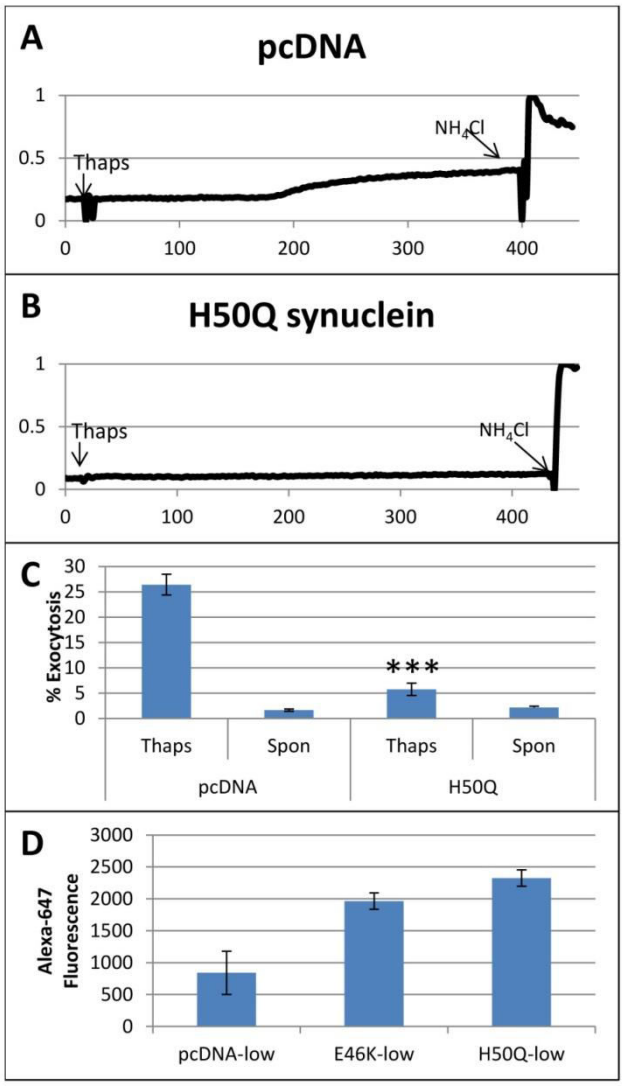

Supplementary Figure 4.2. **Wt-syn-mRFP inhibits stimulated exocytosis at low, but not high concentrations. A-C**: RBL-2H3 cells transfected with VAMP8-pHluorin and low or high concentrations of mRFP or Wt-syn-mRFP and were stimulated with thapsigargin. Summary results from 3 indepdent experiments are displayed in **E**.

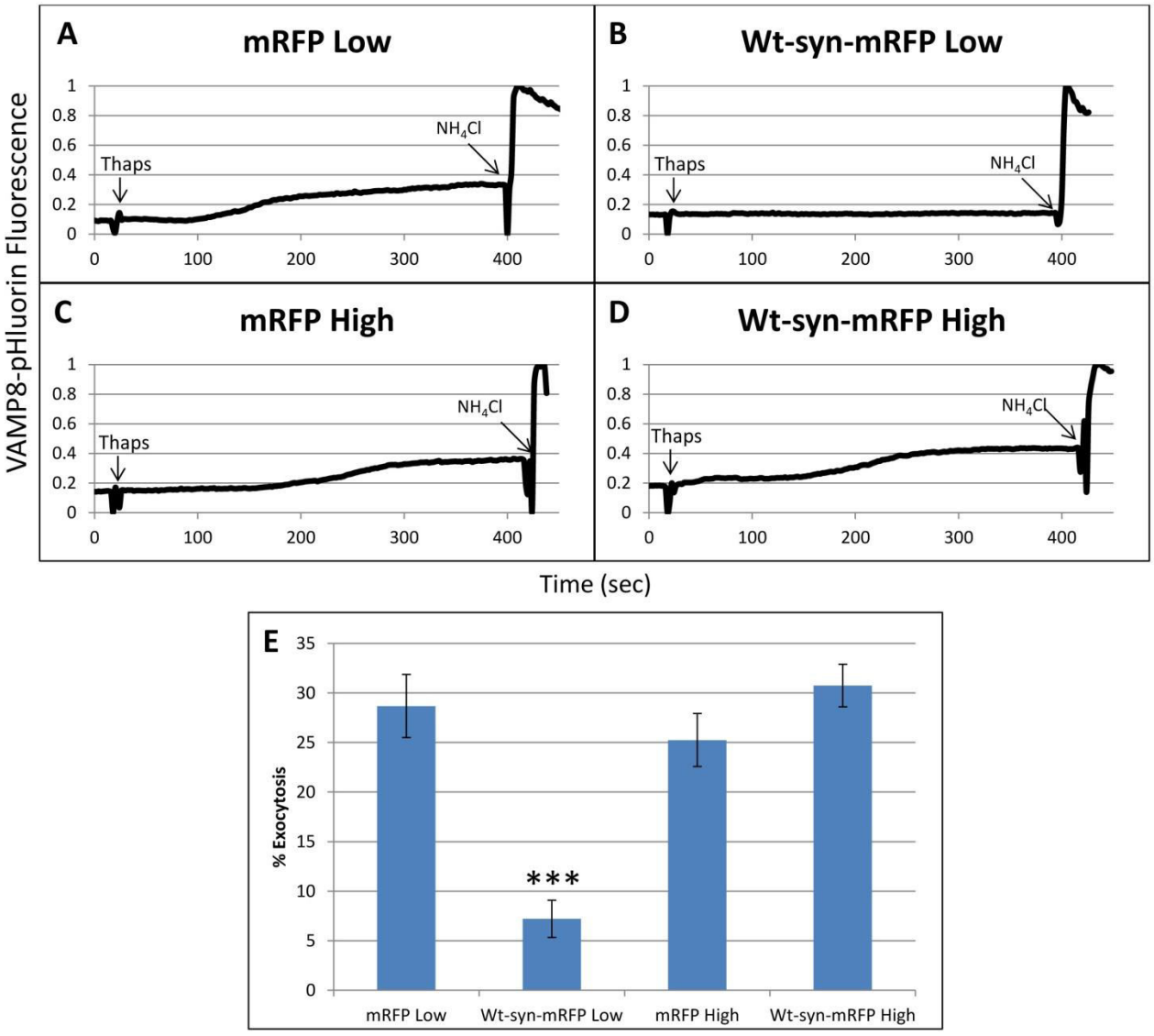

Supplementary Figure 4.3. **A30P human a-syn no longer inhibits stimulated exocytosis after 40 hours of expression.** RBL-2H3 cells expressing VAMP8-pHluorin and high concentrations of pcDNA or A30P human a-syn were stimulated with thapsigargin 40 hours after being transfected.

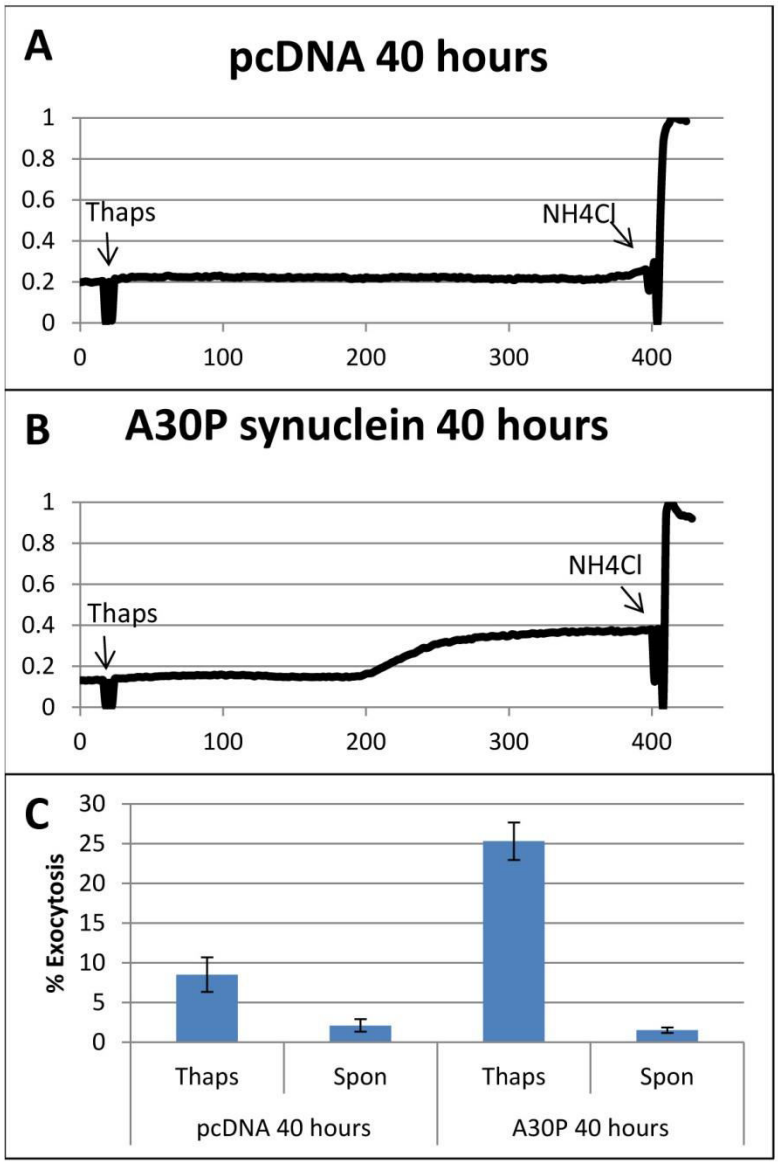

REFERENCES

Barbour, Robin, Kristin Kling, John P. Anderson, Kelly Banducci, Tracy Cole, Linnea Diep, Michael Fox, et al. 2008. "Red Blood Cells Are the Major Source of Alpha-Synuclein in Blood." *Neurodegenerative Diseases* 5 (2): 55–59. doi:10.1159/000112832.

Bodner, Christina R., Alexander S. Maltsev, Christopher M. Dobson, and Ad Bax. 2010. "Differential Phospholipid Binding of α-Synuclein Variants Implicated in Parkinson's Disease Revealed by Solution NMR Spectroscopy." *Biochemistry* 49 (5): 862–71. doi:10.1021/bi901723p.

Breda, Carlo, Marie L. Nugent, Jasper G. Estranero, Charalambos P. Kyriacou, Tiago F. Outeiro, Joern R. Steinert, and Flaviano Giorgini. 2015. "Rab11 Modulates Alpha -Synuclein-Mediated Defects in Synaptic Transmission and Behaviour." *Human Molecular Genetics* 24 (4): 1077–91. doi:10.1093/hmg/ddu521.

Burre, J., M. Sharma, and T. C. Sudhof. 2012. "Systematic Mutagenesis of -Synuclein Reveals Distinct Sequence Requirements for Physiological and Pathological Activities." *Journal of Neuroscience* 32 (43): 15227–42. doi:10.1523/JNEUROSCI.3545-12.2012.

Burré, Jacqueline, Manu Sharma, and Thomas C Südhof. 2015. "Definition of a Molecular Pathway Mediating α-Synuclein Neurotoxicity." *The Journal of Neuroscience : The Official Journal of the Society for Neuroscience* 35 (13): 5221–32. doi:10.1523/JNEUROSCI.4650-14.2015.

Burré, Jacqueline, Manu Sharma, Theodoros Tsetsenis, Vladimir Buchman, Mark R Etherton, and Thomas C Südhof. 2010. "Alpha-Synuclein Promotes SNARE-Complex Assembly in Vivo and in Vitro." *Science (New York, N.Y.)* 329 (5999): 1663–67. doi:10.1126/science.1195227.

Busch, David J, Paul A Oliphint, Rylie B Walsh, Susan M L Banks, Wendy S Woods, Julia M George, and Jennifer R Morgan. 2014. "Acute Increase of α-Synuclein Inhibits Synaptic Vesicle Recycling Evoked during Intense Stimulation." *Molecular Biology of the Cell* 25 (24): 3926–41. doi:10.1091/mbc.E14-02-0708.

Cheng, Hsiao Chun, Christina M. Ulane, and Robert E. Burke. 2010. "Clinical Progression in Parkinson Disease and the Neurobiology of Axons." *Annals of Neurology*. doi:10.1002/ana.21995.

Chiba-Falek, Ornit, Grisel J. Lopez, and Robert L. Nussbaum. 2006. "Levels of Alpha-Synuclein mRNA in Sporadic Parkinson Disease Patients." *Movement Disorders* 21 (10): 1703–8. doi:10.1002/mds.21007.

Chutna, Oldriska, Susana Gonçalves, Anna Villar-Piqué, Patrícia Guerreiro, Zrinka Marijanovic, Tiago Mendes, José Ramalho, et al. 2014. "The Small GTPase Rab11 Co-Localizes with α-Synuclein in Intracellular Inclusions and Modulates Its Aggregation, Secretion and Toxicity." *Human Molecular Genetics* 23 (25): 6732–45. doi:10.1093/hmg/ddu391.

Cooper, A A, A D Gitler, A Cashikar, C M Haynes, K J Hill, B Bhullar, K Liu, et al. 2006. "Alpha-Synuclein Blocks ER-Golgi Traffic and Rab1 Rescues Neuron Loss in Parkinson's Models." *Science (New York, NY)*. doi:10.1126/science.1129462.

Fan, Guo-Huang, Lynne A Lapierre, James R Goldenring, Jiqing Sai, and Ann Richmond. 2004. "Rab11-Family Interacting Protein 2 and Myosin Vb Are Required for CXCR2 Recycling and Receptor-Mediated Chemotaxis." *Molecular Biology of the Cell* 15 (5): 2456–69. doi:10.1091/mbc.E03-09-0706.

Gadi, Deepti, Alice Wagenknecht-Wiesner, David Holowka, and Barbara Baird. 2011. "Sequestration of Phosphoinositides by Mutated MARCKS Effector Domain Inhibits Stimulated Ca(2+) Mobilization and Degranulation in Mast Cells." *Molecular Biology of the Cell* 22 (24): 4908–17. doi:10.1091/mbc.E11-07-0614.

Gaugler, Meret Nora, Ozgur Genc, Wojciech Bobela, Safa Mohanna, Mustafa Taleb Ardah, Omar Mukhtar El-Agnaf, Marco Cantoni, et al. 2012. "Nigrostriatal Overabundance of Alpha-Synuclein Leads to Decreased Vesicle Density and Deficits in Dopamine Release That Correlate with Reduced Motor Activity." *Acta Neuropathologica* 123 (5): 653–69. doi:10.1007/s00401-012-0963-y.

Gosse, JA Julie a, Alice Wagenknecht-Wiesner, David Holowka, Barbara Baird, and David Holowka. 2005. "Transmembrane Sequences Are Determinants of Immunoreceptor Signaling." *The Journal of Immunology* 175 (4): 2123–31. doi:175/4/2123 [pii].

Hibi, T, N Hirashima, and M Nakanishi. 2000. "Rat Basophilic Leukemia Cells Express Syntaxin-3 and VAMP-7 in Granule Membranes." *Biochemical and Biophysical Research Communications* 271 (1): 36–41. doi:10.1006/bbrc.2000.2591.

Holowka, David, Nathaniel Calloway, Roy Cohen, Deepti Gadi, Jinmin Lee, Norah L Smith, and Barbara Baird. 2012. "Roles for Ca2+ Mobilization in Mast Cell Functions." *Frontiers in Immunology* 3: 104. doi:10.3389/fimmu.2012.00104.

Hoopmann, Peer, Annedore Punge, Sina V Barysch, Volker Westphal, Johanna Bückers, Felipe Opazo, Ioanna Bethani, Marcel a Lauterbach, Stefan W Hell, and Silvio O Rizzoli. 2010. "Endosomal Sorting of Readily Releasable Synaptic Vesicles." *Proceedings of the National Academy of Sciences of the United States of America* 107: 19055–60. doi:10.1073/pnas.1007037107.

Irwin, David J., Virginia M-Y M.-Y. Lee, and John Q. Trojanowski. 2013. "Parkinson's Disease Dementia: Convergence of α-Synuclein, Tau and Amyloid-β Pathologies." *Nature Reviews. Neuroscience* 14 (9): 626–36. doi:10.1038/nrn3549.

Kim, Han-Joon. 2013. "Alpha-Synuclein Expression in Patients with Parkinson's Disease: A Clinician's Perspective." *Experimental Neurobiology* 22 (2): 77–83. doi:10.5607/en.2013.22.2.77.

Kramer, Michael L., and Walter J. Schulz-Schaeffer. 2007. "Presynaptic α-Synuclein Aggregates, Not Lewy Bodies, Cause Neurodegeneration in Dementia with Lewy Bodies." *The Journal of Neuroscience* 27 (6): 1405–10. doi:10.1523/JNEUROSCI.4564-06.2007.

Langston, J. William. 2006. "The Parkinson's Complex: Parkinsonism Is Just the Tip of the Iceberg." *Annals of Neurology*. doi:10.1002/ana.20834.

Larsen, Kristin E, Yvonne Schmitz, Matthew D Troyer, Eugene Mosharov, Paula Dietrich, Abrar Z

Quazi, Magali Savalle, et al. 2006. “Alpha-Synuclein Overexpression in PC12 and Chromaffin Cells Impairs Catecholamine Release by Interfering with a Late Step in Exocytosis.” *The Journal of Neuroscience : The Official Journal of the Society for Neuroscience* 26 (46): 11915–22. doi:10.1523/JNEUROSCI.3821-06.2006.

Lemkau, Luisel R., Gemma Comellas, Kathryn D. Kloepper, Wendy S. Woods, Julia M. George, and Chad M. Rienstra. 2012. “Mutant Protein A30P Alpha-Synuclein Adopts Wild-Type Fibril Structure, despite Slower Fibrillation Kinetics.” *Journal of Biological Chemistry* 287 (14): 11526–32. doi:10.1074/jbc.M111.306902.

Lundblad, Martin, Mickael Decressac, Bengt Mattsson, and Anders Björklund. 2012. “Impaired Neurotransmission Caused by Overexpression of α-Synuclein in Nigral Dopamine Neurons.” *Proceedings of the National Academy of Sciences of the United States of America* 109 (9): 3213–19. doi:10.1073/pnas.1200575109.

Maier, Tobias, Marc Güell, and Luis Serrano. 2009. “Correlation of mRNA and Protein in Complex Biological Samples.” *FEBS Letters*. doi:10.1016/j.febslet.2009.10.036.

Marshall, Misty R, Varsha Pattu, Mahantappa Halimani, Monika Maier-Peuschel, Martha-Lena Müller, Ute Becherer, Wanjin Hong, et al. 2015. “VAMP8-Dependent Fusion of Recycling Endosomes with the Plasma Membrane Facilitates T Lymphocyte Cytotoxicity.” *The Journal of Cell Biology* 210 (1): 135–51. doi:10.1083/jcb.201411093.

Murphy, Karen E., Amanda M. Gysbers, Sarah K. Abbott, Nahid Tayebi, Woojin S. Kim, Ellen Sidransky, Antony Cooper, Brett Garner, and Glenda M. Halliday. 2014. “Reduced Glucocerebrosidase Is Associated with Increased Alpha-Synuclein in Sporadic Parkinson’s Disease.” *Brain* 137 (3): 834–48. doi:10.1093/brain/awt367.

Murray, Ian V J, Benoit I Giasson, Shawn M Quinn, Vishwanath Koppaka, Paul H Axelsen, Harry Ischiropoulos, John Q Trojanowski, and Virginia M-Y Lee. 2003. “C-Terminal Truncation: Role of Alpha-Synuclein Carboxy-Terminus on Fibril Formation in Vitro.” *Biochemistry* 42 (28): 8530–40. doi:10.1021/bi027363r.

Naal, Rose Mary Z G, Eric P Holowka, Barbara Baird, and David Holowka. 2003. “Antigen-Stimulated Trafficking from the Recycling Compartment to the Plasma Membrane in RBL Mast Cells.” *Traffic (Copenhagen, Denmark)* 4 (3): 190–200. doi:10.1034/j.1600-0854.2003.00073.x.

Nalls, Mike a, Nathan Pankratz, Christina M Lill, Chuong B Do, Dena G Hernandez, Mohamad Saad, Anita L DeStefano, et al. 2014. “Large-Scale Meta-Analysis of Genome-Wide Association Data Identifies Six New Risk Loci for Parkinson’s Disease.” *Nature Genetics* 056 (9): 1–7. doi:10.1038/ng.3043.

Narkiewicz, Joanna, Gabriele Giachin, and Giuseppe Legname. 2014. “In Vitro Aggregation Assays for the Characterization of α-Synuclein Prion-like Properties.” *Prion* 8 (1): 19–32. doi:10.4161/pri.28125.

Nemani, Venu M., Wei Lu, Victoria Berge, Ken Nakamura, Bibiana Onoa, Michael K. Lee, Farrukh A. Chaudhry, Roger A. Nicoll, and Robert H. Edwards. 2010. “Increased Expression of α-Synuclein Reduces Neurotransmitter Release by Inhibiting Synaptic Vesicle Reclustering after

Endocytosis." *Neuron* 65 (1): 66–79. doi:10.1016/j.neuron.2009.12.023.

Petrucci, Simona, Monia Ginevrino, and Enza Maria Valente. 2016. "Phenotypic Spectrum of Alpha-Synuclein Mutations: New Insights from Patients and Cellular Models." *Parkinsonism and Related Disorders* 22: S16–20. doi:10.1016/j.parkreldis.2015.08.015.

Polymeropoulos, Mihael H, Christian Lavedan, Elisabeth Leroy, Susan E Ide, Anindya Dehejia, Amalia Dutra, Brian Pike, et al. 1997. "Mutation in the Alpha-Synuclein Gene Identified in Families with Parkinson's Disease." *Science (New York, N.Y.)* 276 (5321): 2045–47. doi:doi: 10.1126/science.276.5321.2045.

Posner, R G, B Lee, D H Conrad, D Holowka, B Baird, and B Goldstein. 1992. "Aggregation of IgE-Receptor Complexes on Rat Basophilic Leukemia Cells Does Not Change the Intrinsic Affinity but Can Alter the Kinetics of the Ligand-IgE Interaction." *Biochemistry* 31 (23): 5350–56.

Schulte, Claudia, and Thomas Gasser. 2011. "Genetic Basis of Parkinson's Disease: Inheritance, Penetrance, and Expression." *Application of Clinical Genetics*. doi:10.2147/TACG.S11639.

Scott, D., and S. Roy. 2012. " -Synuclein Inhibits Intersynaptic Vesicle Mobility and Maintains Recycling-Pool Homeostasis." *Journal of Neuroscience* 32 (30): 10129–35. doi:10.1523/JNEUROSCI.0535-12.2012.

Shelby, Sarah A., David Holowka, Barbara Baird, and Sarah L. Veatch. 2013. "Distinct Stages of Stimulated Fcεri Receptor Clustering and Immobilization Are Identified through Superresolution Imaging." *Biophysical Journal* 105 (10): 2343–54. doi:10.1016/j.bpj.2013.09.049.

Snead, David, and David Eliezer. 2014. "Alpha-Synuclein Function and Dysfunction on Cellular Membranes." *Experimental Neurobiology* 23 (4): 292–313. doi:10.5607/en.2014.23.4.292.

Spillantini, M.G. 1999. "Parkinson's Disease, Dementia with Lewy Bodies and Multiple System Atrophy Are α-Synucleinopathies." *Parkinsonism & Related Disorders* 5 (4): 157–62. doi:10.1016/S1353-8020(99)00031-0.

Sulzer, David. 2007. "Multiple Hit Hypotheses for Dopamine Neuron Loss in Parkinson's Disease." *Trends in Neurosciences*. doi:10.1016/j.tins.2007.03.009.

Thayanidhi, Nandhakumar, Jared R Helm, Deborah C Nycz, Marvin Bentley, Yingjian Liang, and Jesse C Hay. 2010. "Alpha-Synuclein Delays Endoplasmic Reticulum (ER)-to-Golgi Transport in Mammalian Cells by Antagonizing ER/Golgi SNAREs." *Molecular Biology of the Cell* 21 (11): 1850–63. doi:10.1091/mbc.E09-09-0801.

van Ijzendoorn, Sven C D. 2006. "Recycling Endosomes." *Journal of Cell Science* 119 (Pt 9): 1679–81. doi:10.1242/jcs.02948.

Vargas, Karina J., Sachin Makani, Taylor Davis, Christopher H. Westphal, Pablo E. Castillo, and Sreeganga S. Chandra. 2014. "Synucleins Regulate the Kinetics of Synaptic Vesicle Endocytosis." *The Journal of Neuroscience : The Official Journal of the Society for Neuroscience* 34 (28): 9364–76. doi:10.1523/JNEUROSCI.4787-13.2014.

Wang, X, T Huang, G Bu, and H Xu. 2014. "Dysregulation of Protein Trafficking in

Neurodegeneration." *Mol Neurodegener* 9 (1): 31. doi:10.1186/1750-1326-9-31.

Wernersson, Sara, and Gunnar Pejler. 2014. "Mast Cell Secretory Granules: Armed for Battle." *Nature Reviews. Immunology* 14 (7): 478–94. doi:10.1038/nri3690.

Wilkes, Marcus M, Joshua D Wilson, Barbara Baird, and David Holowka. 2014. "Activation of Cdc42 Is Necessary for Sustained Oscillations of Ca2+ and PIP2 Stimulated by Antigen in RBL Mast Cells." *Biology Open* 3 (8): 700–710. doi:10.1242/bio.20148862.

Wilson, Joshua D, Sarah A Shelby, David Holowka, Barbara Baird, Regulates Mast, and Cell Exocytosis. 2016. "Rab11 Regulates the Mast Cell Exocytic Response." *Traffic*. doi:10.1111/tra.12418.

Wood, Stephen J., Jette Wypych, Shirley Steavenson, Jean Claude Louis, Martin Citron, and Anja Leona Biere. 1999. "Alpha-Synuclein Fibrillogenesis Is Nucleation-Dependent: Implications for the Pathogenesis of Parkinson's Disease." *Journal of Biological Chemistry* 274 (28): 19509–12. doi:10.1074/jbc.274.28.19509.

Xu, J., X.-S. Wu, J. Sheng, Z. Zhang, H.-Y. Yue, L. Sun, C. Sgobio, et al. 2016. "A-Synuclein Mutation Inhibits Endocytosis at Mammalian Central Nerve Terminals." *Journal of Neuroscience* 36 (16): 4408–14. doi:10.1523/JNEUROSCI.3627-15.2016.

Chapter 5: Summary and Outlook

Summary Part 1. Human life begins with the fertilization of a single cell. Over time this cell multiplies and divides, eventually developing, and differentiating, into all the specialized cell types necessary for life. The majority of the processes required for cellular maturation are controlled by Ca^{2+}. It is Ca^{2+} that triggers life at fertilization. It is Ca^{2+} that regulates differentiation of cells into specialized cell types. It is Ca^{2+} that regulates much of cell signaling, and it is Ca^{2+} that will ultimately signal cell death (Berridge, Bootman, and Lipp 1998). How a single ion can control so many cellular processes is a fascination of many scientists, and the focus of much research.

The Baird-Holowka lab has long been interested in Ca^{2+} signaling, particularly its role in regulating the allergic immune response. As a rotation student I began my first project, which developed into Chapter 2 of this thesis, investigating the importance of the C-terminal di-arginine motif of Cdc42, and its importance for Ca^{2+} signaling. From that rotation project, which began as a follow-up to a study conducted by Dr. Jared Johnson, a former student in the Cerione lab (Johnson, Erickson, and Cerione 2012), I too have developed a fascination, and appreciation, for the role that Ca^{2+} plays in cellular signaling.

Over the course of my Chapter 2 studies we determined that the di-arginine motif was important for Cdc42 to regulate stimulated Ca^{2+} responses. We also began to recognize the important role that Cdc42 plays in regulating sustained Ca^{2+} oscillations, and began to suspect that Cdc42 may regulate mast cell signaling, in part, by controlling Ca^{2+} oscillations indirectly through regulation of PIP_2. We showed that Cdc42 can regulate a Ca^{2+} independent process, stimulated endocytosis, and then showed that Cdc42-G12V can reconstitute stimulated PIP_2 oscillations in mutant B6A4C1 cells.

Building on this work, we attempted to identify a mechanism by which Cdc42 might regulate PIP_2 synthesis in mast cells (Chapter 3). With the help of our collaborator, Dr. Chris Stefan, we demonstrated that antigen-stimulation of RBL-2H3 cells results in an ~40% increase in PIP_2 levels, whereas stimulated-PIP_2 synthesis is not observed in B6A4C1 cells. Stimulated PIP_2 synthesis was also observed in RBL-2H3 cells by using TIRF microscopy to monitor the appearance of PIP_2 puncta, marked with the reporter PH-PLCδ-EGFP, following stimulation. By this method, B6A4C1 cells, again, appeared to be deficient in stimulated PIP_2 synthesis.

Next, we showed that pharmacological inhibitors of Cdc42 (DU40), PKC (BIM), and PI3-kinase (wortmannin), all strongly inhibit antigen and thapsigargin-stimulated degranulation. However, activation of PKC, using PMA, bypassed the inhibition by DU40 and wortmannin. We then investigated if these strong inhibitors of degranulation also showed strong inhibition of stimulated Ca^{2+} responses. DU40 showed only minor inhibition of SOCE, suppressing late, sustained Ca^{2+} oscillations. Wortmannin reduced both stimulated Ca^{2+} release from stores and SOCE, and began to strongly suppress Ca^{2+} oscillations 2-3 min following stimulation. BIM, despite being the strongest inhibitor of degranulation, was found to enhance Ca^{2+} responses, while simultaneously suppressing Ca^{2+} oscillations. We then showed that all three inhibitors decrease the number of RBL-2H3 cells undergoing stimulated PIP_2 synthesis, suggesting that all of these inhibitors can act, at least in part, by controlling levels of PIP_2, the substrate needed for Ca^{2+} signaling. B6A4C1 cells, again showed to be deficient in antigen-stimulated Cdc42 activation by a novel method in Chapter 3, were shown to be partially inhibited in stimulated PKC activity, which can be reconstituted by active Cdc42-G12V. Finally, we showed that low concentrations of wortmannin inhibits stimulated Cdc42 oscillations, and suggest a potential

mechanism for this inhibition, as DOCK GEFs need PIP_3 at the plasma membrane in order to dock, and activate, Rho GTPases. These low concentrations of wortmannin inhibit PIP_3 synthesis.

Future Directions Part 1: Despite the advances we have made over the past several years, many important questions must be addressed to further clarify the role of Cdc42, and other Rho GTPases, in mast cell degranulation and Ca^{2+} signaling. The most pertinent questions arise from our results described in Chapter 3. Many of these results have only recently been obtained. First, as described in Chapter 3, although we have evidence that Cdc42 signals through PKC, the many different PKC isoforms make finding the specific Cdc42 effector difficult. The most straightforward approach to answer this question is to biochemically probe for a stimulated Cdc42-PKC interaction using a pull down assay, and then identifying the PKC isoform, or isoforms, interacting with Cdc42. Realistically, this will be a technically challenging endeavor for many reasons. First, many PKC isoforms exist. Second, because Cdc42 activation is oscillatory in nature, it will, potentially, be easy to miss the time point that Cdc42 and PKC interact. However this could be overcome by expressing the Cdc42-G12V constitutively active mutant in RBL-2H3 cells and performing a pull down assay to probe for a Cdc42-PKC interaction. Finally, it is unclear how strong these two proteins interact, making detecting a protein-protein interaction hypothetically difficult. Despite these challenges, attempting these experiments is a worthwhile pursuit, especially if a novel Cdc42-PKC interaction can be detected. In the case that an interaction can be detected, and a PKC isoform identified in RBL-2H3 cells, B6A4C1 cells could then be probed to verify that this Cdc42-PKC interaction is deficient in the mutant cell line. Knock-downs of Cdc42 or specific PKC isoforms, such as PKCζ, a known Cdc42 effector activated independent of Ca^{2+} influx, are other options for probing a Cdc42-PKC

interaction in RBL-2H3 cells. Cdc42 knock-down will also verify the specificity of DU40, as many proteins, not just Rho GTPases, undergo geranylgeranylation.

An additional explanation as to why we only see partial inhibition of stimulated PKC activation in B6A4C1 cells is that Cdc42 regulates PIP_2 synthesis directly through regulation of PIP5-kinases (Weernink et al. 2004), in addition to its role in PKC activation. Under this circumstance, a redundant PKC isoform might rescue part of the B6A4C1 deficiency, hence we only see partial inhibition of PKC activation, but the capacity to resynthesize PIP_2 would still be lost. This interpretation is supported, in part, by Figure 3.5, which shows that even in the case that MARCKS-ED-mRFP is displaced from the plasma membrane, subsequent MARCKS oscillations are typically suppressed. A recently published study, also conducted in RBL-2H3 cells, demonstrated the importance of constant PIP_2 replenishment for sustained Ca^{2+} oscillations, following G-protein coupled receptor stimulation. This study concludes by asking the question, "How Ca^{2+} influx activates PIP5-kinase and whether this is driven by local Ca^{2+} entry requires further investigation" (Alswied and Parekh 2015). A previous study demonstrated that in order for Cdc42, and Rac1, to be activated, the presence of intracellular Ca^{2+} was necessary (El-Sibai and Backer 2007). Exploring whether receptor-stimulated Ca^{2+} mobilization activates Cdc42, Rho A, and Rac1, which then increase PIP5-kinase activity, leading to PIP_2 synthesis, is a question, whose answer, is of interest to many researchers. Using the CBD-GFP construct we can now explore in live cells, using TIRF microscopy, the timing of these signaling events. We can determine if Cdc42 activation is occurring before or after Ca^{2+} release from stores. In addition future experiments should also probe the effect of receptor-stimulated Rho GTPase activation on PIP5-kinase activity.

Further investigation is also necessary to understand the importance of DOCK GEF proteins in mast cell signaling. Results from both Chapter 2 and Chapter 3 demonstrate that DOCK GEFS most likely play a prominent role in mast cell signaling. However, future experiments are needed to clarify the function of these DOCK GEFs. In Chapter 3 DOCK8 was used to reconstitute stimulated VAMP8-mediated exocytosis in B6A4C1 cells, even though DOCK7 was able to reconstitute Ca^{2+} signaling in Chapter 2. In contrast to DOCK8, DOCK7, in initial experiments, has failed to reconstitute stimulated VAMP8-mediated exocytosis in B6A4C1 cells (data not shown). These initial experiments are being verified, and expression levels of DOCK7 are being confirmed, and final results will be included in a published version of Chapter 3. Assuming this result is true, this finding begs the question, why is DOCK7 capable of reconstituting Ca^{2+} oscillations but not degranulation? Further experiments will probe this question and examine fundamental differences between DOCK8 and DOCK7 in mast cell signaling. One possible explanation is that DOCK GEFs play multiple roles in stimulated exocytosis, some that rely on GEF activity, and others that depend on DOCK proteins as adaptors. A previous study of DOCK5 in RBL-2H3 cells showed that its effect on mast cell signaling was independent of GEF activity, giving credence to the notion that DOCK GEFs can play an important role as adaptors in RBL-2H3 cells. One of the main limitations in conducting reconstitution studies in B6A4C1 cells is consistently obtaining positive transfection. The B6A4C1 cells are notoriously difficult to transfect, and the DOCK7 and DOCK8 plasmids are both large (~14kb). To improve consistency with these studies stable B6A4C1 cell lines, expressing DOCK7 and DOCK8 should be created, potentially using viral transfection systems, which have previously been useful in studying the function of Rho GTPases in B6A4C1 cells (Hong-Geller et al. 2001). Finally, expression levels of DOCK7, DOCK8, and other DOCK

GEFs can be compared between B6A4C1 cells and RBL-2H3 cells using western blotting or immunofluorescence labeling. If differences are not observed, an attempt can be made to clone specific DOCK GEFs out of the RBL-2H3 and B6A4C1 cells to determine if a specific mutation, or mutations, is preventing the capacity of DOCK GEFs to activate Cdc42 and Rac1 in B6A4C1 cells.

Summary Part 2: In March of 2014 I began experiments to determine if the protein alpha-synuclein (a-syn) affected stimulated exocytosis in RBL-2H3 cells. Originally, we had no expectations as to whether exogenous expression of Wt a-syn would increase, decrease, or have no effect on, stimulated responses. We initially discovered an interesting result, that expression of Wt a-syn inhibits stimulated VAMP8-mediated exocytosis (Chapter 4). However, this result was often difficult to reproduce, and sometimes would disappear for weeks at a time. It was only after several months that we finally understood the crucial role that concentration of a-syn played in affecting stimulated exocytosis. Our original experiments expressed a-syn at an intermediate concentration, between the low concentration, and high concentration, described in Chapter 4. Once we identified the importance of a-syn concentration, we were able to quickly optimize our protocol, and consistently see strong inhibition of stimulated VAMP8-mediated exocytosis when a-syn was expressed at low levels. In contrast, we also clearly demonstrate that expression of high levels of a-syn result in the loss of this inhibitory effect. We also demonstrate that Wt a-syn inhibits stimulated exocytosis in PC-12 cells, a dopamine releasing cell line. This suggests that the results observed in RBL-2H3 cells may be transferable to more neuronal like systems.

In Chapter 4 we also investigated whether genetically linked a-syn mutants also inhibit stimulated recycling endosomal exocytosis in RBL-2H3 cells. All of these known genetic mutants (A30P, E46K, G51D, H50Q, and A53T) inhibit stimulated exocytosis when expressed at

low concentrations, and all mutants tested also lose inhibition when expressed at higher levels. With the assistance of our collaborator, Dr. David Eliezer from Weill Cornell Medical College, we explored various structural mutants that could potentially disrupt the inhibitory effect of a-syn at low concentrations. We first truncated the acidic, disordered C-terminus of a-syn, as this region is thought to control protein-protein interactions. However, a-syn still inhibited stimulated exocytosis. We then made a structural mutant, A30P/V70P, similar to other mutants which prevent the capacity of a-syn to bind to membranes (Burre, Sharma, and Sudhof 2012; Burré, Sharma, and Südhof 2015). This mutant does not inhibit stimulated recycling endosomal exocytosis, providing evidence that membrane binding is essential for the inhibitory effect we observe.

As a-syn has been shown to affect stimulated endocytosis in many different cellular systems, we next investigated the role of a-syn in regulating stimulated endocytosis in RBL-2H3 cells. In contrast to our exocytosis results, a-syn did not show significant inhibition of endocytosis at low expression levels. However, at higher expression levels, a-syn begins to inhibit stimulated endocytosis, and this effect appears to be dependent on the C-terminus of a-syn.

Our results, that low expression of a-syn affect stimulated exocytosis, not endocytosis, and that high expression of a-syn affects stimulated endocytosis, but not exocytosis, lead us to believe that we may be observing both physiological and pathological functions of synuclein, depending on concentration level. Future experiments are needed to determine if the differences we see are based on a-syn aggregation state, and if our observed results can also be observed in a neuronal cell line.

Future Directions Part 2: A-syn is known to aggregate within neurons, eventually forming Lewy bodies in the brains of Parkinson's disease (PD) patients. A-syn aggregation has been shown to be a time and concentration-dependent process (Narkiewicz, Giachin, and Legname 2014). As a result, the fact that we see differing results depending on whether we express high or low concentrations of a-syn, in both our exocytosis and endocytosis assays, suggests we may be observing aggregation-mediated signaling effects. However, we have yet to definitively show that high expression of a-syn in RBL-2H3 cells causes a-syn aggregates. Thus, finding an assay that can clearly distinguish a-syn aggregates, from monomeric a-syn, will be important for carrying this project forward.

Initially we performed western blotting experiments in an attempt to see differences in monomeric vs aggregated a-syn. Although interesting results were initially observed, these results proved to be inconsistent and unrepeatable (data not shown). We have reached out to a collaborator, Dr. Jacqueline Burre at Weill Cornell Medical College, who has suggested using Triton X-100 solubility, proteinase K treatment, or limited proteolysis assays, followed by immunoblotting, to detect a-syn aggregates. An alternative option would be to use native PAGE gel electrophoresis. Even with these methods, Dr. Burre admits that identifying and analyzing a-syn aggregates is a tricky endeavor, as aggregates do not form in a consistent manner, varying from experiment to experiment. However these methods should be attempted so that we can definitively determine whether the concentration-dependent differences observed in RBL-2H3 cells is due to a-syn aggregation.

Fluorescent recovery after photobleaching (FRAP) is an alternative method for observing differences in the state of a-syn when expressed at high or low concentrations. Initial experiments have proven promising. In RBL-2H3 cells expressing mRFP only, recovery after

photobleaching can be observed within the nucleus of cells, as shown in Figure 5.1A. However, when Wt-syn-mRFP is expressed at high concentrations, no recovery is observed after photobleaching. This protocol is currently being optimized as technical difficulties have prevented us from doing appropriate control experiments. Under current photobleaching conditions, dim or medium fluorescent cells, are completely photobleached with no recovery observed, for either mRFP or Wt-syn-mRFP. Once this technical difficulty is overcome we will compare FRAP between dim and bright Wt-syn-mRFP expressing cells to see if a difference can be observed. FRAP observed when Wt-syn-mRFP is expressed at low, but not high levels, would provide evidence that a-syn is aggregating when expressed at high concentrations, preventing a-syn from diffusing, and recovering, following photobleaching. Future experiments will aim to improve photobleaching conditions, so that proper control experiments can be performed.

Finally, comparing and applying what we learn from RBL mast cell studies to neuronal systems is crucial for determining the relevance of our results. Our ability to show that low expression of a-syn in PC-12 cells inhibits stimulated recycling endosomal exocytosis was the first step in making this transition. However, even though PC-12 cells release dopamine upon stimulation, they are still not neuronal cells. We have begun growing N2A neuroblastoma cells, and in initial experiments have shown that VAMP8-pHluorin exocytosis can be stimulated and observed using 80 mM KCl (data not shown). Follow-up studies will investigate whether expression of Wt a-syn inhibits KCl-stimulated exocytosis in N2A cells, and whether differing concentrations of Wt a-syn affect this response. Making this transition to a neuronal cell line, and investigating the effect of a-syn on exocytosis induced with a more commonly used neuronal stimulant (KCl instead of thapsigargin + phorbol 12-myristate-13-acetate), is a critical step in moving this project forward. Hopefully, by conducting the experiments described in this

summary section, our lab will move closer to identifying the physiological function of a-syn and improve our understanding of why disruption of this function leads to onset of PD.

Figure 5.1. **Expression of human Wt a-syn inhibits FRAP in RBL-2H3 cells.** RBL-2H3 cells were transfected with high levels of mRFP or Wt-syn-mRFP. Cells were then photobleached using the Zeiss 710 confocal microscope, at 10 seconds, and fluorescent recovery was monitored over 300 seconds.

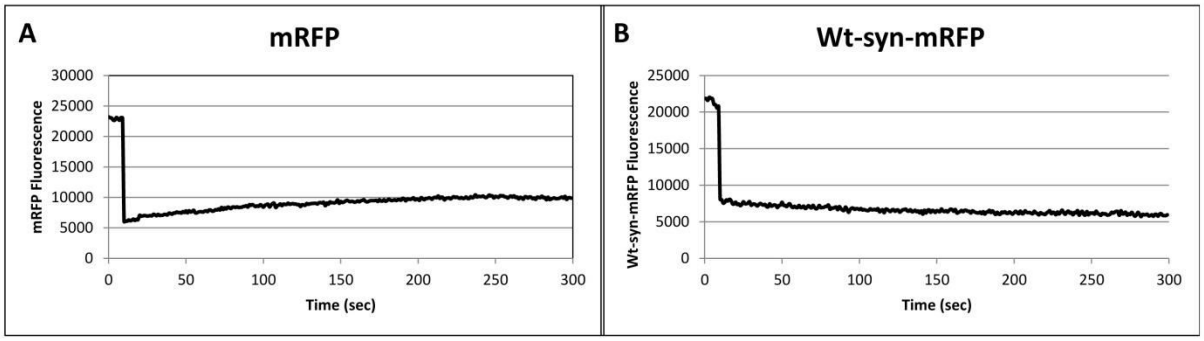

REFERENCES

Alswied, Abdullah, and Anant B. Parekh. 2015. “Ca2+ Influx through Store-Operated Calcium Channels Replenishes the Functional Phosphatidylinositol 4,5-Bisphosphate Pool Used by Cysteinyl Leukotriene Type I Receptors.” *Journal of Biological Chemistry* 290 (49): 29555–66. doi:10.1074/jbc.M115.678292.

Berridge, M J, M D Bootman, and P Lipp. 1998. “Calcium--a Life and Death Signal.” *Nature* 395 (6703): 645–48. doi:10.1038/27094.

Burre, J., M. Sharma, and T. C. Sudhof. 2012. “Systematic Mutagenesis of -Synuclein Reveals Distinct Sequence Requirements for Physiological and Pathological Activities.” *Journal of Neuroscience* 32 (43): 15227–42. doi:10.1523/JNEUROSCI.3545-12.2012.

Burré, Jacqueline, Manu Sharma, and Thomas C Südhof. 2015. “Definition of a Molecular Pathway Mediating α-Synuclein Neurotoxicity.” *The Journal of Neuroscience : The Official Journal of the Society for Neuroscience* 35 (13): 5221–32. doi:10.1523/JNEUROSCI.4650-14.2015.

El-Sibai, Mirvat, and Jonathan M. Backer. 2007. “Phospholipase C?? Negatively Regulates Rac/Cdc42 Activation in Antigen-Stimulated Mast Cells.” *European Journal of Immunology* 37 (1): 261–70. doi:10.1002/eji.200635875.

Hong-Geller, E, D Holowka, R P Siraganian, B Baird, and R a Cerione. 2001. “Activated Cdc42/Rac Reconstitutes Fcepsilon RI-Mediated Ca2+ Mobilization and Degranulation in Mutant RBL Mast Cells.” *Proceedings of the National Academy of Sciences of the United States of America* 98 (3): 1154–59. doi:10.1073/pnas.98.3.1154.

Johnson, Jared L., Jon W. Erickson, and Richard A. Cerione. 2012. “C-Terminal Di-Arginine Motif of Cdc42 Protein Is Essential for Binding to Phosphatidylinositol 4,5-Bisphosphate-Containing Membranes and Inducing Cellular Transformation.” *Journal of Biological Chemistry* 287 (8): 5764–74. doi:10.1074/jbc.M111.336487.

Narkiewicz, Joanna, Gabriele Giachin, and Giuseppe Legname. 2014. “In Vitro Aggregation Assays for the Characterization of α-Synuclein Prion-like Properties.” *Prion* 8 (1): 19–32. doi:10.4161/pri.28125.

Weernink, Paschal A Oude, Konstantinos Meletiadis, Silvia Hommeltenberg, Matthias Hinz, Hisamitsu Ishihara, Martina Schmidt, and Karl H. Jakobs. 2004. “Activation of Type I Phosphatidylinositol 4-Phosphate 5-Kinase Isoforms by the Rho GTPases, RhoA, Rac1, and Cdc42.” *Journal of Biological Chemistry* 279 (9): 7840–49. doi:10.1074/jbc.M312737200.